Universidade de São Paulo
Escola Superior de Agricultura “Luiz de Queiroz”

Mobile terrestrial laser scanner for site-specific management in orange crop

André Freitas Colaço

Thesis presented to obtain the degree of Doctor in Science. Area: Agricultural Systems Engineering

Piracicaba
2016

André Freitas Colaço
Agronomist

Mobile terrestrial laser scanner for site-specific management in orange crop

Advisor: Prof. Dr. **JOSÉ PAULO MOLIN**
Co-advisor: Prof. Dr. **ALEXANDRE ESCOLÀ AGUSTÍ**

Thesis presented to obtain the degree of Doctor in Science. Area: Agricultural Systems Engineering

Piracicaba
2016

Dados Internacionais de Catalogação na Publicação
DIVISÃO DE BIBLIOTECA – DIBD/ESALQ/USP

Colaço, André Freitas

Mobile terrestrial laser scanner for site-specific management in orange crop / André Freitras Colaço. - - Piracicaba, 2016.

87 p.

Tese (Doutorado) - - USP / Escola Superior de Agricultura “Luiz de Queiroz”.

1. Sensor LiDAR 2. Geometria de copa 3. Tecnologia de taxa variada 4. Agricultura de precisão. I. Título

ACKNOWLEDGEMENTS

My sincere thankfulness,

To the University of São Paulo and the 'Luiz de Queiroz' College of Agriculture, for technical, social and scientific education.

To Fapesp and Capes for providing financial means to my formation.

To Jacto and Citrosuco companies, for providing the equipment and experimental fields.

To Prof. José Paulo Molin, for guidance and opportunities throughout my academic life.

To Prof. Alexandre Escolà Agustí, the codirector of this project, for giving good ideas to this work. Also, for kindly hosting me in Spain.

To all my friends in Lleida, the members of the Research Group in AgroICT and Precision Agriculture, especially to Prof. Joan Ramón Rosell Polo for providing me a good experience at the University of Lleida.

To my friends and colleges from the Biosystems Engineering Department, Adriano A. Anselmi, Felippe H. S. Karp, Gustavo Portz, Jeovano G. A. Lima, João Paulo S. Veiga, Leonardo F. Maldaner, Lucas R. Amaral, Marcos N. Ferraz, Mark Spekken, Mateus T. Eitelwein, Natanael S. Vilanova, Nelson C. Franco Jr., Rodrigo G. Trevisan, Tatiana F. Canata and Thiago L. Romanelli.

To my friends for life, Camila, Diego, Erik, Heitor, Leonardo, Mônica and Viviane.

To my family in blood and in law, for the incentive.

To my lovely Larissa, who makes me happy every day with her love and kind companionship.

To my parents, brother and sister, Ailton, Lucy, Rafael and Raquel, my role models to whom I own everything.

“The theory of emptiness…is the deep recognition that there is a fundamental disparity between the way we perceive the world, including our own existence in it, and the way things actually are.”
Dalai Lama XIV, The Universe in a Single Atom: The Convergence of Science and Spirituality

The only true statement,
“I think, therefore I Am”
René Descartes

CONTENTS

RESUMO

Sensor a laser na gestão localizada de pomares de laranja

Sensores baseados em tecnologia LiDAR (*Light Detection and Ranging*) têm o potencial de fornecer modelos tridimensionais de árvores, provendo informações como o volume e altura de copa. Essas informações podem ser utilizadas em diagnósticos e recomendações localizadas de fertilizantes e defensivos agrícolas. Este estudo teve como objetivo investigar o uso de sensores LiDAR na cultura da laranja, uma das principais culturas de porte arbóreo no Brasil. Diversas pesquisas têm desenvolvido sistemas LiDAR para culturas arbóreas. Porém, normalmente tais sistemas são empregados em plantas individuais ou em pequenas áreas. Dessa forma, diversos aspectos da aquisição e processamento de dados ainda devem ser desenvolvidos para viabilizar a aplicação em larga escala. O primeiro estudo deste documento (Capítulo 3) focou no desenvolvimento de um sistema LiDAR (*Mobile Terrestrial Laser Scanner* - MTLS) e nova metodologia de processamento de dados para obtenção de informações acerca da geometria das copas em pomares comerciais de laranja. Um sensor a laser e um receptor RTK-GNSS (*Real Time Kinematics - Global Navigation Satellite System*) foram instalados em um veículo para leituras em campo. O processamento de dados foi baseado na geração de uma nuvem de pontos, seguida dos passos de filtragem, classificação e reconstrução da superfície das copas. Um pomar comercial de laranja de 25 ha foi utilizado para a validação. O sistema de aquisição e processamento de dados foi capaz de produzir uma nuvem de pontos representativa do pomar, fornecendo informação sobre geometria das plantas em alta resolução. A escolha sobre o tipo de classificação da nuvem de pontos (em plantas individuais ou em seções transversais das fileiras) e sobre o algoritmo de reconstrução de superfície, foi discutida nesse estudo. O segundo estudo (Capítulo 4) buscou caracterizar a variabilidade espacial da geometria de copa em pomares comerciais. Entender tal variabilidade permite avaliar se a aplicação em taxas variáveis de insumos baseada em sensores LiDAR (aplicar quantias de insumos proporcionais ao tamanho das copas) é uma estratégia adequada para otimizar o uso de insumos. Cinco pomares comerciais foram avaliados com o sistema MTLS. De acordo com a variabilidade encontrada, a economia de insumos pelo uso da taxa variável foi estimada em aproximadamente 40%. O segundo objetivo desse estudo foi avaliar a relação entre a geometria de copa e diversos outros parâmetros dos pomares. Os mapas de volume e altura de copa foram comparados aos mapas de produtividade, elevação, condutividade elétrica do solo, matéria orgânica e textura do solo. As correlações entre geometria de copa e produtividade ou fatores de solo variaram de fraca até forte, dependendo do pomar. Quando os pomares foram divididos entre três classes com diferentes tamanhos de copas, o desempenho em produtividade e as características do solo foram distintas entre as três zonas, indicando que parâmetros de geometria de copa são variáveis úteis para a delimitação de unidades de gestão diferenciada em um pomar. Os resultados gerais desta pesquisa mostraram o potencial de sistemas MTLS para pomares de laranja, indicando como a geometria de copa pode ser utilizada na gestão localizada de pomares de laranja.

Palavras-chave: Sensor LiDAR; Geometria de copa; Tecnologia de taxa variada; Agricultura de precisão

ABSTRACT

Mobile terrestrial laser scanner for site-specific management in orange crop

Sensors based on LiDAR (*Light Detection and Ranging*) technology have the potential to provide accurate 3D models of the trees retrieving information such as canopy volume and height. This information can be used for diagnostics and prescriptions of fertilizers and plant protection products on a site-specific basis. This research aimed to investigate the use of LiDAR sensors in orange crops. Orange is one of the most important tree crop in Brazil. So far, research have developed and tested LiDAR based systems for several tree crops. However, usually individual trees or small field plots have been used. Therefore, several aspects related to data acquisition and processing must still be developed for large-scale application. The first study reported in this document (Chapter 3) aimed to develop and test a mobile terrestrial laser scanner (MTLS) and new data processing methods in order to obtain 3D models of large commercial orange groves and spatial information about canopy geometry. A 2D laser sensor and a RTK-GNSS receiver (*Real Time Kinematics - Global Navigation Satellite System)* were mounted on a vehicle. The data processing was based on generating a georeferenced point cloud, followed by the filtering, classification and surface reconstruction steps. A 25 ha commercial orange grove was used for field validation. The developed data acquisition and processing system was able to produce a reliable point cloud of the grove, providing high resolution canopy volume and height information. The choice of the type of point cloud classification (by individual trees or by transversal sections of the row) and the surface reconstruction algorithm is discussed in this study. The second study (Chapter 4) aimed to characterize the spatial variability of canopy geometry in commercial orange groves. Understanding such variability allows sensor-based variable rate application of inputs (*i.e*, applying proportional rates of inputs based on the variability of canopy size) to be considered as a suitable strategy to optimize the use of fertilizers and plant protection products. Five commercial orange groves were scanned with the developed MTLS system. According to the variability of canopy volume found in those groves, the input savings as a result of implementing sensor-based variable rate technologies were estimated in about 40%. The second goal of this study was to understand the relationship between canopy geometry and several other relevant attributes of the groves. The canopy volume and height maps of three groves were analyzed against historical yield maps, elevation, soil electrical conductivity, organic matter and clay content maps. The correlations found between canopy geometry and yield or soil maps varied from poor to strong correlations, depending on the grove. When classifying the groves into three classes according to canopy size, the yield performance and soil features inside each class was found to be significantly different, indicating that canopy geometry is a suitable variable to guide management zones delineation in one grove. Overall results from this research show the potential of MTLS systems and subsequent data analysis in orange crops indicating how canopy geometry information can be used in site-specific management practices.

Keywords: LiDAR sensor; Canopy geometry; Variable-rate technology; Precision agriculture

LIST OF FIGURES

LIST OF TABLES

1. INTRODUCTION

Agricultural and forestry management usually follows a sequence of three steps: (1) making observations over the crop, field or phenomena, (2) developing diagnostics and prescriptions and finally, (3) intervening on the crop by applying inputs or carrying out a specific operation. These steps (specially the first and third ones) have been greatly facilitated in the past few decades with the development of new technologies within the scope of precision agriculture (PA) such as the global positioning systems, sensors, geographical information systems and machine automation.

Since the beginning of agriculture, the visual assessment over the fields has been an important source of insight over the crop growth and sanity. However, with the development of agricultural mechanization and consequently, the enlargement of the cropping fields, this simple type of assessment was no longer sufficient to make accurate diagnostics. So, new techniques of observation were designed based mainly on standardized sampling methods in order to provide a more accurate representation of the fields.

Lately, PA has brought awareness over the concept of spatial variability within the fields. This set of technologies enabled the mapping of such variability and also the local management of the field, known as site-specific management. The notion of spatial variability could not be accurately perceived with the use of traditional sampling techniques. Once again, the traditional methods of observation over the fields had to adapt to the new needs of agriculture. A new alternative was the use of sensors, which could provide not only with more information for diagnostics, but also with the spatial distribution of the measured parameter throughout the field. Though slowly deploying, the automatic data collection process through the use of sensors is now taking place in the current agronomical management.

Several types of sensors can be applied in the context of PA. They can be classified based on the sensed target: soil, crop, product (aiming to the quality of the harvested product) and environment. The most widespread type of crop sensing in PA research and in commercial applications is the optical sensing, more specifically the spectroscopy. This technology is based on capturing the reflected light from the crops in different wavelength of the light spectrum. This can be achieved by either terrestrial sensors (proximal sensing) or by aerial or satellite mounted sensors (remote sensing). The information derived from these sensors (vegetation indexes such as the normalized vegetation index - NDVI) can relate to important agronomical parameters such as crop biomass, nutritional and phytosanitary status and yield. The practical application of this technology is to assess the spatial variability of the fields and support variable rate application of inputs. Another important application of spectroscopy in tree crops is the identification of diseases in the groves, which is a priority issue in many crops such as citrus.

Spectroscopy is a known technique in different fields of science and has spread greatly among the PA studies due to its potential application to agriculture. The practical research have proven its functionality for crops such as maize, wheat and others. Nowadays, commercial sensors and also aerial and satellite imagery are available to farmers and can be applied for site-specific management. However, for the majority of the tree crops, research has not yet shown significant results over the application of spectroscopy applied to the site-specific management.

Another type of crop sensor, which is much newer to agriculture than spectroscopy, is the ranging sensor. This technology can be quite simple and straightforward, but it has not yet reached the agricultural market with great expression. Range sensors can measure distances which, with appropriate acquisition setting and data processing, are used to estimate geometrical crop parameters such as height, width, volume and other structural parameters. Radar, ultrasonic and laser are the most important principles used by this kind of sensors. Unlike spectroscopy, the ranging

sensors have been widely tested in tree crops and not as much in stand crops like soybeans and wheat. Radar and laser sensors were successfully introduced into forestry and environmental applications. These sensors are usually mounted on planes for airborne measurements to collect data about canopy height and terrain surface.

The use of terrestrial ultrasonic sensors to estimate canopy geometry such as volume and height was one of the first applications of ranging sensors to tree crops. Further on, the laser sensors based on LiDAR technology (*Light Detection and Ranging*), were also introduced. The purpose of this technology was to provide spatial information about the canopy geometry variability to objectively decide the establishment of management zones within the fields. Additionally, it provides support to implement site-specific management such as variable rate applications. This development was encouraged due to the acknowledgement of spatial variability within the groves. Early research over PA techniques applied to orchards, often referred as "precision horticulture", evidenced the existence of spatial variability within the groves in several attributes of the soil and crop sanity. The effect of such variability can be visually perceived on the tree development and overall performance. The use of ranging sensors to accurately estimate the canopy geometry offered the chance to manage the grove in accordance to the variability of the trees. One of the first uses was the variable rate of plant protection products. Few studies have actually mounted ranging sensor systems on spreaders and sprayers for tree crops in order to realize variable rate applications in "real time", *i.e.*, carrying out the sensor measurements at the same time as the application of inputs. These prototypes permitted the application of inputs in accordance to the size of each tree, which was referred as variable rate application at "single-tree basis".

The introduction of the LiDAR sensor into precision horticulture studies, was a great evolution step over the ultrasonic sensors. The LiDAR technology permits not only a more accurate estimate of the canopy geometry but also the 3D modeling of the canopy structures with great level of detail. This technology was first developed and applied in other fields besides agriculture, such as robotics, architecture and others. Nowadays, it has reach agricultural research and a great number of published scientific material is available. Since this is a relatively young technique for agriculture, the current research is still more focused on developing methods to collect and process data. These methods must be adapted to different crops, scenarios and applications. Scientific work is found for several fruit crops such as vineyard, peach, apple, pear, olive, and citrus trees. However, these studies are usually carried out in small field plots, and large scale tests were not yet conducted.

Brazil is a major producer of several fruit crops. According to the Food and Agriculture Organization of the United Nations (FAO, 2016), Brazil is the third world's largest producer of fruits (FAOSTAT database of 2013 for production of fruits excluding melons). A great portion of this production is exported, supplying the global market with fresh and processed fruit products. Although the research have demonstrated the potential of site-specific management to these crops, the adoption of such techniques is still growing slowly and only in more advanced production systems. Among the fruit crops, the orange production represents to Brazil a particularly outstanding agribusiness. According to the National Company of Food and Supply (COMPANHIA NACIONAL DE ABASTECIMENTO - CONAB, 2013), this crop covers approximately 500,000 hectares of land in the country (the state of São Paulo is the main production region), supplying the internal market of fresh fruit and 52% of the global market of processed orange juice (FAO, 2016). This crop is also highly developed technically and some site-specific practices are already taking place in the management of commercial groves.

The Brazilian orange farms can be as large as thousands of hectares. However, individual groves inside the farms rarely exceeds twenty or thirty hectares each. Even in these relatively small field plots, site-specific techniques still have its purpose. Relieve and soil types can change inside this groves as well as the occurrence of

diseases and insects. Therefore, the variability in the tree performance is noticed in two scales: in large areas within the grove or within short distances (from one tree to the next), which might be referred as variability at "field scale" or at "tree scale", respectively. The evidence of such variabilities encouraged the development and use of site-specific management in Brazilian orange groves. Techniques like yield mapping, georeferenced soil sampling and variable rate application of fertilizers were already validated by research and are considered available to growers.

Disease occurrence is a relevant aspect related to the "tree scale" variability in Brazilian citrus groves. This is also true for the North American groves (the State of Florida in the United States is the second world's largest production region). The *huanglongbing* (HLB) disease is a particularly alarming problem which threatens these two producing regions. The HLB is a bacterial disease transmitted by a flying insect (psyllid, *Diaphorina citri*) with great spreading capability. As a control strategy, the infected trees must be cut out and destroyed, leaving gaps across the groves. Each cut out tree must be replaced by a new tree. Thus, trees in different developing stages might be found in the same grove worsening the variability in the canopy size within the grove.

For all these reasons, the Brazilian orange production is a promising stakeholder of PA techniques, especially of LiDAR technology. Enabling the site-specific management through the use of LiDAR sensors might help growers dealing with canopy variability, greatly optimizing the use of inputs. The importance of this topic was already perceived by researches in Florida in the early beginning of PA applied to citrus. Their research helped greatly on the "state of the art" of ranging sensors applied to tree crops. However, the knowledge they help creating is not entirely applicable to the Brazilian conditions of orange production, indicating the need of local research and development of the technology for Brazilian groves.

Although several researches have been developing LiDAR techniques for tree crops, some aspects of the data processing and 3D modeling are still not entirely solved. The actual variability of the crops was not yet mapped and reported for large commercial groves and thus, the true potential of the technology is still unknown. Also, the use of geometrical parameters like canopy volume or height is not a common type of data for site-specific management, so understanding their relation with other important agronomical variables is crucial on the development of new prescriptions for variable-rate management.

The present work aimed to investigate the use of LiDAR technology in Brazilian orange groves, bridging the aforementioned gaps in the current research. This report is divided into three main sections, corresponding to one literature review, approaching the state of the art of the main topic of this research, and two specific studies with distinct and complementary objectives. The first study described the development of a mobile terrestrial laser scanner based on a LiDAR sensor and new data processing methods to reach 3D modeling of orange crops and retrieve canopy geometry information for site-specific management. The second work, aimed to characterize the spatial variability of canopy geometry in large commercial orange groves. This study assessed the potential benefit of site-specific management based on LiDAR systems. Additionally, it described the relationship between canopy geometry of orange groves and other relevant agronomical attributes usually found on PA management. The understanding of such relationship should help on the use of canopy geometrical information on the site-specific management of orange groves.

References

CONAB. COMPANHIA NACIONAL DE ABASTESCIMENTO. **Acompanhamento de safra brasileira**: laranja, terceiro levantamento, dezembro/2013. Brasília, 16p. 2013.

FAO. **FAOSTAT**: food and agricultural commodities production. Available at: < http://faostat3.fao.org/home/E> accessed on 15, August. 2016

2. LITERATURE REVIEW

2.1. Introduction

The main theme of this research, mobile terrestrial laser scanner applied to the orange crop, results from the interaction between different fields of knowledge within agricultural science. Some of which are primary fields of agronomy and others relate partially with it. Figure 2.1 shows the most relevant areas to this work. The different levels overlapping, interaction and hierarchy among them are not being considered in this scheme. Some of these fields were necessary in order to implement and execute the study (*e.g.* electronics, instrumentation, geostatistics and classical statistics), while others are actually areas affected by the results from this research (*e.g.* horticulture, phytosanitary management, precision agriculture and others).

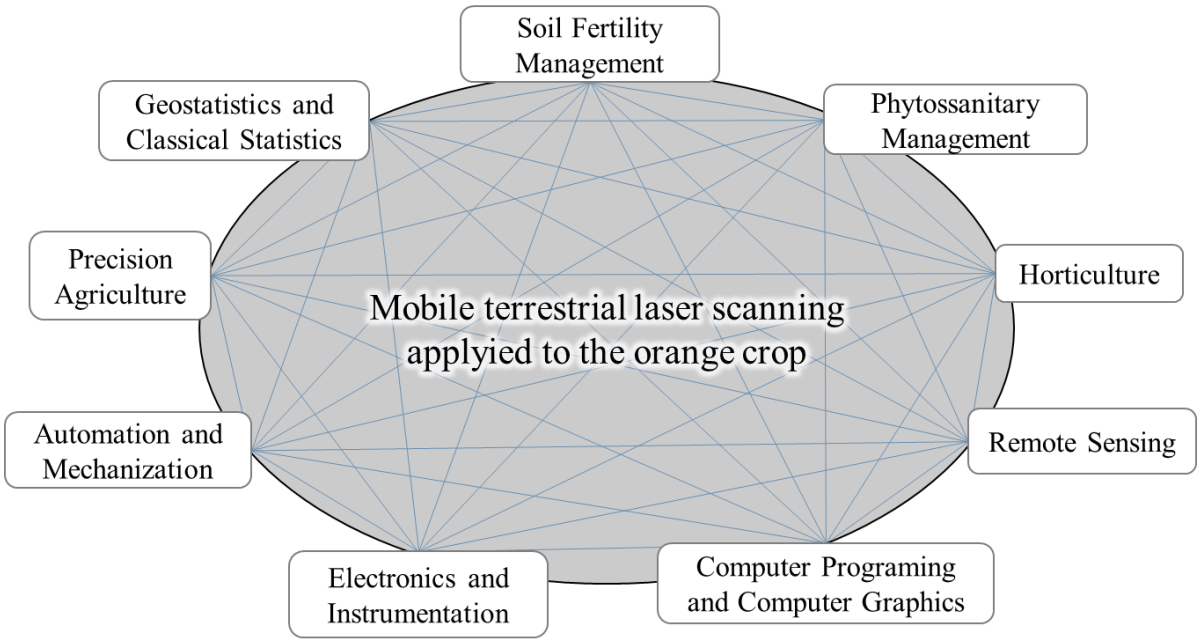

Figure 2.1 - Different fields of knowledge involved in this work

These areas were not reviewed as independent topics. This section does not intend to give deep theoretical knowledge of any particular technology or field neither. For deepening the theory over ranging sensors and geometrical characterization of crops the reviews by Dworak, Selbeck and Ehlert (2011), Rosell and Sanz (2012), Gil et al. (2014) and Lin (2015) are recommended. This literature review aims to explore the "state of the art" regarding ranging sensors applied to tree crops. It focuses on analyzing the most similar studies to this one, characterizing the scientific context of the main topic of this research. A search was carried out using the databases of scientific publication that gathers the most relevant journals in the fields of agricultural and biological engineering. 69 papers were analyzed, accounting for 63 peer reviewed articles and 4 scientific reviews. Two conference full papers were also included due to their relevance to this work. These publications went from 1988 until 2016 (Figure 2.2). About 64% of this material was published in the past decade.

Three main research groups are identified as the main contributors to the theme of ranging sensors applied to tree crops (Figure 2.2). The first is the Research Group in AgroICT & Precision Agriculture,

headquartered in the University of Lleida, Catalonia, Spain. Researchers from the Citrus Research and Education Center at Lake Alfred, Florida, USA, from the University of Florida represents the second group. The third is a smaller group of researchers from the Silsoe Research Institute at Silsoe, UK. Other works come from USA (excluding Florida), Germany, Canada, China, Spain (excluding Lleida), Slovenia, Finland, Iran and Chile.

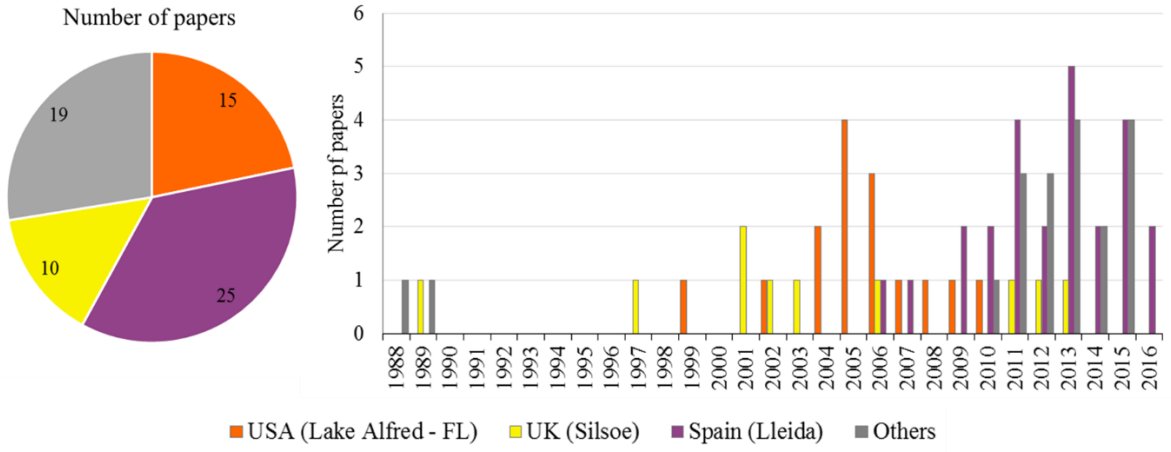

Figure 2.2: Sources of the reviewed papers and publication rate of different research groups

The first research group is responsible for the most recent research. They stand out with studies dedicated to LiDAR applications to several fruit crops, especially apple trees and vineyards. They might be considered focused on the LiDAR technology itself and not on a specific crop. The second group is focused on the development of ranging sensors specifically to the citrus crop. In fact, the research from Florida comes from a citrus devoted research center, which investigates all subjects related to this crop. Most of their work employed ultrasonic sensors, although some important studies with laser sensors were also conducted. The studies from UK are more dedicated to the spraying technology applied mostly to apple orchards. This group is responsible for presenting one of the first approaches of LiDAR sensors applied to tree crops.

The major topics found in the reviewed material were: i) the capability of ultrasonic and LiDAR sensors on estimating tree canopy attributes such as leaf area index, canopy volume and canopy height; ii) the performance of fertilizer spreaders and mostly sprayers instrumented with ranging sensors and automatic control of flow rate, and iii) the 3D modeling of tree crops by terrestrial laser scanning through the construction of 3D point clouds. Less frequent subjects were: i) the assessment of input savings by sensor-based variable rate applications; ii) the evaluation of 3D reconstruction algorithms and iii) variations over the method of laser scanning data acquisition. The most frequent crops were citrus, apples trees and vineyards. The less frequent crops were pear, olive trees and forest crops.

2.2. Ranging sensors applied to tree crops

The early application of ranging sensors for measuring crop geometry was presented by Giles, Delwiche and Dodd (1988, 1989) in California, USA. In their first work, an ultrasonic measuring system composed by three sensors was designed and evaluated. The sensors were arranged in different heights along a vertical pole, facing the side of the tree. Each ultrasonic unit measured its distance from the canopy every 0.5 second. The system moved along the side of the tree row at constant speed. Combining the measured distances from the sensors, the system

provided estimates of volume for each section along the tree row (similar example of this method in Figure 2.3 a). The authors found it to be an effective and reliable way to measure the canopy volume of fruit trees. This type of data acquisition set up was later employed in practically all ultrasonic measurements of tree crops. In their second work (GILES; DELWICHE; DODD, 1989), they instrumented a sprayer with the measuring system which guided variable rate applications according to the measured tree sizes. They accounted for 28 up to 52% savings of plant protection products by using this application method in different fruit crops.

Since those works, recent studies still use similar technology for variable rate applications. Escolà et al. (2011) equipped a sprayer for apple orchard with ultrasonic sensors. They assessed the accuracy of canopy geometry estimations by such sensors. Maghsoudi et al. (2015) equipped a sprayer machine with three ultrasonic sensors for measuring the canopy volume of pistachio trees and controlling the spraying rate. They accounted for a 34% reduction on pesticide usage using such technology. Another interesting application of ultrasonic sensors was recently tested by Osterman et al. (2013), where the sensors were actually used to control the position of the spraying sections of the machine, providing the optimal spraying deposition in each part of the tree.

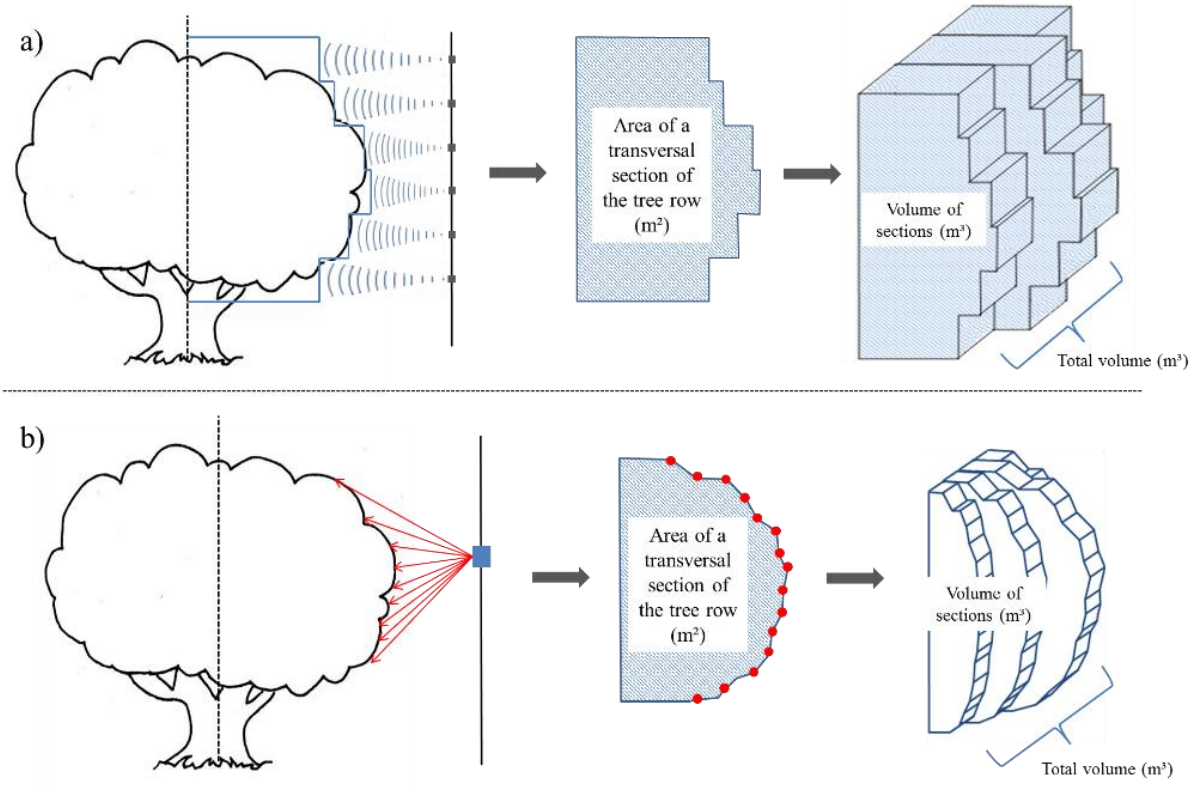

Figure 2.3: Example of canopy volume estimation by ultrasonic (a) and LiDAR (b) sensors

In the UK, Walklate (1989) used a 2D LiDAR sensor in barley crop and later they also applied it to tree crops (WALKLATE et al., 1997). The proposed set up of the laser sensor, facing the side of the tree vertically and moving along the grove alleys to measure transversal sections of the row, was later used by most of the studies in the application of LiDAR to tree crops. Nowadays, after many developments, this data acquisition system is referred as "mobile terrestrial laser scanner" (MTLS). Unlike the ultrasonic sensors, the 2D LiDAR scanner can measure distances in several directions within a plane, providing a much more realistic profile of the target (Figure 2.3 b). In

the study by Walklate et al. (1997), the interception of light by the canopy of apple trees was evaluated as an indicator of the crop density and as an estimator of spraying deposition.

Later on, these authors measured the effects of constant flow rate spraying of apple trees of different sizes, indicating the need for accounting the variability of canopy size to determine the optimal spraying rate (CROSS et al., 2001a, 2001b, 2003). Simultaneously, Walklate et al. (2002) investigated the use of a LiDAR system in order to adjust the models to calculate spraying volume and deposition based on new variables which would represent tree size and density. This initiative looked towards a coordinate adjustment on the label-recommended dose rate of agrochemicals in European orchards and vineyards (WALKLATE et al., 2006; WALKLATE; CROSS; PERGHER, 2011; WALKLATE; CROSS, 2012, 2013). The authors estimated that such adjustments would result in significant reduction on agrochemical consumption.

The application of ranging sensors to citrus crops was first mentioned by Whitney et al. (1999), in Florida, USA. They presented the main topics that should be developed in order to advance the use of precision agriculture in citrus. The canopy volume and height estimations by ranging sensors were mentioned among yield mapping, variable rate technology, GPS (*Global Positioning Systems*) and GIS (*Geographic Information Systems*) topics. Later on, the investigation of LiDAR and ultrasonic sensors in Florida evolved simultaneously. Zaman and Salyani (2004), Schumann and Zaman (2005), Zaman and Schumann (2005) evaluated several aspects of ultrasonic estimations of citrus canopy volume. They found that ultrasonic measurements were highly correlated with manual measurements ($R^2 > 0.90$) and that canopy volume varied significantly in commercial groves. The sensor readings were stable even in different ground speeds. Estimation of canopy volume were more reliable in densely foliated trees. The trees were not symmetrical, so they should be scanned from both sides. The works by Zaman, Schumann and Hostler (2006) and Schumann et al. (2006a) found a high correlation (R^2 of 0.80 and 0.64 respectively) between canopy volume estimated by ultrasonic sensors and fruit yield in commercial citrus plots. Schumann et al. (2006b) adapted a fertilizer spreader machine with a control system in order to perform variable rate application based on a single-tree prescription map. Zaman, Schumann and Miller (2005) got up to 40% savings of nitrogen by using this practice.

One work which actually compared ultrasonic and laser sensors in the Florida citrus was carried out by Tumbo et al. (2002). They implemented a laser measuring system and an ultrasonic system with twenty sensors and compared their capability to estimate canopy volume. The methods correlated well with each other ($R^2 = 0.90$) and with manually measurements of canopy volume. However, the authors concluded that, due to the higher resolution of laser sensor, it could provide better estimations of canopy volume especially in groves with small replants. The laser sensor was subsequently investigated with greater depth by Wei and Salyani (2004, 2005). They found high accuracy and repeatability of the distance measurements by the sensor. The estimated volume of a template box got an average error of 4.4%. The authors have also proposed a data processing method to estimate foliage density of citrus trees based on the occupancy proportion of actual tree surface measured by the laser and the smoothed canopy boundary created with the outer points of the canopy. Both Tumbo et al. (2002) and Wei and Salyani (2005) transformed the laser data into a 2D distance images (Figure 2.4), from which canopy volume and other parameters were retrieved.

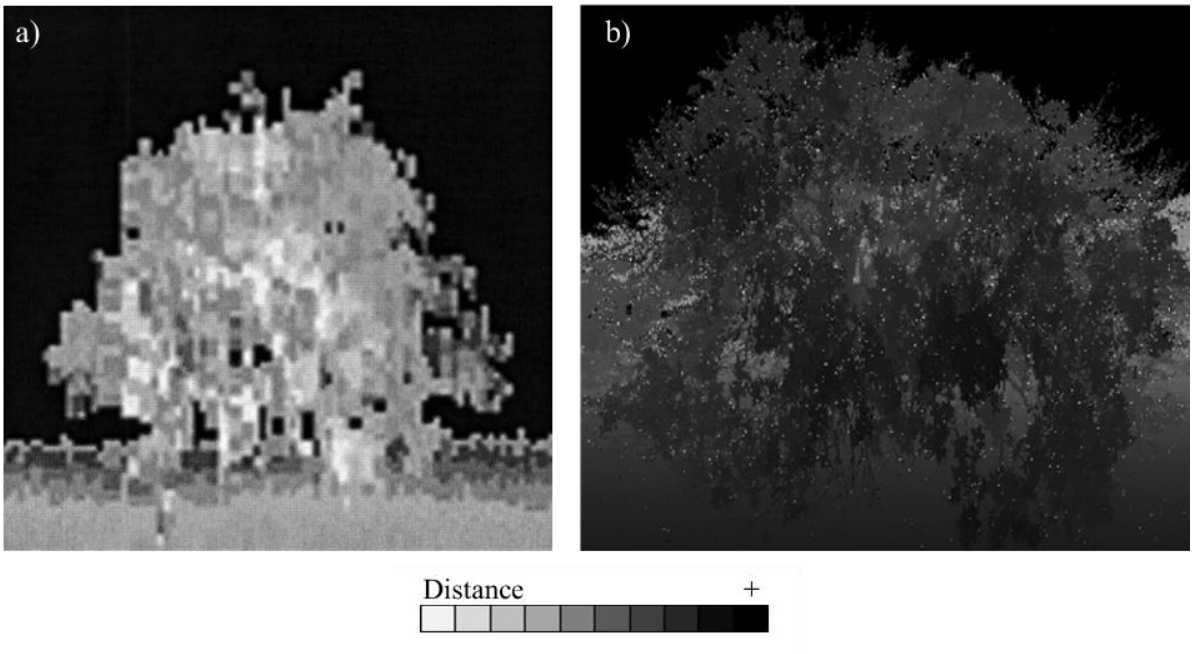

Figure 2.4: Transformed LiDAR data into a distance image; adapted from Tumbo et al. (2002) and Wei and Salyani (2005) (b)

The most recent LiDAR studies applied to citrus conducted in Florida were carried out by Lee and Ehsani (2008, 2009). After analyzing several performance aspects of two commercial laser sensors the authors proposed a data acquisition and new processing method for quantifying tree height, width, canopy surface area and volume. The canopy volume was computed for vertical sections of the tree. A similar example of canopy volume computation is shown in Figure 2.3 b. They got an error against manual measurements of canopy volume of 5.9 %.

While research in Florida have advanced significantly the ranging sensor technology, similar studies were conducted in Spain, but mostly with other tree crops besides citrus. Several works have developed and demonstrated ultrasonic ranging systems for spraying control in different tree crops. Solanelles et al. (2006) got 70%, 28% and 39% savings of plant protection products in olive, pear and apple groves, respectively, when using the variable rate application guided by the ultrasonic sensors. Using a similar prototype sprayer, Gil et al. (2007) and Llorens et al. (2010) reported almost 60% savings of input consumption in vineyards. Figure 2.5 shows the analysis used by Escolà et al. (2013) and Gil et al. (2013) to estimate input savings by variable rate spraying. Considering that there is an optimal application coefficient based on the canopy volume (in Figure 2.5, 0.12 L m^{-3}), it is noticeable that sensor-based variable rate applications can provide closer application rates to the objective than the conventional application (notice that, in the given example, the conventional application is based on the maximum canopy volume). It is also perceived that even in variable rate applications the machine does not perfectly follow the objective rate, especially in small size canopies.

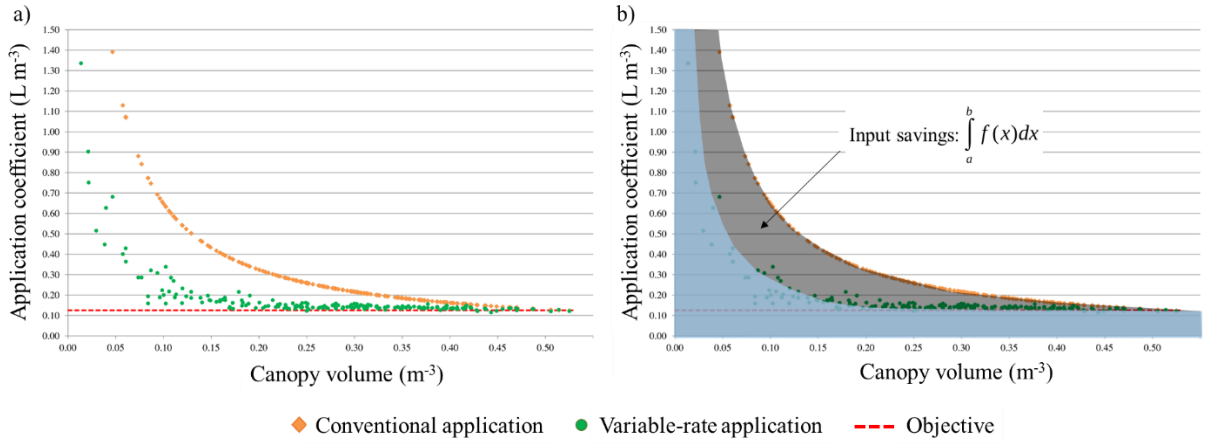

Figure 2.5: Application coefficient (L m^{-3}) in different canopy sizes by constant and variable rate spraying, adapted from Escolà et al. (2013) (a) and input savings estimation, adapted from Escolà et al. (2013) and Gil et al. (2013) (b)

This prototype used in vineyards was described and evaluated by Gil et al. (2013) (Figure 2.6). The spraying system was composed by three ultrasonic sensors and three nozzles which were controlled independently by solenoid valves. The flow rate was proportional to the canopy volume estimated by the sensors. The authors found that the accuracy of ultrasonic sensors was considered sufficient to estimate canopy structures and guide variable rate sprayings. Jeon et al. (2011), evaluating a similar system, also attested that ultrasonic sensor were robust enough for field operation. However, as similar studies from Florida (ZAMAN; SCHUMANN; HOSTLER, 2007; LEE; EHSANI, 2009), Gil et al. (2013) pointed to some challenges to be overcomed such as the error from deviating the driving path from the centerline between two rows and technical limitation of the sensors and solenoid valves. Escolà et al. (2011) showed that ultrasonic sensors might lose accuracy when mounted too close together due to interference effect between the units when there is not synchronization in their operation.

In order to deal with some of these issues and evolve the earlier prototypes, a new prototype sprayer was later designed with a LiDAR sensor (ESCOLÀ et al., 2013). The laser scanning enabled a more accurate estimation of canopy structures. The authors also reported a strong relationship between intended and sprayed flow rates (R^2 = 0.93). Chen, Zhu and Ozkan (2012) also instrumented a sprayer with a LiDAR scanning system where the application rate was given by the estimated tree height, width and foliage density. The spraying nozzles were also controlled by solenoid valves, which got sufficient response time for variable rate applications. Llorens et al. (2011) estimating crop geometrical parameters on vineyard, found the LiDAR system to be much more powerful and accurate than the ultrasonic sensors.

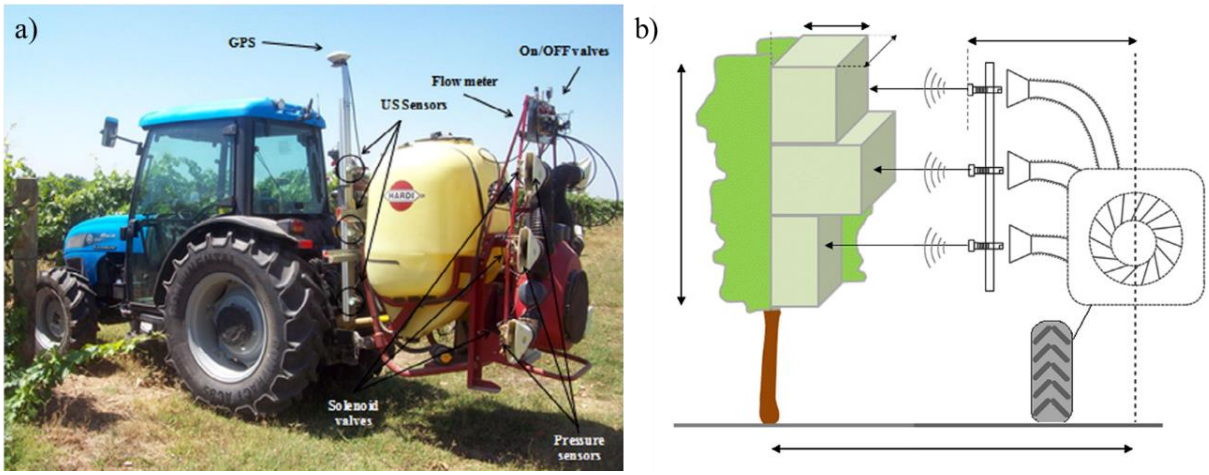

Figure 2.6: Prototype sprayer with ultrasonic measuring system (a) and scheme of ultrasonic estimation of canopy volume (arrows indicate the distances required for canopy volume estimation) (b), adapted from Gil et al. (2013)

Once the machine control and automation got fairly resolved, and as the LiDAR technology gained attention from researchers (ROSELL and SANZ, 2012), a new study line appeared towards the high accurate 3D characterization of tree canopies. An approach for transforming and processing LiDAR data from MTLS systems was presented in Spain which worked with actual 3D point cloud generation and 3D modeling (ROSELL et al., 2009a) (Figure 2.7). This new method permitted actual 3D visualization of the data and the creation of structures over the laser beam impacts, which could retrieve volume information. The capability of generating 3D models of tree crops from LiDAR scanning using the point cloud approach was attested in laboratory (KEIGHTLEY; BAWDEN, 2010; SANZ et al., 2011b), in field conditions (MOORTHY et al., 2011) and also virtually through simulation software (MÉNDEZ et al., 2012, 2013).

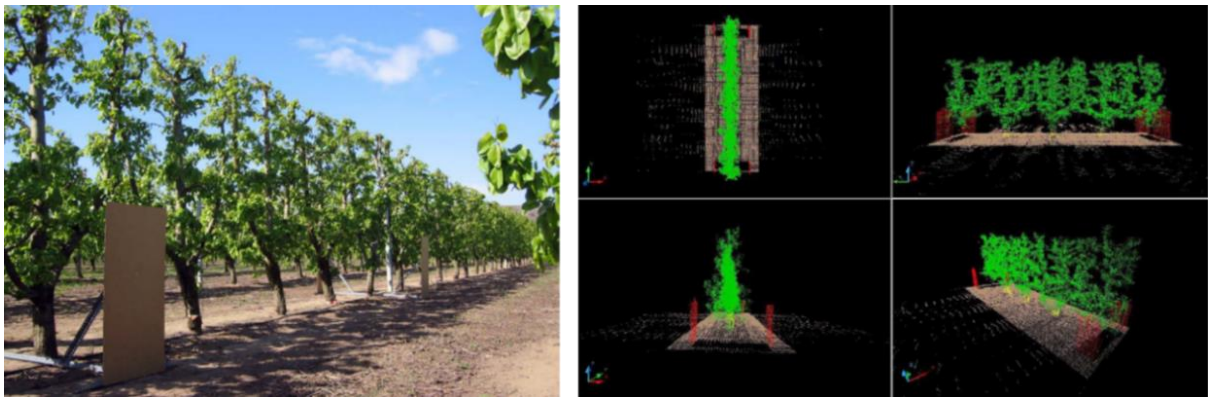

Figure 2.7: 3D point cloud generated by MTLS in a pear orchard; adapted from Rosell et al. (2009a)

The reconstruction of the target's surface based on the obtained laser points was a challenge explored for several fruit and forest crops. Highly accurate reconstruction models from dense point clouds were presented for obtaining wood volume and other forestry applications (RAUMONEN et al., 2013; DELAGRANGE; JAUVIN; ROCHON, 2014; HACKENBERG et al., 2014, 2015; MÉNDEZ et al., 2014). These studies focused on the modeling of trunks and small branches of the trees (Figure 2.8). The surface reconstructions based on involucre objects (hull-based approach) were also reported for cherry (HACKENBERG et al., 2015), olive (AUAT CHEEIN; GUIVANT, 2014), pear and apple trees (AUAT CHEEIN et al., 2015; ROSELL et al., 2009b) (Figure 2.9). Taking

the potential use of LiDAR 3D modeling as a possible new reference for canopy structures, other studies suggested new dendrometry methods for computing tree volume (VELÁZQUEZ-MARTÍ et al., 2012; XU et al., 2013; MIRANDA-FUENTES et al., 2015).

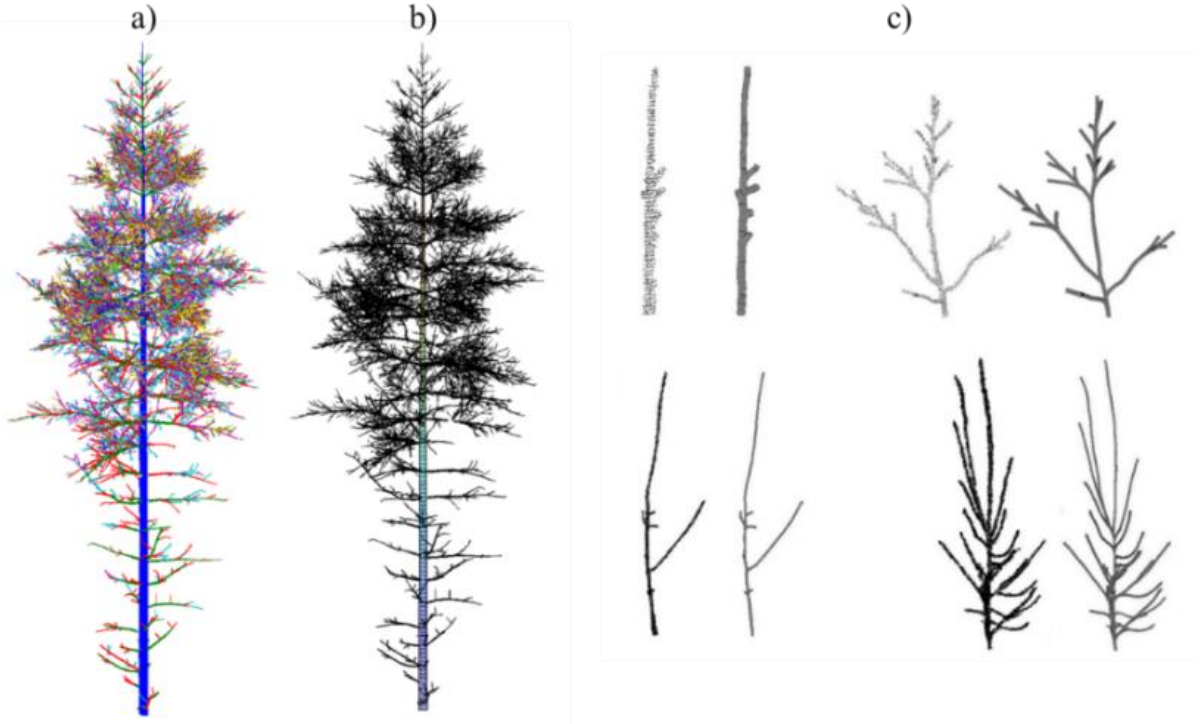

Figure 2.8: Reconstruction of tree's structures (b) from dense point cloud (a); in each pair of images, the right hand image represents the reconstructed surface from the point cloud (left hand image) (c), adapted from Delagrange, Jauvin and Rochon (2014)

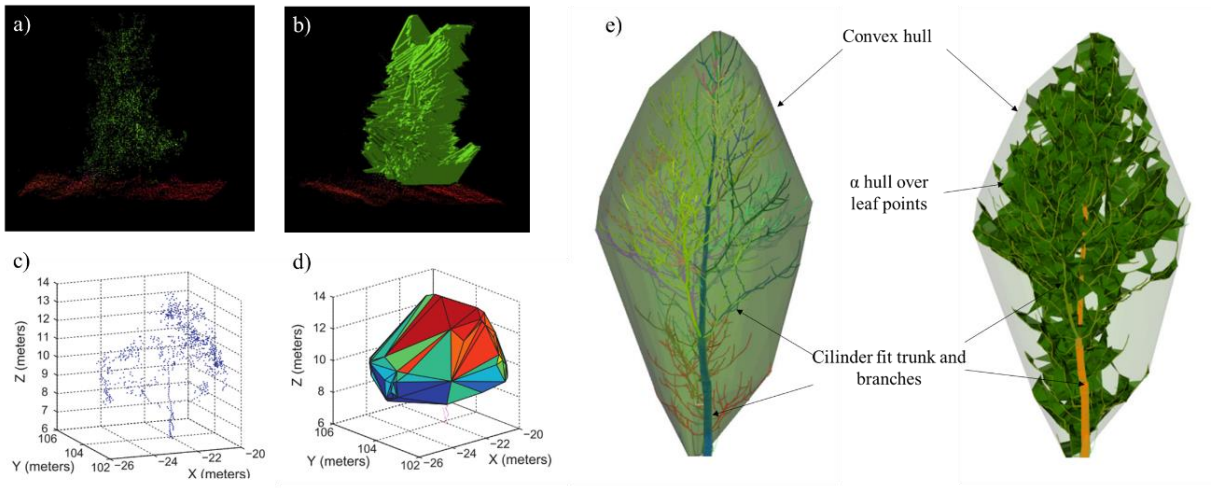

Figure 2.9: Reconstruction algorithms applied over 3D point clouds; hull structure (b) created over sections of a point cloud from an apple tree (a), adapted from Rosell et al. (2009b); convex-hull (d) applied over point cloud from an olive tree (c)

The 3D modeling itself does not reach its purpose if relevant agronomical parameters are not retrieved from it. For that matter, several research developed different algorithms for extracting parameters of vineyards and other fruit trees in Spain. Some reported parameters were tree height, width, volume, tree area index (TAI), leaf area index (LAI), and leaf wall area (LWA), leaf area density (LAD) and others. Canopy volume calculated from LiDAR

and the leaf area was well correlated in apple, pears and vineyard (SANZ et al., 2013). Sanz et al. (2011a), testing a LiDAR sensor in laboratory conditions, got a good correlation ($R^2 = 0.89$) between the number of impacts of the laser beam and the leaf area of a ficus tree (*Ficus benjamina*). The LAI, which is one of the most widely used index to characterize grapevines vigour, was well estimated using the TAI from LiDAR scanning ($R^2 = 0.91$, in ROSELL et al. 2009b and $R^2 = 0.92$, in ARNÓ et al. 2013). The TAI, originally proposed by Walklate et al. (2002), uses the probability of the laser beam transmission trough the vegetation to estimate crop area. While these studies employed LiDAR scanning from the side of the tree rows, Pforte, Selbeck and Hensel (2012) tested the scanning from the top of the trees in a plum grove in Germany. They compared the results from the laser scanning with a NIR (near infrared) image analysis. Correlations between crop coverage and the leaf area using the LiDAR system yielded better results ($R^2 = 0.86$) than the image approach.

Besides the processing of data in order to get relevant tree parameters, other studies focused on evaluating some aspects of the laser data acquisition method. Arnó et al. (2015) evaluated the influence of the scanned side of the row in MTLS in vineyards. They found that, for mapping purposes, the LAI could be estimated from only one side of the row, increasing the efficiency of field operation. The specific row length for accurately estimating LAI from MTLS was also recommended by Arnó, Escolà and Rosell (2016). In order to produce a reliable map of LAI in vineyards, these measurements do not need to be taken continuously (DEL-MORAL-MARTÍNEZ et al., 2016). The discontinuous use of MTLS following a specific sampling scheme is a viable option to overcome difficulties of dealing with large amounts of data from the laser sensor.

Regarding the use of GNSS (*Global Navigation Satellite System*) in laser scanning, besides enabling the mapping of the measured parameter it solves many problems related with the error of the laser beam positioning from readings without a GNSS reference. As shown in Figure 2.6, the estimation of the canopy boundaries, by either laser or ultrasonic measurements, was usually given based on the distance of the sensor from the central line of the row, in other words, the sensor must be kept at a constant distance from the central tree line. Therefore, the vehicle must move along the row in a perfect parallel track from the row axis. When plotting a point cloud from a LiDAR scanning in that acquisition system, all points have actually a relative position to the center of the sensor. As pointed by Lee and Ehsani (2009) and Pallejà et al. (2010) any deviation of the vehicle from the centerline of the alley is transmitted to the 3D positioning of the laser impacts resulting in errors on the final estimated parameter of the trees. When a high accuracy GNSS receiver is attached and synchronized with the acquisition system, the position of the laser impacts can be given relatively to a real geographical positioning of the sensor, therefore the vehicle does not need to follow a predefined track. Besides, the geographical positioning of the point cloud permits the matching of the two scanned sides of the rows because the points follow the same positioning reference. Figure 2.7 shows a point cloud from two independent non-georeferenced scanning of a pear grove, one for each side of the row. The carton boards viewed in the picture were actually used as references to match the point clouds from each side. Del-Moral-Martínez et al. (2015) gave a detailed description on how to attribute the GNSS coordinates to each impact of the laser.

Another device that can minimize positioning errors of the laser impacts is an inertial measurement unit (IMU). Irregularities of the terrain during the scanning can cause deviations of the angular orientation of sensor (PALLEJÀ et al., 2010). The IMU can help correcting such positioning error. In the early investigation of LiDAR scanning in tree crops, the laser sensor was commonly used without any additional sensor. Later on, the IMU was reported in some studies (LEE; EHSANI, 2009), and most recently the IMU and high accuracy GNSS positioning were reported (GIL et al., 2014; DEL-MORAL-MARTÍNEZ et al., 2015, 2016).

In the reviewed material it was noticed that, although research over the ranging technology aimed the site-specific management, the actual maps of canopy volume, LAI or other parameters were rarely shown for the scanned groves (maps found in the reviewed material are shown in Figures 2.10 and 2.11). In fact, many of the studies were conducted in small plots and without georreferencing. The map of the measured attribute is after all probably the main information for precision agriculture systems.

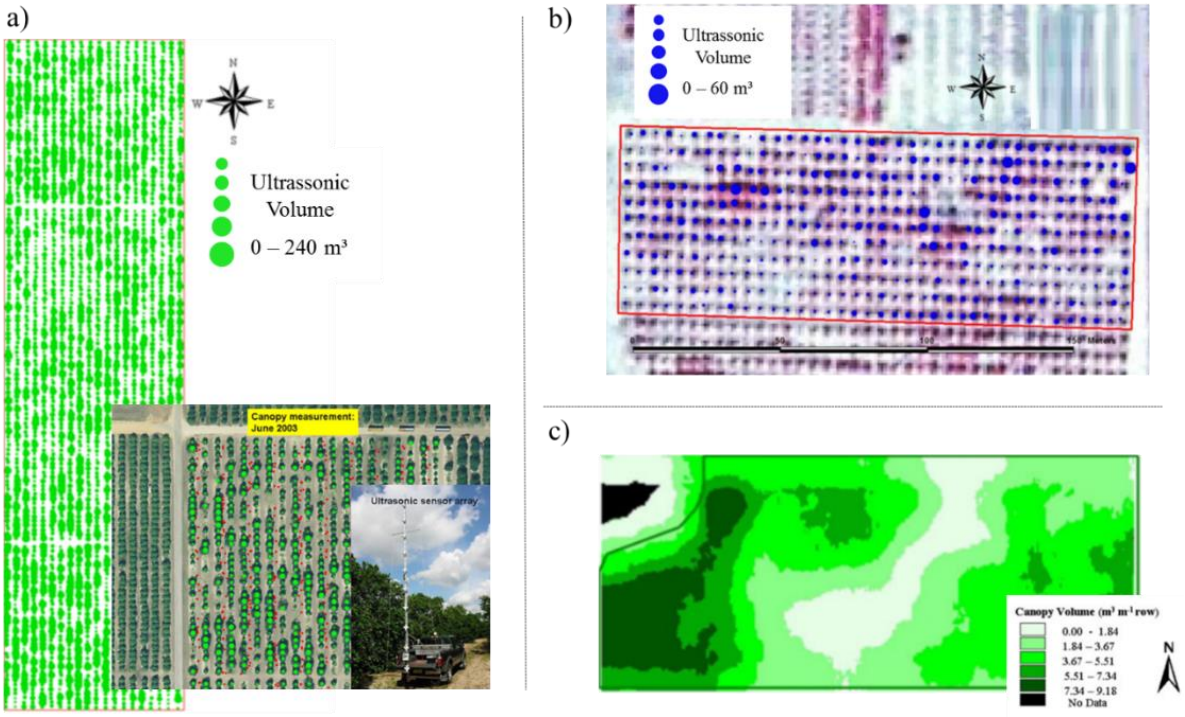

Figure 2.10: Citrus canopy volume maps by ultrasonic sensor; adapted from Zaman, Schumann and Miller (2005) and Schumann et al. (2006a) (a), Schumann and Zaman (2005) (b) and Mann, Schumann and Obreza (2010) (c)

Citrus canopy volume maps were shown in studies from Florida, which used ultrasonic measuring systems. Schumann and Zaman (2005) presented a map of citrus canopy volume for a 1 ha grove to validate the acquisition system. This system was later used in a 17 ha commercial grove presented in works of Zaman, Schumann and Miller (2005), Zaman and Schumann (2005), Schumann et al. (2006a, 2006b) and Zaman, Schumann and Hostler (2006) (Figure 2.10). Mann, Schumann and Obreza (2010) combined a canopy volume map from ultrasonic measurements with yield, NDVI (*normalized difference vegetation index*) and other maps to produce management zones in a 10 ha citrus grove. They found visual resemblance between the maps of canopy volume, yield and NDVI. In Spain, maps of LAI in vineyard were shown by Gil et al. (2014) recommending regions in the field for different management. Canopy volume maps of olive trees (ESCOLÀ et al. 2015) were obtained in different dates in a 1 ha grove. The authors estimated the growth rate of the trees during one season (Figure 2.11 b). These maps were obtained using a georeferenced MTLS system.

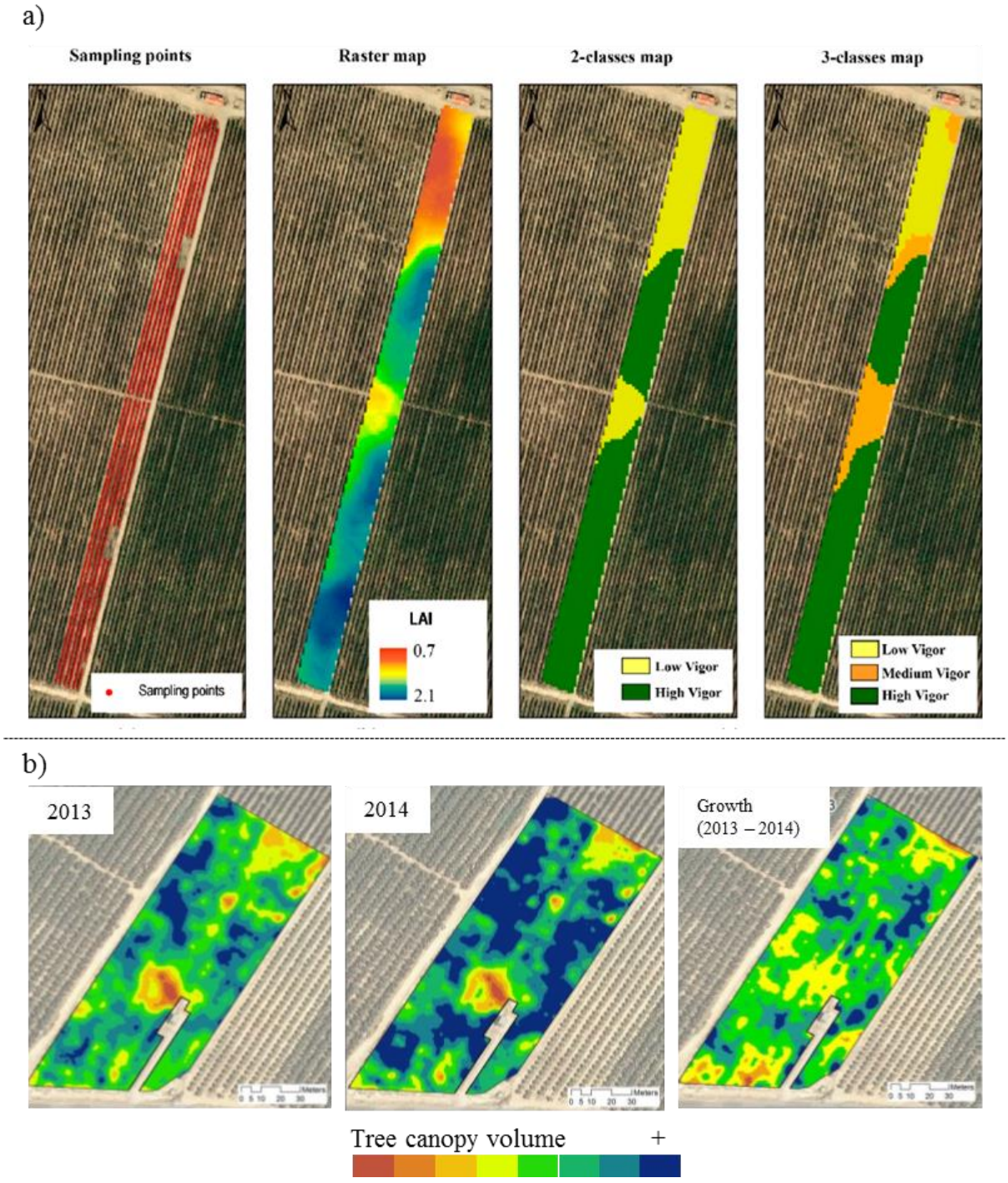

Figure 2.11: Maps of LAI in vineyard (a) adapted from Gil et al. (2014) and canopy volume in an olive grove (b) adapted from Escolà et al. (2015)

References

ARNÓ, J.; ESCOLÀ, A.; MASIP, J.; ROSELL, J. R. Influence of the scanned side of the row in terrestrial laser sensor applications in vineyards: practical consequences. **Precision Agriculture**, Dordrecht, v. 16, n. 2, p. 119–128, 2015.

ARNÓ, J.; ESCOLÀ, A.; ROSELL, J. R. Setting the optimal length to be scanned in rows of vines by using mobile terrestrial laser scanners. **Precision Agriculture**, Dordrecht, online, 2016.

ARNÓ, J.; ESCOLÀ, A.; VALLÈS, J. M.; LLORENS, J.; SANZ, R.; MASIP, J.; PALACÍN, J.; ROSELL, J. R. Leaf area index estimation in vineyards using a ground-based LiDAR scanner. **Precision Agriculture**, Dordrecht, v. 14, n. 3, p. 290–306, 4 dez. 2013.

AUAT CHEEIN, F. A.; GUIVANT, J. SLAM-based incremental convex hull processing approach for treetop volume estimation. **Computers and Electronics in Agriculture**, Amsterdam, v. 102, p. 19–30, mar. 2014.

AUAT CHEEIN, F. A.; GUIVANT, J. SANZ, R.; ESCOLÀ, A.; YANDÚN, F.; TORRES-TORRITI, M.; ROSELL, J. R. Real-time approaches for characterization of fully and partially scanned canopies in groves. **Computers and Electronics in Agriculture**, Amsterdam, v. 118, p. 361-371, 2015.

CHEN, Y.; ZHU, H.; OZKAN, H. E. Development of a variable-rate sprayer with laser scanning sensor to synchronize spray outputs to tree structures. **Transactions Of The Asabe**, St. Joseph, v. 55, n. 3, p. 773–781, 2012.

CROSS, J. V.; WALKLATE, P. J.; MURRAY, R. A.; RICHARDSON, G. M. Spray deposits and losses in different sized apple trees from an axial fan orchard sprayer: 2 . Effects of spray quality. **Crop Protection**, Guildford, v. 20, p. 333 – 343, 2001a.

CROSS, J. V.; WALKLATE, P. J.; MURRAY, R. A.; RICHARDSON, G. M. Spray deposits and losses in different sized apple trees from an axial fan orchard sprayer: 3 . Effects of spray quality. **Crop Protection**, Guildford, v. 22, p. 381–394, 2003.

CROSS, J.; WALKLATE, P. .; MURRAY, R. .; RICHARDSON, G. . Spray deposits and losses in different sized apple trees from an axial fan orchard sprayer: 1. Effects of air volumetric flow rate. **Crop Protection**, Guildford, v. 20, n. 2, p. 13–30, 2001b.

DELAGRANGE, S.; JAUVIN, C.; ROCHON, P. PypeTree: a tool for reconstructing tree perennial tissues from point clouds. **Sensors**, New York, v. 14, n. 3, p. 4271–4289, 2014.

DEL-MORAL-MARTÍNEZ, I.; ARNÓ, J.; ESCOLÀ, A.; SANZ, R.; MASIP-VILALTA, J.; COMPANY-MESSA, J.; ROSELL, J. R. Georeferenced Scanning System to Estimate the LeafWall Area in Tree Crops. **Sensors**, New York, v. 15, n. 4, p. 8382–8405, 2015.

DEL-MORAL-MARTÍNEZ, I.; ROSELL, J. R.; COMPANY, J.; SANZ, R.; ESCOLÀ, A.; MASIP, J.; MARTÍNEZ-CASASNOVAS, J.; ARNÓ, J. Mapping Vineyard Leaf Area Using Mobile Terrestrial Laser Scanners: Should Rows be Scanned On-the-Go or Discontinuously Sampled? **Sensors**, New York, v. 16, n. 1, p. 119, 2016.

DWORAK, V.; SELBECK, J.; EHLERT, D. Ranging sensors for vehicle-based measurement of crop stand and orchard parameters: a review. **Transactions Of The Asabe**, St. Joseph, v. 54, n. 4, p. 1497–1510, 2011.

ESCOLÀ, A.; PLANAS, S.; ROSELL, J. R.; POMAR, J.; CAMP, F.; SOLANELLES, F.; GRACIA, F.; LLORENS, J.; GIL, E. Performance of an ultrasonic ranging sensor in apple tree canopies. **Sensors**, New York, v. 11, n. 3, p. 2459–77, 2011.

ESCOLÀ, A.; ROSELL, J. R.; PLANAS, S.; GIL, E.; POMAR, J.; CAMP, F.; LLORENS, J.; SOLANELLES, F. Variable rate sprayer. Part 1 – Orchard prototype: Design, implementation and validation. **Computers and Electronics in Agriculture**, Amsterdam, v. 95, p. 122–135, 2013.

ESCOLÀ, A. MARTINEZ-CASASNOVAS, J. A.; RUFAT, J. ARBONÉS, A.; SANZ, R.; SEBÉ, F.; ARNÓ, J.; MASIP, J.; PASCUAL, M.; GREGORIO, E.; RIBES-DASI, M.; VILLAR, J. M.; ROSELL-POLO, J. R. A monile terrestrial laser scanner for tree crops: point cloud generation, information, extraction and validation in an intensive olive orchard. In: EUROPEAN CONFERENCE ON PRECISION AGRICULTURE, 10., 2015, Tel Aviv. **Proceedings**... Wageningen: Wageningen Academic Publishers, 2015. p. 337 - 344.

GIL, E.; ARNÓ, J.; LLORENS, J.; SANZ, R.; LLOP, J.; ROSELL, J. R.; GALLART, M.; ESCOLÀ, A. Advanced Technologies for the Improvement of Spray Application Techniques in Spanish Viticulture: An Overview. **Sensors**, New York, v. 14, n. 1, p. 691–708, 2014.

GIL, E.; ESCOLÀ, A.; ROSELL, J. R.; PLANAS, S.; VAL, L. Variable rate application of plant protection products in vineyard using ultrasonic sensors. **Crop Protection**, Guildford, v. 26, n. 8, p. 1287–1297, 2007.

GIL, E.; LLORENS, J.; LLOP, J.; FÀBREGAS, X.; ESCOLÀ, A.; ROSELL, J. R. Variable rate sprayer. Part 2 – Vineyard prototype: Design, implementation, and validation. **Computers and Electronics in Agriculture**, Amsterdam, v. 95, p. 136–150, 2013.

GILES, D. K.; DELWICHE, M. J.; DODD, R. B. Electronic measurement of tree canopy volume. **Transactions Of The Asae**, St. Joseph, v. 31, n. 1, p. 264–273, 1988.

GILES, D. K.; DELWICHE, M. J.; DODD, R. B. Sprayer control by sensing orchard crop characteristics: Orchard architecture and spray liquid savings. **Journal of Agricultural Engineering Research**, London, v. 43, p. 271–289, 1989.

HACKENBERG, J.; MORHART, C.; SHEPPARD, J.; SPIECKER, H.; DISNEY, M. Highly accurate tree models derived from terrestrial laser scan data: A method description. **Forests**, Basel, v. 5, n. 5, p. 1069–1105, 2014.

HACKENBERG, J.; SPIECKER, H.; CALDERS, K.; DISNEY, M.; RAUMONEN, P. SimpleTree - An efficient open source tool to build tree models from TLS clouds. **Forests**, Basel, v. 6, n. 11, p. 4245–4294, 2015.

JEON, H. Y.; ZHU, H.; DERKSEN, R.; OZKAN, E.; KRAUSE, C. Evaluation of ultrasonic sensor for variable-rate spray applications. **Computers and Electronics in Agriculture**, Amsterdam, v. 75, n. 1, p. 213–221, 2011.

KEIGHTLEY, K. E.; BAWDEN, G. W. 3D volumetric modeling of grapevine biomass using Tripod LiDAR. **Computers and Electronics in Agriculture**, Amsterdam, v. 74, n. 2, p. 305–312, 2010.

LEE, K. H.; EHSANI, R. Comparison of two 2D laser scanners for sensing object distances, shapes and surface patterns. **Computers and Electronics in Agriculture**, Amsterdam, v. 60, n. 2, p. 250–262, 2008.

LEE, K. H.; EHSANI, R. A laser scanner based measurement system for quantification of citrus tree geometric. **Applied Engineering in Agriculture**, St. Joseph, v. 25, n. 5, p. 777–788, 2009.

LIN, Y. LiDAR: An important tool for next-generation phenotyping technology of high potential for plant phenomics? **Computers and Electronics in Agriculture**, Amsterdam, v. 119, p. 61–73, 2015.

LLORENS, J.; GIL, E.; LLOP, J.; ESCOLÀ, A. Variable rate dosing in precision viticulture: Use of electronic devices to improve application efficiency. **Crop Protection**, Guildford, v. 29, n. 3, p. 239–248, 2010.

LLORENS, J.; GIL, E.; LLOP, J.; ESCOLÀ, A. Ultrasonic and LIDAR sensors for electronic canopy characterization in vineyards: advances to improve pesticide application methods. **Sensors**, New York, v. 11, n. 2, p. 2177–94, 2011.

MAGHSOUDI, H.; MINAEI, S.; GHOBADIAN, B.; MASOUDI, H. Ultrasonic sensing of pistachio canopy for low-volume precision spraying. **Computers and Electronics in Agriculture**, Amsterdam, v. 112, p. 149–160, 2015.

MANN, K. K.; SCHUMANN, A. W.; OBREZA, T. a. Delineating productivity zones in a citrus grove using citrus production, tree growth and temporally stable soil data. **Precision Agriculture**, Dordrecht, v. 12, n. 4, p. 457–472, 2010.

MÉNDEZ, V.; CATALÁN, H.; ROSELL, J. R.; ARNÓ, J.; SANZ, R. LiDAR simulation in modelled orchards to optimise the use of terrestrial laser scanners and derived vegetative measures. **Biosystems Engineering**, London, v. 115, n. 1, p. 7–19, 2013.

MÉNDEZ, V.; CATALÁN, H.; ROSELL, J. R.; ARNÓ, J.; SANZ, R.; TARQUIS, A. SIMLIDAR – Simulation of LIDAR performance in artificially simulated orchards. **Biosystems Engineering**, London, v. 111, n. 1, p. 72–82, 2012.

MÉNDEZ, V.; ROSELL, J. R.; SANZ, R.; ESCOLÀ, A.; CATALÁN, H. Deciduous tree reconstruction algorithm based on cylinder fitting from mobile terrestrial laser scanned point clouds. **Biosystems Engineering**, London, v. 124, p. 78–88, 2014.

MIRANDA-FUENTES, A.; LLORENS, J.; GAMARRA-DIEZMA, J. L.; GIL-RIBES, J. A.; GIL, E. Towards an optimized method of olive tree crown volume measurement. **Sensors**, New York, v. 15, n. 2, p. 3672–3687, 2015.

MOORTHY, I.; MILLER, J. R.; BERNI, J. A. J.; ZARCO-TEJADA, P.; HU, B.; CHEN, J. Field characterization of olive (Olea europaea L.) tree crown architecture using terrestrial laser scanning data. **Agricultural and Forest Meteorology**, Amsterdam, v. 151, n. 2, p. 204–214, 2011.

OSTERMAN, A.; GODEŠA, T.; HOČEVAR, M.; ŠIROK, B.; STOPAR, M. Real-time positioning algorithm for variable-geometry air-assisted orchard sprayer. **Computers and Electronics in Agriculture**, Amsterdam, v. 98, p. 175–182, 2013.

PALLEJÀ, T.; TRESANCHEZ, M.; TEIXIDO, M.; SANZ, R.; ROSELL, J. R.; PALACÍN, J. Sensitivity of tree volume measurement to trajectory errors from a terrestrial LIDAR scanner. **Agricultural and Forest Meteorology**, Amsterdam, v. 150, n. 11, p. 1420–1427, 2010.

PFORTE, F.; SELBECK, J.; HENSEL, O. Comparison of two different measurement techniques for automated determination of plum tree canopy cover. **Biosystems Engineering**, London, v. 113, n. 4, p. 325–333, 2012.

RAUMONEN, P.; KAASALAINEN, M.; ÅKERBLOM, M.; KAASALAINEN, S.; KAARTINEN, H.; VASTARANTA, M.; HOLOPAINEN, M.; DISNEY, M.; LEWIS, P. Fast Automatic Precision Tree Models from Terrestrial Laser Scanner Data. **Remote Sensing**, Basingstoke, v. 5, n. 2, p. 491–520, 2013.

ROSELL, J. R.; LLORENS, J.; SANZ, R.; ARNÓ, J.; RIBES-DASI, M.; MASIP, J.; ESCOLÀ, A.; CAMP, F.; SOLANELLES, F.; GRÀCIA, F.; GIL, E.; VAL, L.; PLANAS, S.; PALACÍN, J. Obtaining the three-dimensional structure of tree orchards from remote 2D terrestrial LIDAR scanning. **Agricultural and Forest Meteorology**, Amsterdam, v. 149, n. 9, p. 1505–1515, 2009a.

ROSELL, J. R.; SANZ, R. A review of methods and applications of the geometric characterization of tree crops in agricultural activities. **Computers and Electronics in Agriculture**, Amsterdam, v. 81, p. 124–141, fev. 2012.

ROSELL, J. R.; SANZ, R.; LLORENS, J.; ARNÓ, J.; ESCOLÀ, A.; RIBES-DASI, M.; MASIP, J.; CAMP, F.; GRÀCIA, F.; SOLANELLES, F.; PALLEJÀ, T.; VAL, L.; PLANAS, S.; GIL, E.; PALACÍN, J. A tractor-mounted scanning LIDAR for the non-destructive measurement of vegetative volume and surface area of tree-row plantations: A comparison with conventional destructive measurements. **Biosystems Engineering**, London, v. 102, n. 2, p. 128–134, 2009b.

SANZ, R.; LLORENS, J.; ESCOLÀ, A.; ARNÓ, J.; RIBES, M.; MASIP, J.; CAMP, F.; GRÀCIA, F.; SOLANELLES, F.; PLANAS, S.; PALLEJÀ, T.; PALACÍN, J.; GREGORIO, E.; MARTÍNEZ, I.; ROSELL, J. R. Innovative LIDAR 3D Dynamic Measurement System to estimate fruit-tree leaf area. **Sensors**, New York, v. 11, n. 6, p. 5769–91, 2011a.

SANZ, R.; LLORENS, J.; ROSELL, J. R.; GREGORIO, E.; PALACÍN, J. Characterisation of the LMS200 laser beam under the influence of blockage surfaces. Influence on 3D scanning of tree orchards. **Sensors**, New York, v. 11, n. 3, p. 2751–72, 2011b.

SANZ, R.; ROSELL, J. R.; LLORENS, J.; GIL, E.; PLANAS, S. Relationship between tree row LIDAR-volume and leaf area density for fruit orchards and vineyards obtained with a LIDAR 3D Dynamic Measurement System. **Agricultural and Forest Meteorology**, Amsterdam, v. 171-172, p. 153–162. 2013.

SCHUMANN, A. W.; HOSTLER, K. H.; BUCHANON, S.; ZAMAN, Q. U. Relating citrus canopy size and yield to precision fertilization. **Proceedings of Florida State Horticultural Society**, Tallahassee, v. 119, p. 148–154, 2006a.

SCHUMANN, A. W.; MILLER, W. M.; ZAMAN, Q. U.; HOSTLER, K. H.; BUCHANON, S.; CUGATI, S. A. Variable rate granular fertilization of citrus groves: Spreader performance with single-tree prescription zones. **Applied Engineering in Agriculture**, St. Joseph, v. 22, n. 1, p. 19–24, 2006b.

SCHUMANN, A. W.; ZAMAN, Q. U. Software development for real-time ultrasonic mapping of tree canopy size. **Computers and Electronics in Agriculture**, Amsterdam, v. 47, n. 1, p. 25–40, 2005.

SOLANELLES, F.; ESCOLÀ, A.; PLANAS, S.; ROSELL, J. R.; CAMP, F.; GRÀCIA, F. An electronic control system for pesticide application proportional to the canopy width of tree crops. **Biosystems Engineering**, London, v. 95, n. 4, p. 473–481, 2006.

TUMBO, S. D.; SALYANI, M.; WHITNEY, J. D.; WHEATON, T. A.; MILLER, W. M. Investigation of laser and ultrasonic ranging sensors for measurements of citrus canopy volume. **Applied Engineering in Agriculture**, St. Joseph, v. 18, n. 3, p. 367–372, 2002.

VELÁZQUEZ-MARTÍ, B.; ESTORNELL, J.; LÓPEZ-CORTÉS, I.; MARTÍ-GAVILÁ, J. Calculation of biomass volume of citrus trees from an adapted dendrometry. **Biosystems Engineering**, London, v. 112, n. 4, p. 285–292, 2012.

WALKLATE, P. J. A laser scanning instrument for measuring crop geometry. **Agricultural and Forest Meteorology**, Amsterdam, v. 46, p. 275–284, 1989.

WALKLATE, P. J.; CROSS, J. V. An examination of Leaf-Wall-Area dose expression. **Crop Protection**, Guildford, v. 35, p. 132–134, 2012.

WALKLATE, P. J.; CROSS, J. V. Regulated dose adjustment of commercial orchard spraying products. **Crop Protection**, Guildford, v. 54, p. 65–73, 2013.

WALKLATE, P. J.; CROSS, J. V.; PERGHER, G. Support system for efficient dosage of orchard and vineyard spraying products. **Computers and Electronics in Agriculture**, Amsterdam, v. 75, n. 2, p. 355–362, 2011.

WALKLATE, P. J.; CROSS, J. V.; RICHARDSON, G. M.; BAKER, D. E. Optimising the adjustment of label-recommended dose rate for orchard spraying. **Crop Protection**, Guildford, v. 25, n. 10, p. 1080–1086, 2006.

WALKLATE, P. J.; CROSS, J. V.; RICHARDSON, G. M.; MURRAY, R. A.; BAKER, D. E. Comparison of different spray volume deposition models using LIDAR measurements of apple orchards. **Biosystems Engineering**, London, v. 82, n. 3, p. 253–267, 2002.

WALKLATE, P. J.; RICHARDSON, G. M.; BAKER, D. E.; RICHARDS, P. A.; CROSS, J. V. Short-range LIDAR measurement of top fruit tree canopies for pesticide applications research in the UK. (R. M. Narayanan, J. E. Kalshoven, Jr., Eds.) In: ADVANCES IN LASER REMOTE SENSING FOR TERRESTRIAL AND OCEANOGRAPHIC APPLICATIONS, Orlando. **Proceedings**... 1997. p. 143 - 151.

WEI, J.; SALYANI, M. Development of a laser scanner for measuring tree canopy characteristics: phase 1. Prototype development. **Transactions Of The Asabe**, St. Josehp, v. 47, n. 6, p. 2101–2108, 2004.

WEI, J.; SALYANI, M. Development of a laser scanner for measuring tree canopy characteristics: Phase 2. Foliage density measurement. **Transactions Of The Asabe**, St. Joseph, v. 48, n. 4, p. 1595–1602, 2005.

WHITNEY, J. D.; MILLER, W. M.; WHEATON, T. A.; SALYANI, M.; SCHUELLER, J. K. Precision farming applications in Florida citrus. **Applied Engineering in Agriculture**, St. Joseph, v. 15, n. 5, p. 399–403, 1999.

XU, W.; SU, Z.; FENG, Z.; XU, H.; JIAO, Y.; YAN, F. Comparison of conventional measurement and LiDAR-based measurement for crown structures. **Computers and Electronics in Agriculture**, Amsterdam, v. 98, p. 242–251, 2013.

ZAMAN, Q. U.; SALYANI, M. Effects of foliage density and ground speed on ultrasonic measurement of citrus tree volume. **Applied Engineering in Agriculture**, St. Joseph, v. 20, n. 2, p. 173–178, 2004.

ZAMAN, Q. U.; SCHUMANN, A. W. Performance of an ultrasonic tree volume measurement system in commercial citrus groves. **Precision Agriculture**, Dordrecht, v. 6, p. 467–480, 2005.

ZAMAN, Q. U.; SCHUMANN, A. W.; HOSTLER, H. K. Quantifying sources of error in ultrasonic measurements of citrus orchards. **Applied Engineering in Agriculture**, St. Joseph, v. 23, n. 4, p. 449–453, 2007.

ZAMAN, Q. U.; SCHUMANN, A. W.; HOSTLER, K. H. Estimation of citrus fruit yield using ultrasonically-sensed tree size. **Applied Engineering in Agriculture**, St. Joseph, v. 22, n. 1, p. 39–44, 2006.

ZAMAN, Q. U.; SCHUMANN, A. W.; MILLER, W. M. Variable rate nitrogen application in Florida citrus based on ultrasonically-sensed tree size. **Applied Engineering in Agriculture**, St. Joseph, v. 21, n. 3, p. 331–336, 2005.

3. ORANGE CROP GEOMETRY AND 3D MODELING USING A MOBILE TERRESTRIAL LASER SCANNER

ABSTRACT

Sensors based on LiDAR (*Light Detection and Ranging*) technology are sources of primary data, which, with appropriate data acquisition and processing, might produce information about geometrical attributes of tree crops. When this information is available in sufficient quantity and assigned to specific locations throughout the field, it can be used in site-specific management practices. Several research have developed acquisition and processing methods based on LiDAR sensor data for different tree crops. However, they usually apply such methods in individual trees or in small field plots. Besides, some challenges related to the data processing must be overcome. The main objective of this study was to develop a method of 3D modeling for canopy volume and height computation based on a mobile terrestrial laser scanner (MTLS) suited for large commercial orange groves. In addition, it aimed to demonstrate and compare variations over the data processing method. The data acquisition system was based on a 2D LiDAR sensor and a RTK-GNSS (*Real Time Kinematics - Global Navigation Satellite System)*. The devices were mounted on an all-terrain vehicle. The sensor faced the side of the trees colleting distance values along a vertical transect of the row. The data processing started with the construction of a georeferenced point cloud. The point cloud was subsequently filtered and segmented by classifying points into transversal sections along the row or according to individual trees (using a cluster classification). The *convex-hull* and the *alpha-shape* reconstructions algorithms were tested in order to connect the outer points of the cloud and reproduce the shape of the tree crowns. The information of canopy volume and height retrieved from each section or individual tree was used to produce canopy volume and height maps. The data acquisition and processing methods were tested in a 25 ha commercial grove in São Paulo, Brazil. The developed MTLS was robust for field application. The data processing was also efficient when dealing with large amount of data. The system was able to accurately reproduce a 3D model of the crop in the format of a georeferenced point cloud. The *alpha-shape* algorithms were able to reproduce concave structures of the canopies yielding smaller canopy volumes than the *convex-hull* algorithm. However, when applied to sections of the row, undesirable concavities were formed in the areas between each section, leading to an underestimating the total canopy volume of the trees. For that reason this algorithm was only considered suitable for treating point clouds classified by individual trees, and not by sections. The *convex-hull* algorithm overestimated the canopy volume because it was unable to reproduce concave structures. However, this effect was reduced when slicing the row into transversal sections. The canopy volume and height maps produced by two methods (cluster segmentation followed by the *alpha-shape* reconstruction or the transversal section segmentation followed by the *convex-hull* reconstruction) were similar, showing the same patterns of spatial variability. The proposed MTLS system was able to produce useful information for the site-specific management in commercial orange groves.

Keywords: laser scanner; LiDAR; 3D surface reconstruction; convex-hull; alpha-shape

3.1. Introduction

The 3D modeling of canopies has become an important research topic among precision agriculture studies, especially in tree crops. This technique provides with accurate information about canopy dimensions and foliage density, which relates to the crop development and health. Among several available techniques, the LiDAR (*Light Detection and Ranging*) scanning, either airborne or ground-based, has proven to be a viable option for modeling geometrical features of tree crops. An advantage of the terrestrial acquisition systems, often referred as "terrestrial

laser scanner" (TLS), is that the sensors can be attached to spreaders and spraying machines. Therefore, it would not require an extra operation in order to acquire the data from orchards or groves. Besides, this arrangement enables variable-rate applications on a real-time basis.

Research groups have developed and tested several TLS systems and data processing methods in different tree crops. Usually, 2D LiDAR sensors are mounted on a vehicle that moves along the alleys of the grove to vertically scan the side of the tree rows. This setting, referred as "mobile terrestrial laser scanner" (MTLS), permits the laser beam to impact the side of the rows in several points along a vertical transect, configuring a detailed profile of the trees. 3D information is formed with the combination of subsequent 2D transects as the vehicle moves along the grove alleys.

This type of MTLS was applied to citrus crops in Florida, USA, in early developments. The first studies applied relatively simple data processing techniques to compute geometrical parameters of the trees. Tumbo et al. (2002), Wei and Salyani (2004) and Lee and Ehsani (2009) used methods based on attributing local rectangular coordinates to the laser beam impacts. They achieved this considering the polar coordinates from the sensor and the vehicle movement along the side of the tree. From this 3D information, different algorithms were applied to retrieve geometrical parameters from the trees. Those authors applied their methods in the measurement of individual trees and compared that new approach with current methods based on ultrasonic sensors and manual measurements. They concluded that LiDAR scanning could provide with more accurate information of the canopies than the former available technologies.

However, due to the application of local coordinates to the laser data, the vehicle had to maintain a steady linear track parallel to the tree row in order to keep a reference position of the sensor. Those systems also did not permit a practical way of matching the two scanned sides of the trees. Thus, all geometrical computation was carried out based on the assumption that the canopies were symmetrical and only one side of the trees was scanned.

Rosell et al. (2009) also proposed and demonstrated a MTLS system in several tree crops in Catalonia, Spain. They used a similar acquisition system to the one developed in Florida, but developed innovative data processing and manipulation. After the computation of local coordinates from the raw LiDAR sensor data, they constructed point clouds, which could be treated and manipulated using *computer aided design* (CAD) software. Point clouds from the two sides of the tree row could be manually matched trough the CAD software using a reference object that was placed close to the target tree during the scanning of each side. The geometrical attributes of the canopy were also obtained using the CAD tools and modeling. This type of data processing was also reported in several other studies (ROSELL and SANZ, 2012).

A great improvement of the data acquisition and data processing was achieved when high accuracy GNSS (*Global Navigation Satellite System*) positioning systems were incorporated in MTLS methods (DEL-MORAL-MARTÍNEZ et al., 2015). The use of GNSS positioning solves most of the problems derived from the use of local coordinates to the collected data. The synchronous acquisition of LiDAR sensor and GNSS data permits each laser impact to be georeferenced and plotted in a common absolute geographical coordinate system. This system allows independent scanning (*e. g.* the scanning of the two sides of the tree row) to be accurately put together. Else, the vehicle do not need to keep a previously stablished path in order to maintain a reference position of the laser sensor.

After creating the point cloud, the 3D modeling of the canopies and the actual computation of geometrical parameters of the trees must be carried out. Along with the leaf area index (LAI), the canopy volume is one of the most important and studied parameters that can be derived from 3D modeling. The canopy height is also an important parameter but its computation algorithm is not as complex as the aforementioned parameters. In order

to compute the canopy volume, two main approaches are possible. The first is a discretization-based method, which creates a grid of small regular geometries (*e.g.* cubes or prisms) inside the point cloud structure. This approach is referred as the "occupancy grid". The second is a 3D surface reconstruction, which usually employs triangulation algorithms to connect the outer points of the cloud and create the shape of the represented object. Auat Cheein and Guivant (2014) have applied the *convex-hull* surface reconstruction to compute canopy volume of individual trees in a small olive crop. Auat Cheein et al. (2015) applied the segmented *convex-hull* and the occupancy grid approaches in a point cloud from four pear trees and over a virtual template object. Although a few drawbacks were pointed out, both approaches proved to be effective on characterizing the trees canopies.

It is noticeable that, so far, most studies have performed MTLS and 3D modeling over small field plots or over individualized trees in order to develop and test different data processing methods. The actual representation of the crop geometrical features in the format of maps, which can be used to investigate spatial variability of the entire grove and guide site-specific management, is rarely found on published research. Del-Moral-Martínez et al. (2016) created LAI maps from MTLS in vineyards approaching several options for data acquisition and processing. Escolà et al. (2015) also presented maps of canopy volume of olive trees in a 1 ha commercial grove.

The Brazilian orange groves present a great potential for MTLS application, but the data acquisition and processing methods must be developed and tested for this environment. Some relevant features of this crop worth mentioning are: Brazil is the largest world producer of oranges; this crop cover extensive areas in the country; its agribusiness has great economic and social importance; there is a high level of agronomical management and use of technology; this crop is highly demanding regarding energy and inputs; precision agriculture practices have shown a potential to optimize the use of resources and provide economical and environmental benefits (COLAÇO and MOLIN, 2016).

The research in the past few years have greatly improved the 3D modeling of tree crops based on MTLS data. However, several aspects of this technique are yet to be solved, especially for the environment of the Brazilian orange groves. As mentioned, most of the studies have not used large commercial fields in order to test the acquisition system and data processing in more realistic environment. Thus, robust and replicable methods must be designed for large fields and large data. When dealing with large data from continuous scanning, a segmentation of the data into smaller batches should be carried out prior to the 3D modeling, *e. g.* each batch representing one tree or a segment of the row. Different combinations of the type of segmentation and the 3D modeling algorithms must be tested considering different configurations of the orange trees.

3.2. Objective

The main objective of this study is to develop a method of 3D modeling for canopy volume and height computation in commercial orange groves based on a MTLS. Secondly, this study aims to demonstrate and compare several variations on the proposed method (varying the type of cloud segmentation and 3D modeling algorithm). The proposed data acquisition method and data processing must be able to reproduce the spatial variability of the trees supplying information for site-specific management of the grove.

3.3. Materials and Methods

This section is divided into two main parts. The first part is devoted to describe the MTLS system used in this study. In addition, it describes each step of the data processing, from producing a georeferenced point cloud, to modeling the canopy structures and computing the canopy volume and height.

The second part describes how this method and its variations were tested and demonstrated in laboratory and in field conditions.

3.3.1. Description of the data acquisition and processing

The method described in this study was developed to adapt to commercial orange groves in which the trees were planted in straight rows. The crowns might be touching each other along the row, closing partially or totally the gaps between plants.

The equipment and data acquisition

The LiDAR sensor used in this study was a terrestrial 2D laser scanner, model LMS 200 (Sick, Waldkirch, Germany) (Figure 3.1 a). As any LiDAR-based technology, this sensor measures the distance between its center and the nearest obstacle in a given direction. The distance is estimated based on the "time-of-flight" principle. The sensor emits a laser beam, it travels until it reaches the target and it is then reflected back to the sensor. The time between the emission and reception of the laser beam is directly related with the distance between the sensor and the target. This LiDAR sensor is classified as an eye-safe sensor (safety class 1) emitting laser light in the infrared wavelength (905 nm).

As a 2D laser scanner, this sensor calculates distances in several directions within a plane. This is achieved due to an internal rotational mirror, which orientates the laser beam along the plane. For each rotation of the mirror several distance measurements are collected in different directions. The angular range of the scan can be set to 100 or 180° (Figure 3.1 b). The angular resolution can be set to 1°, 0.5° or 0.25° (0.25° only permitted for 100° angular range). The range of the sensor can be set to 8 m or to 80 m. The distance values can be obtained with a resolution of 1 mm for a range of 8 m, or of 1 cm for range of 80 m. The specified distance error is ± 5 mm for a 8 m range.

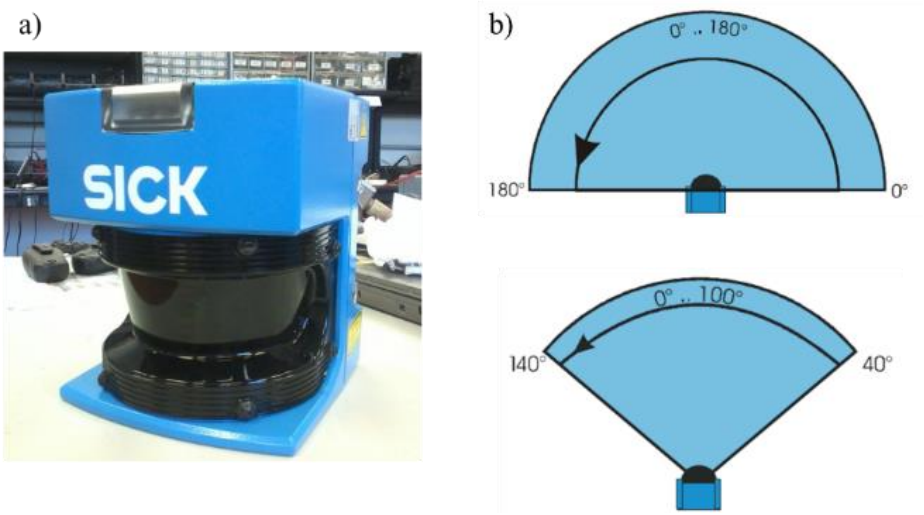

Figure 3.1: LiDAR sensor Sick, LMS 200 (a) and angular range on 2D scanning plane (b) (adapted from SICK AG., 2002)

A desktop or laptop computer must be connected to the sensor for general communication and data acquisition. By default, the communication is stablished by a serial RS 232 interface with a baud rate of 9600 bps. With this connection the maximum update rate of achieved by the sensor was around 15 Hz. However, the maximum permitted acquisition rate, 75 Hz, was achieved by configuring a 500 kbps baud rate communication through a RS 422 serial interface.

To collect data from a commercial orange grove, the LiDAR sensor and a GR3 RTK (*Real Time Kinematics*) GNSS receiver (Topcon, Tokyo, Japan) (with ±10 mm accuracy on kinematic mode) were arranged in a customized metallic structure mounted on an all-terrain vehicle (Figure 3.2 a). The sensor faced the side of the tree row perpendicularly and the RTK rover unit was on top and aligned with the center of the sensor. With this setting, the sensor collected data on a 2D vertical transect along the tree row and as the vehicle moved along the alleys of the grove the third dimension of the data was formed (Figure 3.2 b).

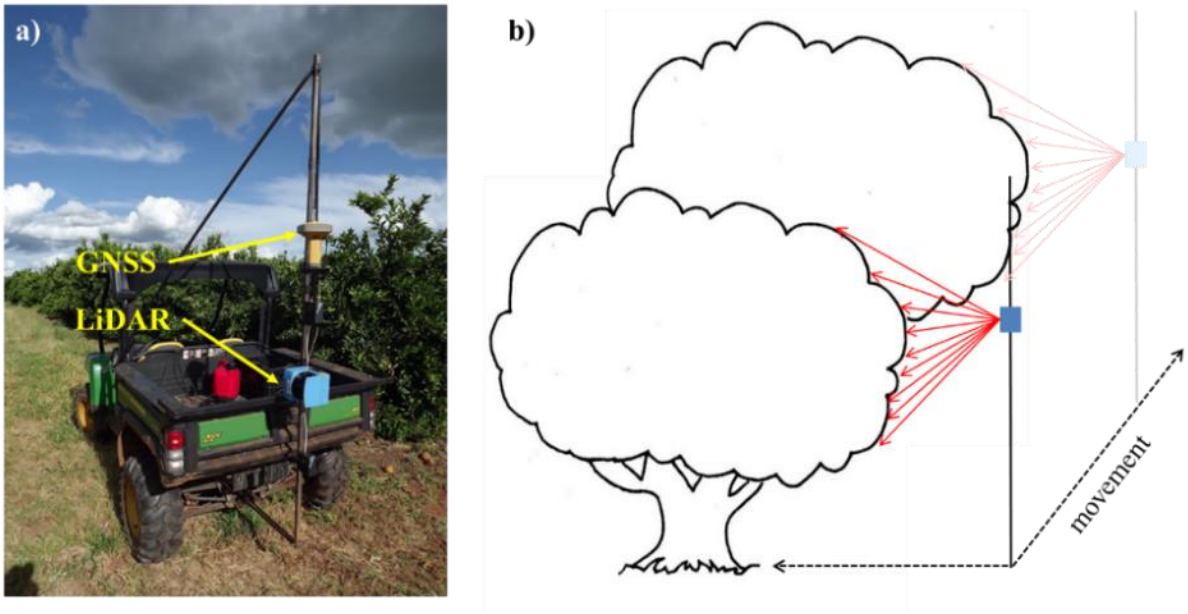

Figure 3.2: LiDAR sensor and RTK-GNSS receiver mounted on an all-terrain vehicle (a); diagram of LiDAR sensor displacement along the alleys (b)

To acquire data from the LiDAR sensor and the RTK-GNSS receiver synchronously a piece of software was developed. The chosen programming environment was Processing 2, which uses the JAVA programming protocol. All communication between the computer and the LiDAR sensor was carried out by a series of messages that were sent to and from the device following a hexadecimal telegram code (SICK AG. 2003). The communication with the RTK-GNSS receiver was carried out according to the NMEA (*National Marine Electronics Association*) standard. The developed acquisition software started by configuring the communication ports and the baud-rate for both the LiDAR sensor and the GNSS receiver to stablish communication with the devices. Afterwards, the sensors was configured, setting its angular resolution and range. Finally, a command was sent to both devices to start streaming the data.

The final output from the acquisition software was a text file containing information about time, GNSS location (latitude, longitude and altitude) and distance values from the LiDAR sensor. Figure 3.3 is an example of one output file where the lines represents each scan of the sensor and the columns labeled as A00, A01, until A180, represent the measured distance at each angle from the scanner in the 2D transect.

The maximum data acquisition frequency of the GNSS receiver was 10 Hz whereas the LiDAR sensor was 75 Hz. The software was synchronized with the LiDAR frequency, so during the acquisition process the GNSS was linearly interpolated and assigned to the LiDAR data so that every scan had a distinct GNSS positioning.

Time (s)	Latitude (degrees)	Longitude (degrees)	Elevation (m)	A00 (mm)	A01 (mm)	A02 (mm)	A03 (mm)	A04 (mm)	A05 (mm)	A06 (mm)	A07 (mm)	A08 (mm)	A09 (mm)	A10 (mm)	A...
0.0813	-22.833714	-49.127940	640.4520	1652	1617	1662	1672	1711	1800	1824	1851	1832	1912	1955	...
0.0947	-22.833714	-49.127939	640.4604	1670	1686	1658	1718	1759	1784	1809	1843	1854	1893	1961	...
0.1080	-22.833714	-49.127939	640.4616	1545	1692	1681	1705	1761	1764	1793	1833	1908	1947	1955	...
0.1213	-22.833713	-49.127936	640.4761	1599	1632	1670	1771	1782	1792	1766	1860	1804	1960	2000	...
0.1347	-22.833713	-49.127935	640.4793	1621	1663	1669	1632	1676	1797	1847	1899	1910	1927	1968	...
0.1480	-22.833713	-49.127934	640.4836	1645	1641	1679	1704	1790	1810	1814	1835	1803	1841	1955	...
0.1613	-22.833713	-49.127934	640.4857	1548	1629	1670	1689	1739	1770	1828	1833	1873	1875	1925	...
0.1747	-22.833713	-49.127933	640.4845	1598	1600	1646	1717	1732	1775	1761	1831	1813	1893	1950	...
0.1880	-22.833712	-49.127932	640.4866	1613	1631	1663	1698	1755	1783	1805	1853	1897	1856	1872	...
0.2013	-22.833712	-49.127931	640.4880	1609	1631	1681	1677	1732	1730	1794	1776	1812	1892	1902	...
0.2147	-22.833712	-49.127930	640.4853	1573	1599	1668	1665	1712	1706	1732	1771	1782	1764	1826	...
0.2280	-22.833712	-49.127928	640.4769	1556	1600	1658	1688	1673	1747	1720	1832	1856	1797	1857	...
0.2413	-22.833711	-49.127927	640.4806	1592	1620	1636	1632	1653	1723	1733	1760	1785	1764	1893	...
0.2547	-22.833711	-49.127927	640.4825	1531	1563	1643	1675	1691	1738	1778	1750	1727	1755	1820	...
0.2680	-22.833711	-49.127926	640.4825	1516	1554	1636	1661	1700	1755	1775	1822	1819	1834	1904	...
0.2813	-22.833711	-49.127924	640.4821	1497	1548	1610	1643	1630	1716	1727	1758	1826	1838	1836	...
0.2947	-22.833710	-49.127923	640.4815	1575	1595	1617	1652	1692	1697	1666	1766	1824	1841	1901	...
0.3080	-22.833710	-49.127923	640.4797	1526	1558	1598	1623	1668	1678	1721	1756	1814	1797	1842	...
0.3213	-22.833710	-49.127922	640.4779	1525	1552	1613	1616	1604	1703	1670	1762	1748	1732	1753	...
0.3347	-22.833710	-49.127920	640.4745	1532	1554	1551	1572	1625	1645	1671	1667	1782	1764	1855	...
0.3480	-22.833709	-49.127919	640.4693	1540	1550	1546	1556	1609	1617	1672	1718	1778	1826	1865	...
0.3613	-22.833709	-49.127917	640.4458	1416	1556	1591	1627	1659	1673	1702	1715	1764	1802	1828	...
0.3747	-22.833708	-49.127915	640.4554	1395	1429	1519	1599	1573	1637	1647	1751	1835	1856	1879	...
0.3880	-22.833708	-49.127915	640.4578	1607	1442	1606	1623	1708	1642	1784	1816	1828	1879	1945	...
0.4013	-22.833708	-49.127913	640.4847	1553	1527	1492	1661	1603	1612	1627	1761	1731	1763	1794	...
0.4147	-22.833707	-49.127911	640.4992	1524	1599	1645	1659	1657	1744	1776	1760	1774	1795	1812	...
0.4280	-22.833707	-49.127910	640.5078	1535	1599	1598	1708	1730	1690	1773	1828	1900	1882	1946	...
0.4413	-22.833707	-49.127909	640.5165	1574	1495	1574	1612	1739	1723	1787	1842	1806	1877	1864	...
0.4547	-22.833706	-49.127908	640.5203	1526	1645	1679	1718	1752	1783	1808	1843	1888	1902	1908	...
...	...	...	...	...	...	...	...	...	...	...	...	...	...	...	...

Figure 3.3: Output file from the data acquisition software containing information of the RTK-GNSS receiver and the measured LiDAR distances in mm

For data acquisition at the groves, the RTK-GNSS base unit was mounted at the highest corner of the field. Before starting the acquisition, the RTK-GNSS base was kept fixing its position during 30 minutes. The data collection was only carried out when the correction signal was actually being received by the RTK-GNSS rover unit. During the measurements, the vehicle moved along the alleys at constant speed, scanning one side of the tree row at a time (Figure 3.4). The data was saved separately for each tree row.

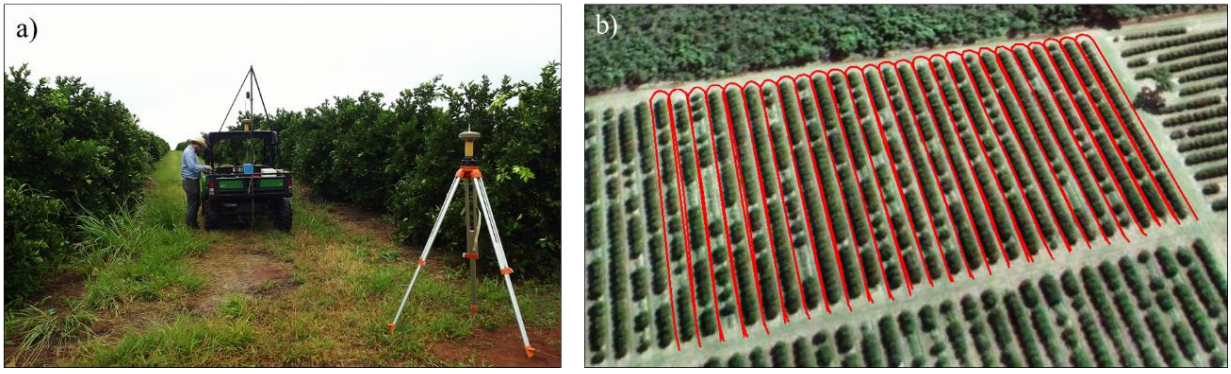

Figure 3.4: RTK base station (a); track of the vehicle for scanning both sides of the tree rows (b)

Data Processing

The objective of the data processing was to transform the raw data from the acquisition software into a shapefile ready to be imported into a GIS software to produce thematic maps of geometrical attributes of the trees. This goal was achieved in four steps: i) attributing RTK-GNSS coordinates to each impact of the laser beam and generating a georeferenced 3D point cloud; ii) filtering points of interest; iii) classifying points into groups, each representing one individual tree or a transversal section of the tree row; iv) calculating the canopy volume and height of each group. The processing algorithm was developed using R 3.2.2 software. R software was chosen due to its versatility and the availability of 3D modeling tools as well as 2D spatial mapping tools. Since the acquisition software saved independent text files for each row in the grove, the processing algorithm also treated each row individually.

i) Generating a georeferenced 3D point cloud

The first step consisted in transforming the raw data which were polar coordinates (angles and distances) of the laser impacts into rectangular coordinates (x, y, z) in which the x and y are actually UTM (Universal Transverse Mercator) coordinates derived from the RTK-GNSS receiver and z is the height of the point to the ground.

To obtain geographical coordinates for each laser impact, the actual position of the sensor (obtained from the RTK-GNSS receiver) was shifted in the x and y axes based on the respective dx and dy deviations for each point (Equations 1 and 2).

$$x_p = x_s + dx \quad (1)$$

$$y_p = y_s + dy \quad (2)$$

where,

x_p and y_p, UTM coordinates of the laser impact (point) (m);

x_s and y_s, UTM coordinates of the sensor (m);

dx and dy, deviations in x and y axes between the sensor and the point (m).

The deviations dx and dy were calculated based on the distance from the sensor and the laser impact in the x, y plane (dxy) and the angle α (Figure 3.5 a) (Equation 3 and 4). a corresponded to the direction of the

measurement in relation to the North, counted clockwise. This angle is the subtraction of 90° from the vehicle direction in relation to the North (the LiDAR sensor is arranged perpendicularly to the vehicle longitude, facing the left side). The direction of the vehicle at a given moment is defined by the median values of direction from 30 consecutive points along the vehicle track. Finally, *dxy* was calculated based on the original polar coordinates of the laser impacts (distance *d* and angle *β*) (Figure 3.5 b) (Equation 5). The *z* coordinate (point height) is also derived from the polar coordinates as exposed in Equation 6.

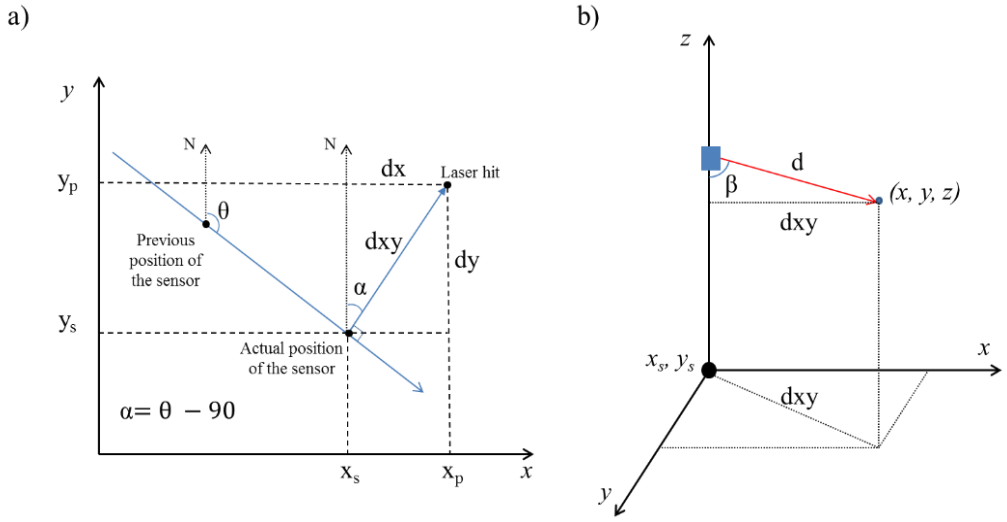

Figure 3.5: dx and dy deviations based on the angle α and dxy (a); dxy based on distance d and angle β (b)

$$dx = \operatorname{sen}\alpha \ . dxy \quad (3)$$

$$dy = \cos\alpha \ . dxy \quad (4)$$

$$dxy = \operatorname{sen}\beta \ . d \quad (5)$$

$$z_p = z_s - (\cos\beta \, . d) \quad (6)$$

where,

dxy, the distance between the sensor and the laser impact in the *x*, *y* plane (m);

α, angle of the direction of the measurement in relation to the North (degrees);

β, angle from LiDAR scanning (0 to 180°);

d, the distance value from the LiDAR scanning (m);

z_p, coordinate z (height) of the point (m);

z_s, coordinate z (height) of the sensor (m).

ii) Filtering points of interest

After the transformation from polar to rectangular coordinates, the data is then given by a matrix of three columns (*x*, *y* and *z*) and *n* lines, where *n* is the number of laser impacts. Those data can be visualized in the form of a 3D point cloud using the CloudCompare 2.6.1 software. Figure 3.6 shows an example of an original point cloud from a LiDAR scanning in one crop row. It is to be noticed a dotted line along the two sides of the tree row, which are the laser beam hitting the GNSS antenna. Also, whenever there is a gap between the plants the laser reached the

neighbor tree row. Because the aim of the data processing was to assess canopy geometry from each tree row separately, any point that does not represent the canopy of the trees from one single row must be removed from the original point cloud. For that, the next step of the processing was to apply filters to select only the points of interest (Figure 3.6 b).

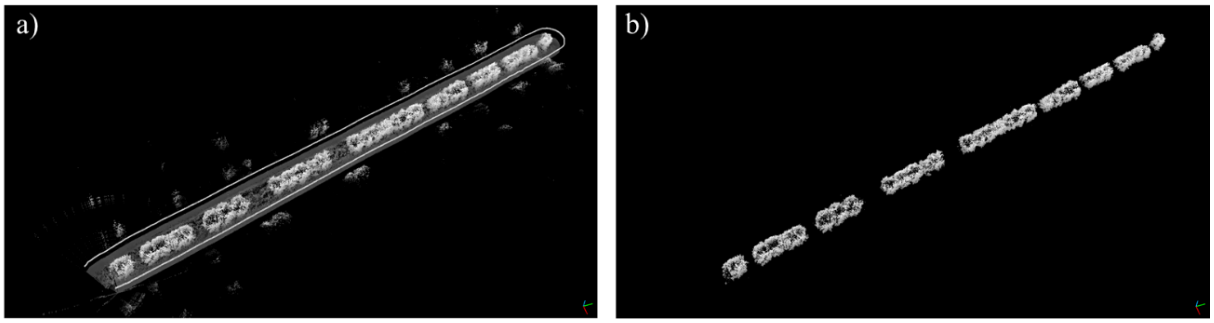

Figure 3.6: Original point cloud from one tree row (a); point cloud after the filtering process (b)

Points that were relatively far away from the target tree row were excluded by setting a maximum distance (*d*) for the LiDAR readings. A minimum distance value was also set to exclude obstacles that were too close to the sensor (the GNSS antenna, for example). The points which represented the soil were excluded by establishing a minimum threshold for the height (z coordinate) of each point. The output data after filtering was a point cloud representing only the crowns of the trees from one tree row (Figure 3.6 b).

iii) Classifying points into groups

Because each file contained the 3D point cloud from one entire tree row, the point cloud must be segmented into smaller batches prior to the computation of geometrical parameters. Two approaches were developed for this matter: the first one divided the original point cloud from the tree row into smaller groups, each representing one individual tree; the second divided the point cloud into transversal sections along the row.

The reason for these approaches is that they are applicable to two different crop scenarios. Analyzing trees individually is an appropriate approach for young crops or crops which are implanted in sparse tree spacing. Analyzing sections of the tree is applicable when the grove reaches a mature stage and the plants are large enough to fill up the gaps between them forming a vegetative wall along the row. In the past few years, it is noticeable a tendency of reducing the tree spacing in the Brazilian orange groves. In such arrangement, the grove is better adapted to the mechanical harvesting system and is also more resilient to the eradication of trees infected by diseases.

Both approaches permit the generation of thematic maps to investigate spatial variability. Also, both methods supply information for variable rate applications based on canopy variability, but with distinct resolutions. Analyzing the geometry of each plant individually produces useful information to investigate spatial variability at tree scale. In addition, it permits the generation of a database with individual plant information. The method of analyzing sections of the tree row allows the evaluation of variability in a finer scale, which suits variable rate applications with greater resolution.

In order to classify points among individual trees automatically, a clustering method was applied. According to Fridgen et al. (2004), the cluster analysis is the grouping of similar individuals into distinct classes called clusters. In the case of this study, the mentioned "individuals" were the laser beam impacts and the "clusters" were

the trees. Among several clustering algorithms available, the chosen algorithm was the k-means. This is a common non-supervised partitioning algorithm, which is available in R software through the *stats* package. This algorithm seeks to maximize the similarity between individuals inside the clusters and minimize it between the clusters.

This method requires the desired number of groups prior to the classification or an initial estimation of the centers of each cluster. After classification, each group should represent one individual tree, so the number of trees in one row should be known or estimated and then informed to the algorithm. To improve the accuracy of the classification, the estimation of the centers of each cluster were informed to the algorithm. This estimation was based on the spacing between the trees and the direction of the row. The algorithm used this information as an initial guess of the cluster centers. The points were then classified (Figure 3.7) according to their position in space so the information accounted by the algorithm was the *x* and *y* coordinates from each point.

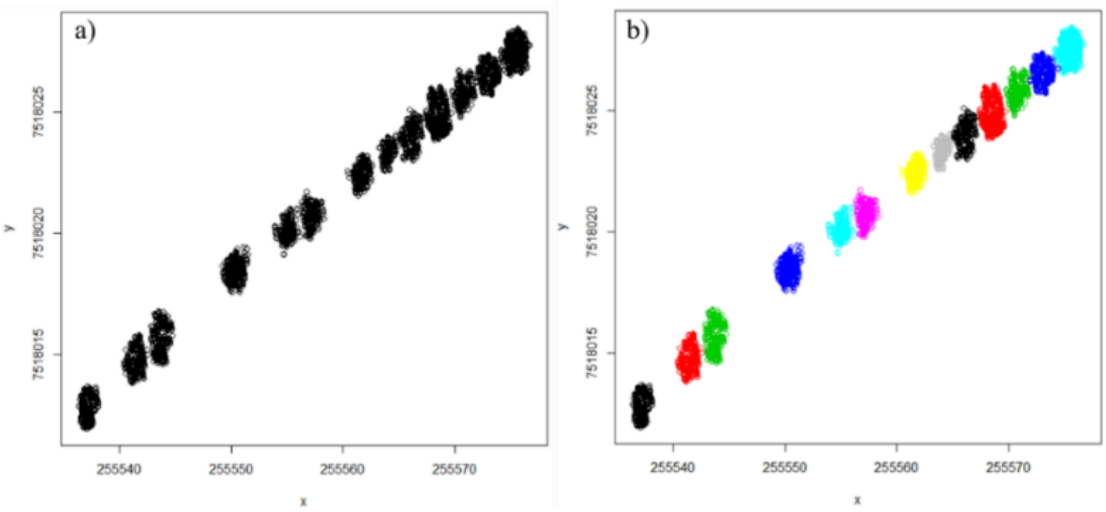

Figure 3.7: The x and y coordinates of a point cloud from orange trees (a); and clustering classification into groups each representing one individual tree (b)

The second approach of grouping the points was based on segmenting the row perpendicularly to its longitude, creating transversal sections with fixed width and length. The boundary lines of each transect were automatically drawn using the R package *sp* which allows delineation of lines and polygons using geographical information. The first step was to compute a linear regression with the *x* and *y* coordinates of the filtered point cloud. This represented a central longitudinal line of the tree row. A deviation was applied from this central line to both sides of the row. Finally, the row was segmented lengthwise based on a given distance (Figure 3.8) and the points within each section were assigned the section identification number.

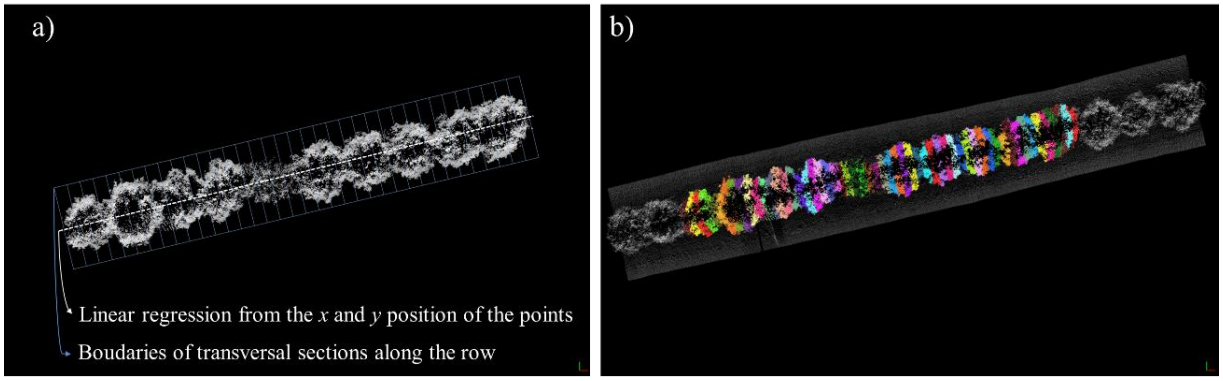

Figure 3.8: Top view of a point cloud; segmentation of the tree row (a); classified points in transversal sections (b)

iv) Calculating canopy volume and height

In order to compute geometrical attributes such as canopy volume, a 3D object was modeled over each classified point cloud (cluster or section). Two 3D modeling algorithms available in the software R were tested in this study: the *convex-hull* (package *grDevices*); and the *alpha-shape* (package *alphashape3d*). Both algorithms were designed to produce the smallest involucre able to enclose a set of 3D point cloud. The first one produces a convex object and the second permits an object with concavities. The level of concavity is defined by the index α (higher α produce less concavity). The canopy volume was automatically retrieved by the algorithm. By its definition, the *convex-hull* should produce larger object volumes and probably overestimate the canopy volume since each salient branch from the tree will pull out the hull structure. On the other hand, the *alpha-shape* should better suit the irregularities from the canopy reducing the effect of salient branches on the canopy volume computation, especially by setting a lower α index.

The canopy height was simply obtained by assessing the point of maximum height (z) within each group (cluster or transversal section). The final output of the processing steps was a GIS shapefile containing the polygons and the canopy volume and height information for each cluster or section boundaries.

3.3.2. Demonstrating and testing the proposed methods

Assessing the point cloud accuracy

Although the accuracy of the laser sensor is known and considered sufficient to produce accurate point clouds, the overall data acquisition method and the arrangement of the LiDAR sensor, RTK-GNSS receiver and vehicle might produce unknown errors over the point cloud. For this reason, a test procedure was carried out to assess the accuracy of the point cloud generated by the proposed method.

Objects with regular geometry were selected as targets to be scanned by the LiDAR-based system. A platform carrying the sensor and the RTK-GNSS receiver was designed to run over a rail at constant speed powered by means of an electric motor. Such a testing set up was develop to minimize the effect of vibration during the data acquisition. A second scanning over the objects was carried out with the actual all-terrain vehicle mounting the same equipment as in the real reading in the groves. During the tests the vehicle moved over a leveled lawn.

The accuracy of the point cloud was assessed by simply comparing the dimensions of the objects in the point cloud with the actual dimensions of the objects. The virtual dimensions (from the point clouds) were obtained using a distance measurement tool available in the CloudCompare software.

Data acquisition in a commercial grove

In order to demonstrate the proposed methods for data acquisition and processing, a 25 ha orange grove located in the state of São Paulo, Brazil, was scanned. The variety of the trees was "Valencia" grafted to "Swingle" rootstock. Trees were planted in 2009 and were six years old at the time of this study. The spacing was 2.6 m between trees and 6.8 m between rows. At the time of the readings, the tree canopies were already touching each other along the row, partially closing the gaps between them (Figure 3.9). This grove was grown in a rain-fed system.

Figure 3.9: 25 ha commercial orange grove scanned with the laser sensor

The aforementioned equipment and data acquisition method were applied. The vehicle moved along the alleys at 3.3 m s^{-1}, scanning one side of the tree row at a time. The configuration of the sensor used is shown in Table 3.1.

Due to a 13 m gradient in elevation, this field was implemented with terraces on terrain contours for soil conservation. The tree rows were planted as straight lines which occasionally crossed over the terraces. The areas surrounding the terraces were more suited to errors during the readings due to the movement of the vehicle to cross over them. These areas were subsequently excluded from the analysis.

Table 3.1: Configuration used for the LiDAR sensor

Communication		Angle		Distance		Scan
Protocol	Baud Rate	Range	Resolution	Range	Resolution	frequency
Serial RS 422	500 kbps	0 – 180°	1°	8 m	1 mm	75 Hz

Modeling of 3D objects from the point cloud

As shown during the data processing description, several alternatives can be used during the processing of a point cloud in order to model a 3D object over the points. To compare these possibilities, different methods to

create 3D objects were applied over a set of point clouds from 25 individual orange trees. These trees were extracted from the original point cloud obtained from the entire field. The selection of these trees aimed to capture different canopy sizes. The 3D objects were modeled over each plant individually and over transversal sections of 0.86 m, 0.52 m, 0.37 m and 0.26 m wide, which were equivalent to dividing the trees into three, five, seven or ten transversal parts, respectively. The *convex-hull* and the *alpha-shape* algorithms were applied. Variations over the *alpha-shape* were also tested by setting the index α to 0.25, 0.50 or 0.75.

The tree volumes from each method were compared against each other. The volume of each individual tree was also computed by two methods based on manual measurement of the canopy dimensions. In the first manual method, referred here as "cylinder-fit", the canopy volume of a citrus tree is considered as two-thirds the volume of the smallest cylinder able to enclosure the tree (Mendel, 1956). The second method, referred here as "cube-fit", is the current method adopted in most of the Brazilian groves. The volume of the tree is simply given by the volume of a cube, which encloses the canopy. The dimension of this cube is given by multiplying the two widths of the canopy (along the row axis and perpendicular to the row axis) with the height of the canopy. The dimensions of the canopy for the manual methods were measured from the point cloud of each tree by using a distance measurement tool available in the CloudCompare software.

These processing methods were also applied over a point cloud from a 26 m segment of a tree row. 3D visualization of the modeling and general observations over the results were carried out.

Mapping of canopy volume and height in a commercial orange grove

To produce a map of canopy volume from the scanned grove, the point cloud was processed in two different ways. The first method was based on computing the canopy volume for each individual tree (cluster) and applying the *alpha-shape* algorithm with the index α set to 0.75. The second approach was based on dividing the rows into sections of 0.26 m width and applying the *convex-hull* algorithm. These setting were chosen after evaluating the results from the previous analysis, which tested several options for modeling the tree's canopies.

Because the trees were partially touching each other, some error in the cluster classification was expected. The accuracy of this classification was assessed by visually recognizing 678 trees from the point cloud and comparing them with the outcome of the cluster classification using the CloudCompare software.

The canopy volume and height maps were produced by importing the shapefiles from the data processing output into the QGIS 2.10 software. A map of points, each representing one tree or a transversal section of the row, was created by generating a centroid point within each polygon. Points close up to 10 m to the field boundary were excluded. Due to maneuvering of the vehicle the point cloud might lose accuracy and the clustering algorithm was more suited to errors in that region. In addition, the points within a 15 m buffer around the terraces in the field were excluded. The point cloud lost accuracy in those regions because of the movement of the vehicle to cross over the terraces.

To produce the final canopy volume and height maps, the points that represented each tree or section were interpolated in a regular pixel grid in order to produce a continuous surface across the grove. Prior to the interpolation, the values from the row sections were converted into values equivalent to individual trees, otherwise the final map would represent volume of row sections and not of individual trees. Therefore, sections were merged in groups of 10 along the row forming segments of 2.6 m of length, which was equivalent to the tree spacing (Figure 3.10). The canopy volume of each segment was given by adding the volume of the 10 sections inside it and the

height value was given by the maximum height of the 10 sections. Those parameters were attributed to a central point within each segment.

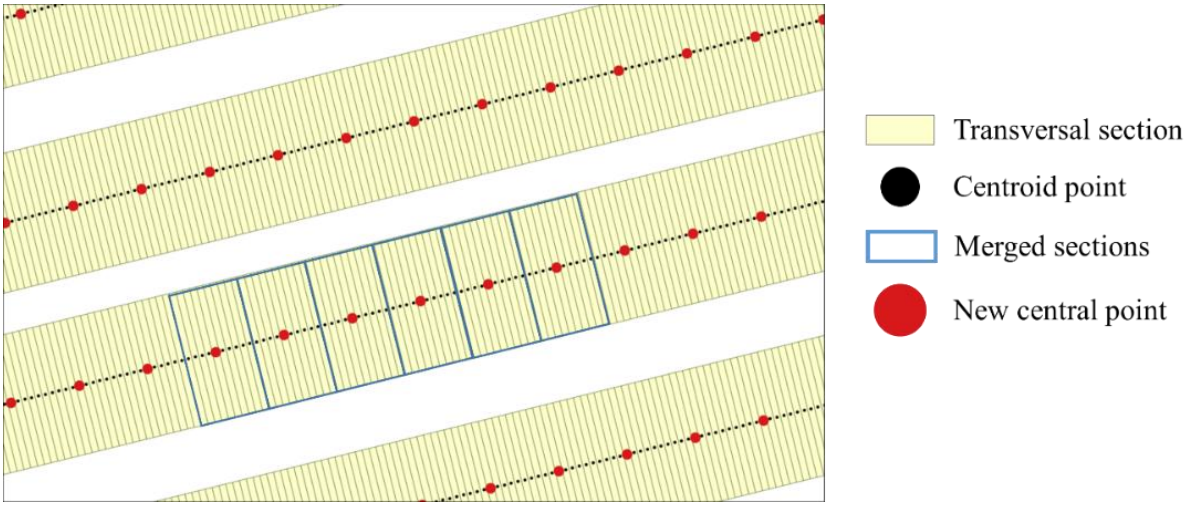

Figure 3.10: Merging of adjacent sections of the row into segments equivalent to the tree spacing

Finally, volume and height data of at each point across the grove (representing row segments or clusters) were interpolated in a pixel grid of 5 m to produce the final canopy volume and height maps. The interpolation method was ordinary kriging and it was carried out with the use of the Vesper 1.6 software.

In order to compare the resulting maps of the two methods (cluster segmentation using *alpha-shape* reconstruction and transversal section segmentation using *convex-hull* reconstruction) a similarity analysis between maps was carried out with the use of the Map Comparison Kit 3.2 software. The chosen algorithm was the *fuzzy numerical cell-by-cell comparison*. The measure of similarity (fuzzy similarity index) is given at each pixel based on Equation 7 in a scale from 0 to 1, being 1 identical values.

$$s(a,b)_i = 1 - \frac{|a_i - b_i|}{\max(|a_i|,|b_i|)} \quad (7)$$

where,

a, value in pixel i from map 1

b, value in pixel i from map 2

$s(a,b)$, fuzzy similarity index in pixel i between the two maps

The fuzzy logic implemented in this algorithm considers a level of uncertainty in the value in each pixel based on the neighboring pixels, which is referred as "fuzziness of location". It means that the neighboring pixels affect the considered value in the central pixel. The searching radius was set to four pixels. Other configuration for the fuzziness of location, such as the decay type function was kept to default. More information about the algorithm is available in Hagen (2002). The relationship between maps of canopy volume and canopy height was assessed by a pixel-based correlation analysis.

3.4. Results and Discussion

3.4.1. Point cloud generation - laboratory testing

The accuracy of the point cloud derived from the developed MTLS was assessed by using template objects as targets for scanning. Figure 3.11 shows the point clouds from a cylinder, a body of cone, a square, triangle and circle shaped objects scanned by the MTLS mounted on the all-terrain vehicle (the same data acquisition setting applied in the groves). These results seems coherent by a visual assessment. The same objects were also scanned with the MTLS mounted on a platform running over a rail.

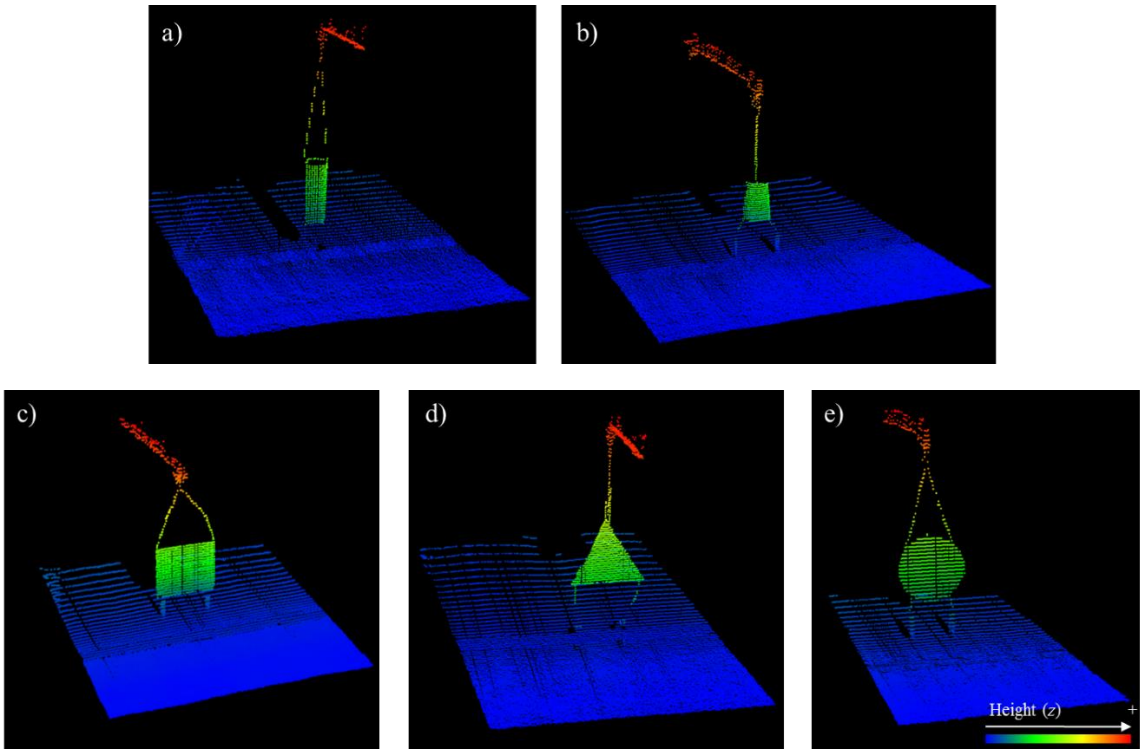

Figure 3.11: Point clouds from objects scanned by a mobile terrestrial laser scanner mounted on an all-terrain vehicle; cylinder (a), body of cone (b), square (c), triangle (d) and circle (e)

The dimensions of the objects obtained by the two scanning systems are viewed in Table 3.2. It should be noticed that, in order to simplify the design of such tests, the accuracy of the point cloud was evaluated based on the obtained dimensions of the objects and not by assessing the actual positioning error of each laser beam impact (as it would be ideal). Generally, both scanning systems provided very similar dimensions to the actual dimensions of the objects, with, as expected, slightly better results when the MTLS was running over the rail. The overall average difference between the laser measurements and the actual dimensions of the objects was 0.69 cm, reaching a maximum of 5.77 cm ('b' dimension of the square with the MTLS mounted on the vehicle). The surface area and the volume of the objects calculated from these measurements were also close to the actual areas and volumes.

Table 3.2: Object dimensions measured manually and by a mobile terrestrial laser scanner mounted on an all-terrain vehicle and on a platform running over a rail

Objects	--- a ---			--- b ---			--- c ---			A. (m^2), Vol. (m^3)		
	(i)	(ii)	(iii)	(i)	(ii)	(iii)	(i)	(ii)	(iii)			
	(cm)									(i)	(ii)	(iii)
Square	98.60	98.29	100.00	94.23	100.25	100.00	-	-	-	0.9290	0.9853	1.0000
Triangle	98.22	98.33	100.00	84.64	88.48	87.00	-	-	-	0.4162	0.4350	0.4350
Circle	101.17	99.96	100.00	-	-	-	-	-	-	0.8040	0.7848	0.7854
Cylinder I	79.58	79.78	80.00	29.58	30.13	30.00	-	-	-	0.0549	0.0569	0.0565
Cylinder II	80.92	83.21	83.00	19.74	20.28	20.00	-	-	-	0.0250	0.0269	0.0262
Body of cone	62.65	63.31	64.00	44.95	45.05	45.00	31.15	30.90	31.00	0.0721	0.0725	0.0736

* Header abbreviations: (i), laser scanner mounted on an all-terrain vehicle; (ii), laser scanner mounted on a platform running over a rail; (iii) actual dimension (by measurement tape); A., surface area of square, triangle and circle; Vol., volume of cylinders and body of cone

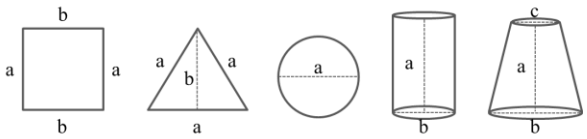

The main sources of error in such measurements are the embodied errors in the laser sensor (± 5 mm) and in the RTK-GNSS (± 10 mm) and the rotations of the sensor along its three axes (pitch, yaw and roll). The obtained errors in the performed tests were fairly low considering these three main sources of error. As pointed out in the literature review, some studies reported the importance of implementing an inertial measurement unit (IMU) during the scanning in order to register such angular displacements and correct the position of the laser impacts. During the field operations, although the alleys of the groves were well leveled, higher errors might have occurred occasionally due to irregularities of the terrain.

3.4.2. Field scanning and 3D modeling

Results from the LiDAR data acquisition and processing of a 3D point cloud over a 25 ha orange grove can be seen in Figure 3.12. The grove was successfully scanned at its hole. This was a particularly encouraging result since previous research which employed terrestrial laser scanners to model tree crops normally used smaller field plots. Large scale enterprise was not yet reported.

The equipment setting proved to be relatively robust for large field scanning. One issue that should be reported is the sensitivity of the LiDAR sensor to intense sun light exposure. The sensor used in this study was developed for indoor scanning and do not operate properly under excessive light exposure. Several times during the data acquisition in the field, the operation was interrupted due to malfunctioning of the sensor. Sensors developed for outdoor purpose are available in the market and would be more adequate for agricultural use. Otherwise, a structure to protect the sensor against direct sunlight without blocking its field of vision towards the targets should be required. Avoiding readings during hours of intense light exposure is also an option to deal with this issue.

It is noticeable that the achieved density of points was able to capture the shape of the rows and of individual trees with good level of detail. Due to the georeferencing of the readings, each individual point in the cloud has precise RTK-GNSS position, so every point or tree can be traced in the field. With the applied data

acquisition configuration (75 Hz scanning frequency at 3.3 m s^{-1} speed) the distance between each scan was around 4 cm. A total of approximately 2.3 million points were acquired for each row (approximately 12,100 point per plant). The total grove accounted for approximately 175 million points, which corresponds to approximately 700 points per m^2. Airborne LiDAR scanning applied over urban or forest areas usually produces point clouds with 0.5 to 5 points per m^2. Escolà et al. (2015) reported a density of 8,000 points per m^2 using a multi-echo LiDAR device on a MTLS on an olive grove.

To achieve a proper density of points in the scanned orange grove the vehicle movement was set to a relatively low speed resulting in a low working efficiency for data acquisition. Nevertheless, this speed is compatible with several mechanical operations in the grove such as spraying, which means that the LiDAR-based scanning system could be attached to the machines in the field to collect data while performing other agricultural operations.

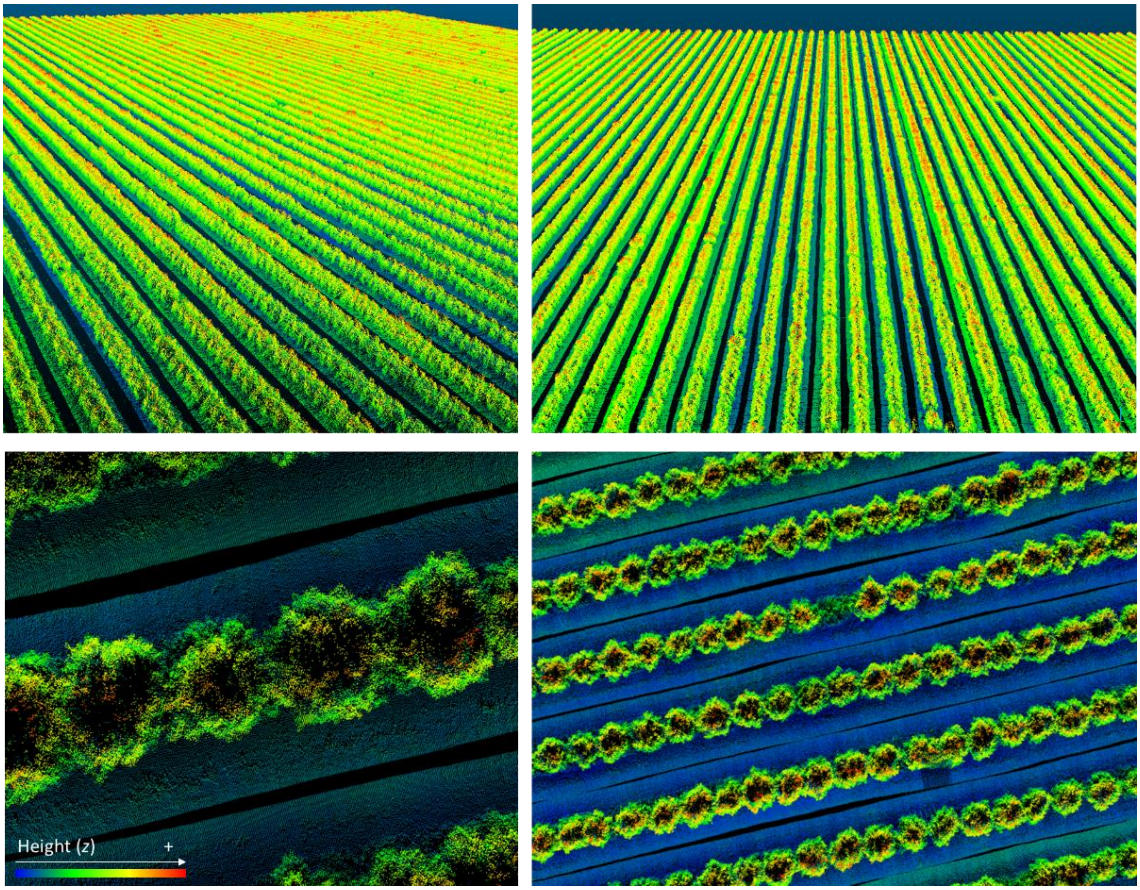

Figure 3.12: Point cloud derived from the developed terrestrial laser scanning system in a 25 ha commercial orange grove

The results of the proposed 3D modeling algorithms applied to a segment of tree row of 26 m is showed in Figure 3.13. It is noticeable how the *convex-hull* model apparently produced larger objects, which occurs because salient branches enlarges the hull structure. As expected, salient branches were better represented by the *alpha-shape* algorithm with lower α index. However, the index α should be appropriately set (not too high neither too low). A low index might produce disconnected structures forming holes inside the canopy, which is not desirable. Because this algorithm permits the representation of concave structures, it is reasonable to consider the *alpha-shape* a suited model for representing the tree canopy. Likewise, it is noticeable that slicing the row into transversal sections instead of maintaining the tree as a whole also helped the representation of the canopies with greater level of detail. The

segmentation of the trees was particularly important in the *convex-hull* model, because it reduced the effect of over estimation caused by outer branches on the tree. This issue was more severe when the model was created over the entire plant. The importance of segmenting the point cloud when applying the *convex-hull* algorithm to estimate volume was also evidenced by Auat Cheein et al. (2015).

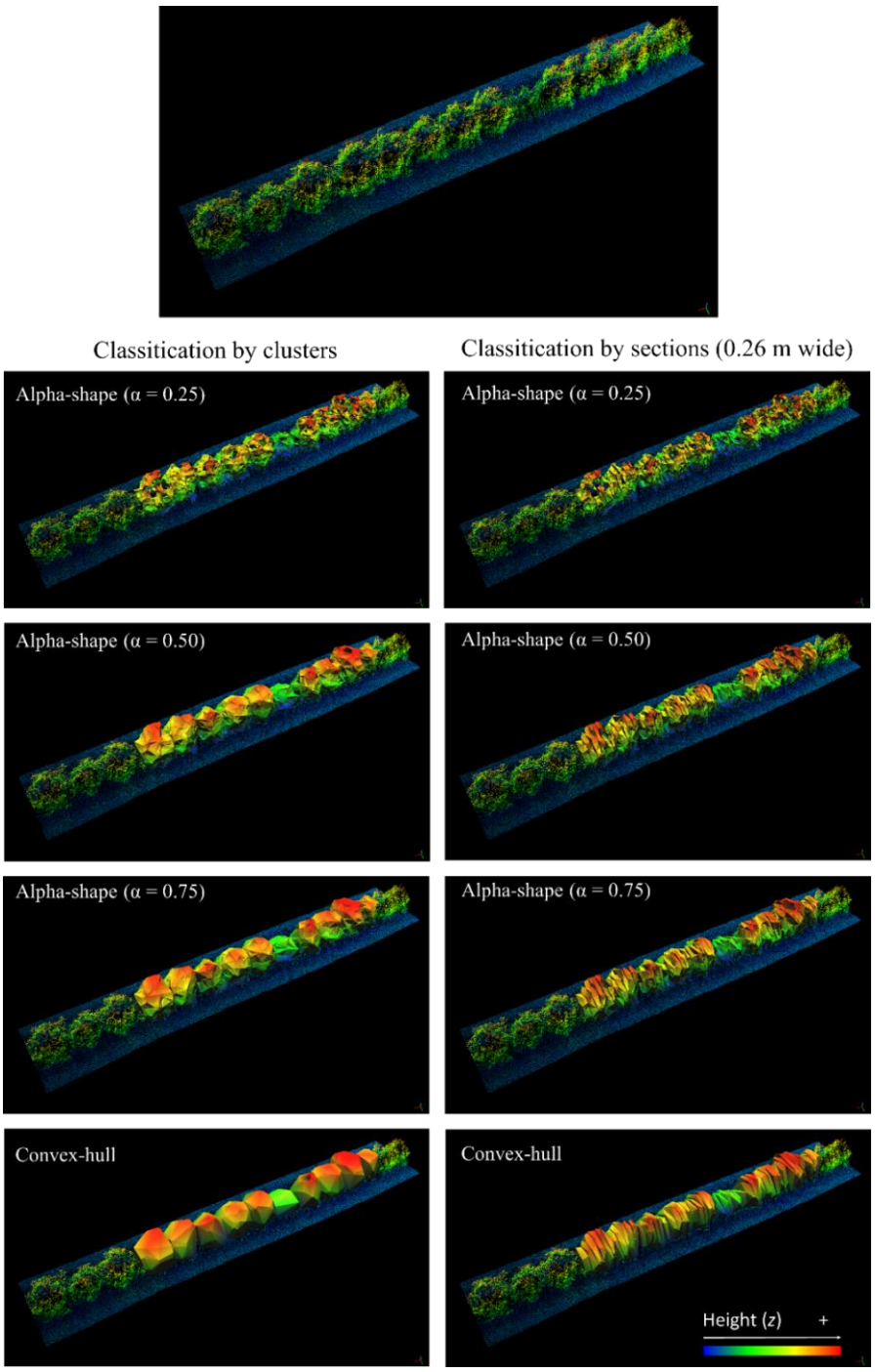

Figure 3.13: Convex-hull and alpha-shape algorithms to model orange trees by two approaches: clusters (individual tree) and transversal sections of the row (0.26 m wide)

However, when slicing the trees to produce 3D models of continuous canopies a problem with the *alpha-shape* algorithm was evidenced. While the algorithm produced desirable concavities on the outer part of the canopy,

which helped detailing the silhouette of the canopy, it also created undesirable depressions in the transversal slicing plane and in the bottom of the trees (Figure 3.14). When all the sections were put together, the concavities in the transversal wall of the sections produced voids, which affected the final computation of canopy volume. The voids between sections were also present in the *convex-hull* models but they were considered insignificant (Figure 3.15_. They are inherent to the approach of slicing the rows and are directly related with the scanning frequency during the data acquisition (which determines the spacing between scans). Because of the high scanning frequency, the space between each scan was very narrow and so was the voids between the *convex-hull* objects (Figure 3.15). Thus, the *convex-hull* algorithm was considered better than the *alpha-shape* to represent transversal sections of the row.

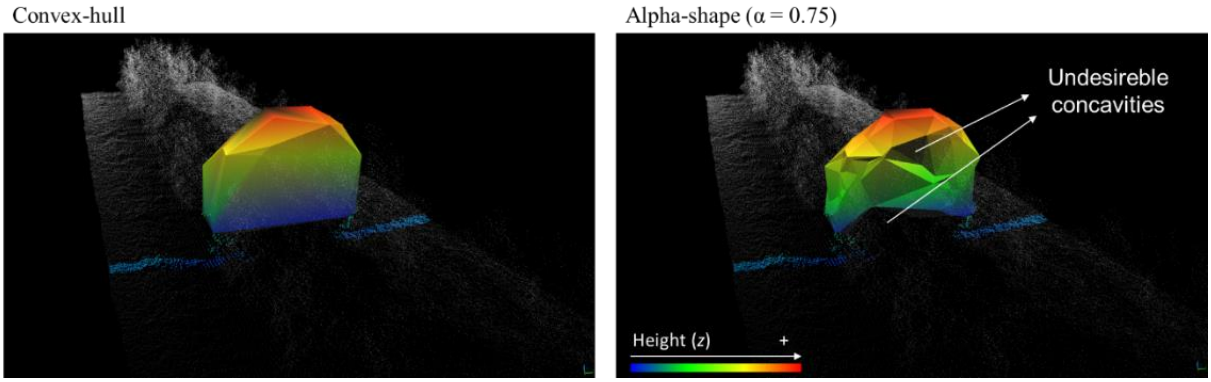

Figure 3.14: Detail of the convex-hull and alpha-shape modeled over a single 0.26 m wide transversal section of a tree row

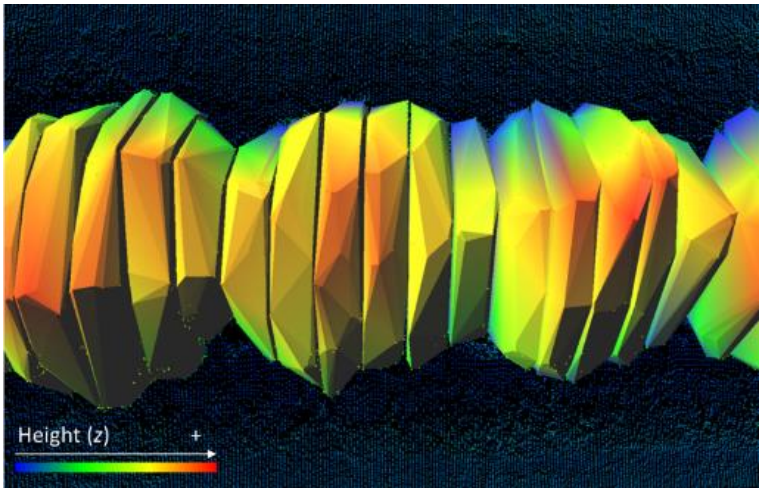

Figure 3.15: Top view of the convex-hull modeling over transversal sections of an orange tree row

Nevertheless, the *alpha-shape* algorithm remained a better option when the model was applied over the entire tree. The best index α should be the one which does not produce voids inside the canopy. In the Figure 3.16 it is noticeable that this result was obtained when the index α was set to 0.75.

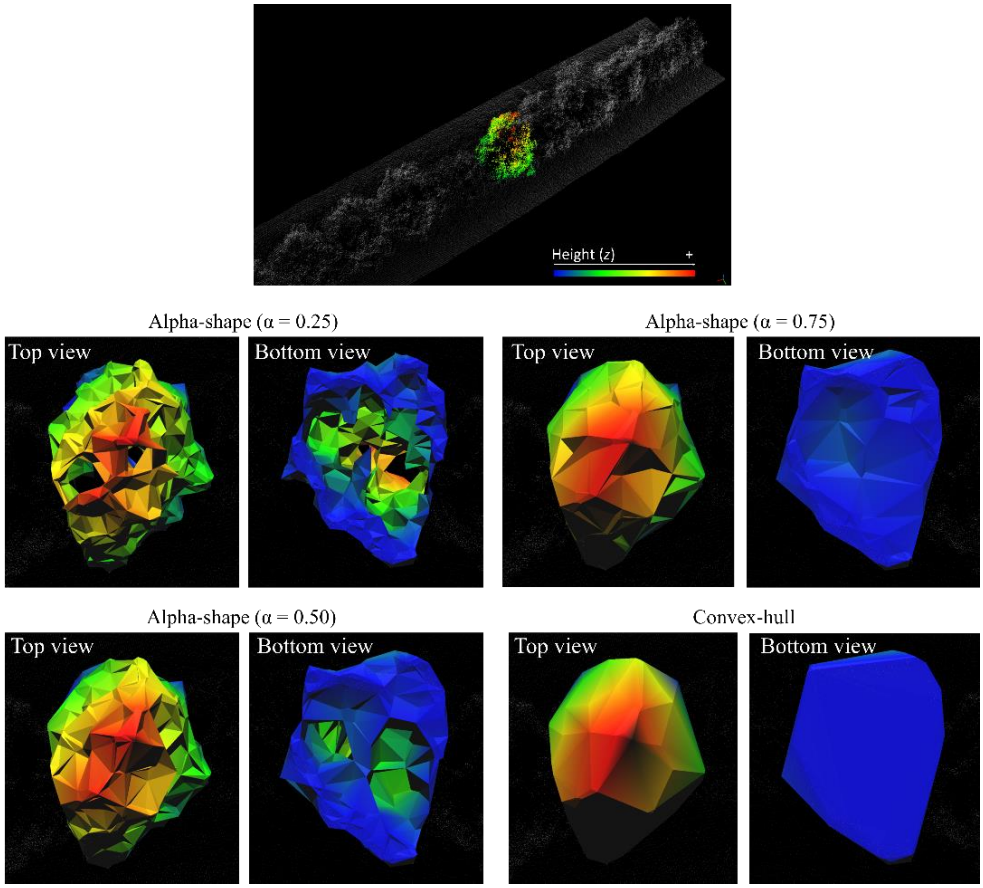

Figure 3.16: 3D canopy structure of a single tree modeled by different algorithms

The results from the measurements of 25 individual trees extracted from the scanned grove also confirmed the observations made from the previous analysis (Table 3.3). The *convex-hull* model resulted in the highest canopy volume, followed by the *alpha-shape* with higher index α. The canopy volume also decreased as the number of slices of the trees increased. This decrease is higher in *alpha-shape* algorithm (Figure 3.17), probably due to the increase of voids between sections as mentioned. When using the *alpha-shape* algorithm, there was a 2-fold range in the volume computation by computing the volume of the tree as a whole or by dividing it into 10 sections (Table 3.3).

Table 3.3: Mean canopy volume of 25 individual trees by different methods and by dividing the trees into different number of sections

Method / Algorithm	Number of sections per tree				
	1	3	5	7	10
	Mean canopy volume of 25 individual trees (m^3)				
Manual (cube-fit)	23.01	-	-	-	-
Manual (cilinder-fit)	12.15	-	-	-	-
Convex-hull	16.95	15.61	14.85	14.29	13.67
α-shape (α =0.75)	14.92	12.12	10.31	8.89	7.58
α-shape (α =0.50)	12.66	10.21	8.43	7.19	5.92
α-shape (α =0.25)	6.43	5.51	4.89	4.28	3.45

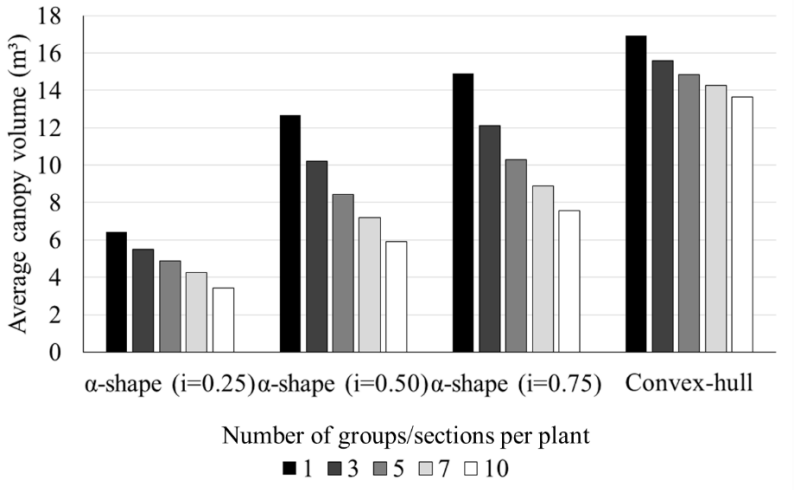

Figure 3.17: Canopy volume computation by different algorithms for individual trees and by dividing each tree into three, five, seven and ten transversal sections

The volumes for each individual tree calculated by the proposed algorithms and by the manual methods are showed in the Figure 3.18. These results were computed over the entire point cloud of each tree and not by sections. The plants IDs were given based on a rank from the smallest to the largest tree according to the *alpha-shape* ($\alpha = 0.75$) and *convex-hull* computation. It is to be noticed that this ranking is roughly followed by all the other algorithms. Generally, the manual methods produced a ranking with some disagreement with the other algorithms, which indicated a certain level of randomness in the manual measurements. The rough simplification of the canopy structure by the manual method based on the cube-fit overestimated the canopy volume in relation to all the other algorithms. The measurements from the cylinder-fit method were mainly close to the ones computed with the *alpha-shape* with index of 0.50, which produced voids inside the plant as shown in Figure 3.16, but sometimes closer to index 0.75 and other to 0.25. The average volume obtained from the *alpha-shape* with index of 0.75, which was previously considered the best alpha index, was 14.9 m³, whereas the volume from the manual measurements based on the cube-fit and the cylinder-fit were 23 m³ and 12.1 m³, respectively (Table 3.3).

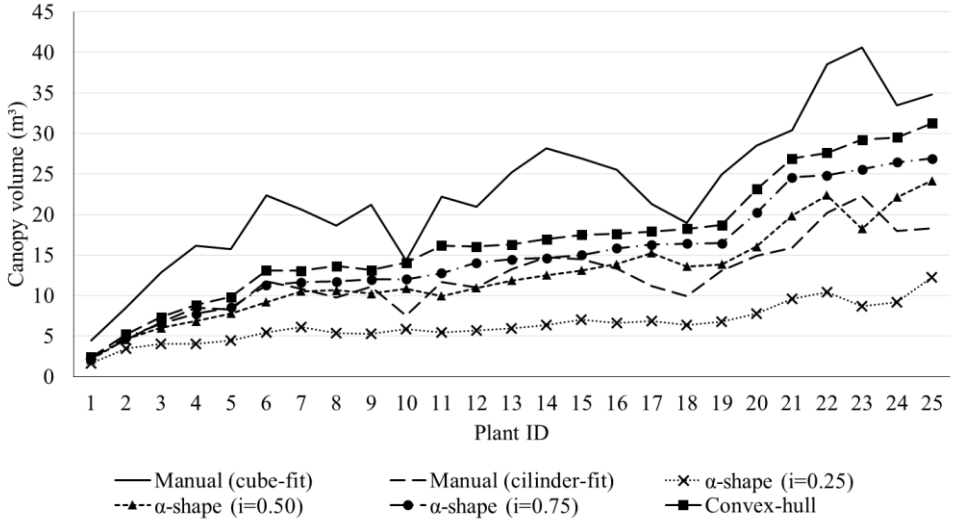

Figure 3.18: Canopy volume of 25 individual trees computed by different methods

The difference in canopy volume obtained from different methods evidenced the importance of the adoption of a reference method. The choice of the best method based on the one which is more close to a reference is simply not possible since the "real" canopy volume is not known and cannot be measured without the establishment of a standardized method. At this stage, it is reasonable to consider that the method of canopy volume computation based on the terrestrial laser scanner and 3D modeling is clearly more capable of capturing the geometry of the canopy than the current available manual methods. The proposed methods are also applicable in the field and, for those reasons, could be adopted as a new standard method of canopy volume computation.

These first considerations about the 3D modeling methods led to the conclusions that, among the tested options, the best algorithm for modeling the canopy of individual trees was the *alpha-shape* with index α set to 0.75, because it permits the representation of salient structures from the canopy while keeping the canopy as a solid without voids inside it. The *convex-hull* algorithm was a better option for modeling of sections of the trees, because it produced minimum voids between the sections. The weakness of this algorithm, which is overestimating the structure in outer parts of the tree, is less relevant when the tree is divided into sections.

3.4.3. Mapping of canopy volume and height

The final canopy volume and height maps were produced by two methods: by classifying the point cloud into individual tress (cluster) and subsequently applying the *alpha-shape* algorithm (α = 0.75); and by dividing the rows into sections of 0.26 m wide and further applying the *convex-hull* algorithm to model the canopies. The two data processing methods produced shapefiles of polygons where each polygon contained the information of canopy volume and height computed by the algorithms (Figure 3.19 and 3.20). The slicing of the rows produced approximately ten polygons per tree (prior to interpolation every ten subsequent section were merged together to produce the final map). Inside each polygon approximately 6 laser scans were found.

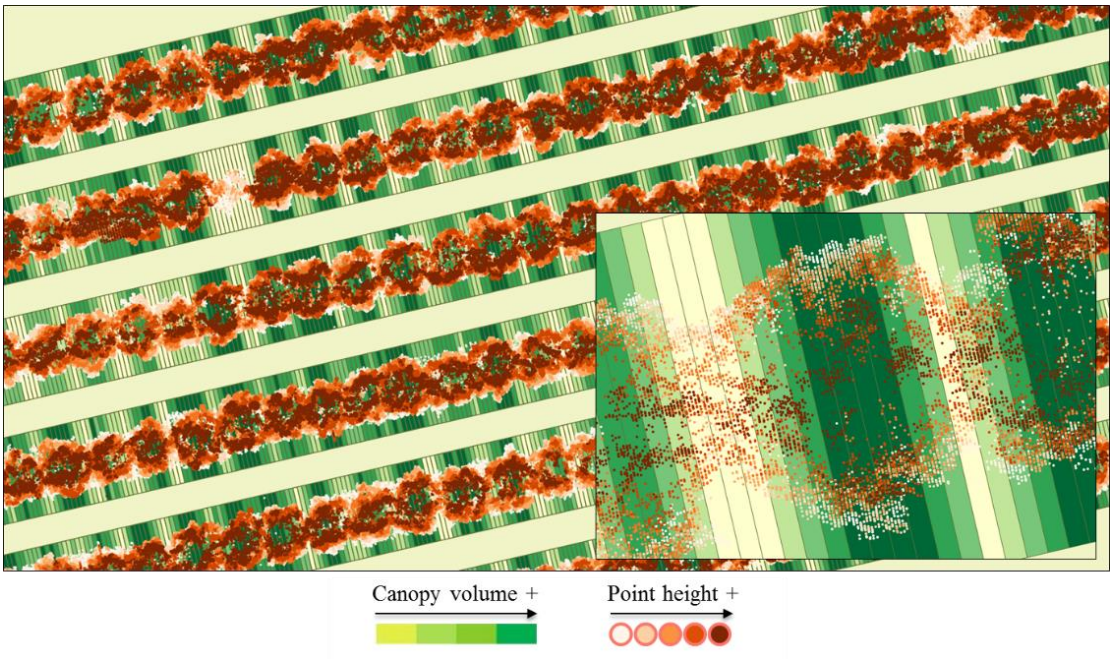

Figure 3.19: Shapefile resulted from data processing according to the method based on segmenting the row into transversal section

Regarding the representation of individual trees, the classification accuracy was assessed by measuring by the number of corrected clusters representing a single tree. The accuracy of the cluster analysis obtained for this field was 90.2% (percent of correctly classified clusters over the total number of clusters). This was considered sufficient to produce reliable information, but this accuracy may vary from different groves.

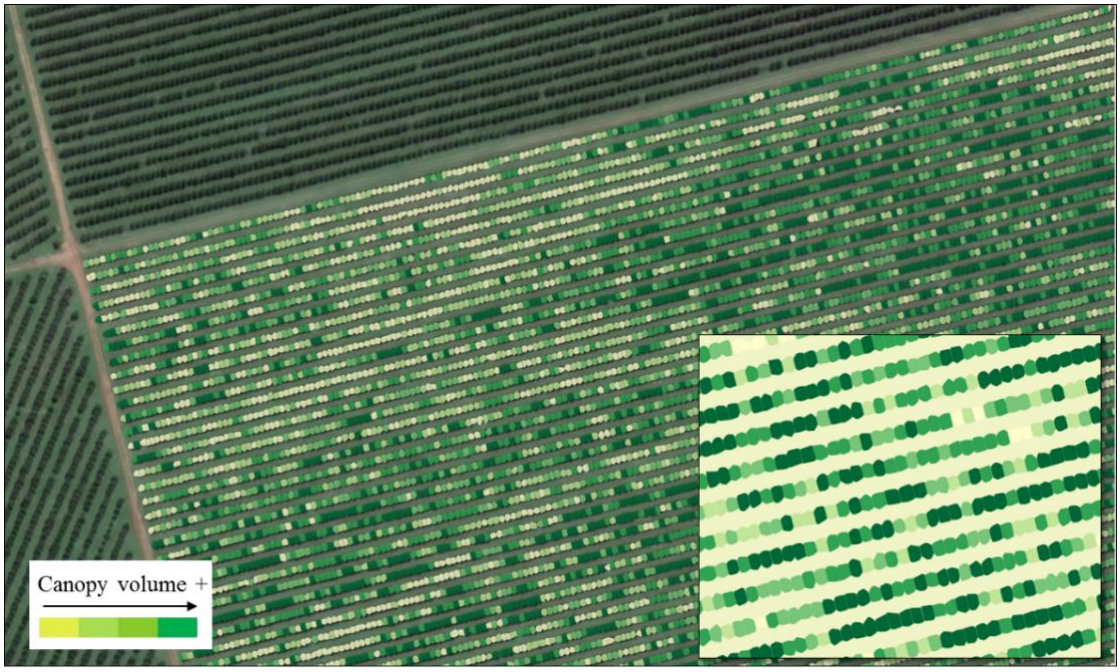

Figure 3.20: Shapefile resulted from the data processing method based on cluster analysis and single-tree computation of canopy volume

The proposed algorithm applied to transform the raw data from the LiDAR scanning into shapefiles ready to be imported into a GIS software to produce canopy volume and height maps was robust and effective. The developed programing in R software ran all data processing steps sequentially one row at a time, taking approximately 30 minutes to complete the entire grove. Besides the required time, R software was considered a good choice to process the data, since it provided a variety of packages and functionalities to proceed with different tasks along the processing steps.

Table 3.4 shows the descriptive statistics over the data prior to the interpolation. All statistics parameters were very similar between the two methods. One noticeable difference was found on the total number of clusters and row segments (the merging of 10 subsequent sections). This is probably due because the cluster analysis was programmed to exclude clusters which were too small, probably representing a tree gap. This was applied in order to improve the cluster accuracy. The segmentation was continuous along the row so, the logic of this method considered tree gaps as very small canopies. The minimum value of canopy volume was also obtained by this method.

Table 3.4: Descriptive statistics of canopy volume and height for the two methods

Canopy variable	Method*	Mean	Minimum	Maximum	Coef. of variation	Observations
		----- m³ (volume) or m (height) -----				
Volume	1	11.94	1.29	26.50	0.20	9119
	2	12.15	0.25	26.30	0.21	9669
Height	1	2.85	1.03	3.80	0.09	9119
	2	2.86	0.95	3.80	0.09	9669

*Method 1: *Alpha-shape* modeling over individual trees

**Method 2: *Convex-hull* modeling over sections of the row

The two methods produced similar results for canopy volume and height. The final maps were visually similar (Figure 3.21 and 3.22). The similarity between the maps assessed by the fuzzy similarity index was higher for the canopy height (fuzzy similarity index = 0.99) than for the canopy volume (Figure 3.23). This is because both methods applied the same rational to compute the height. The height of each cluster or section of the row was equal to the height of the point with maximum height inside the cluster or section. The canopy volume maps were computed by two different algorithms, so the fuzzy comparison resulted in slightly lower index (fuzzy similarity index = 0.96).

Some relation between height and canopy volume was also expected. This correlation was higher when the two parameters were computed using the cluster analysis (r = 0.71). The grouping of sections along the row did not necessarily match with individual plants, so the correlation of height and volume was not as high (r = 0.61).

Generally, both methods resulted similarly. They were both able to represent the spatial variability of canopy geometry in the grove. These maps are useful information for site-specific management, providing information for variable rate applications or to divide the field into management zones.

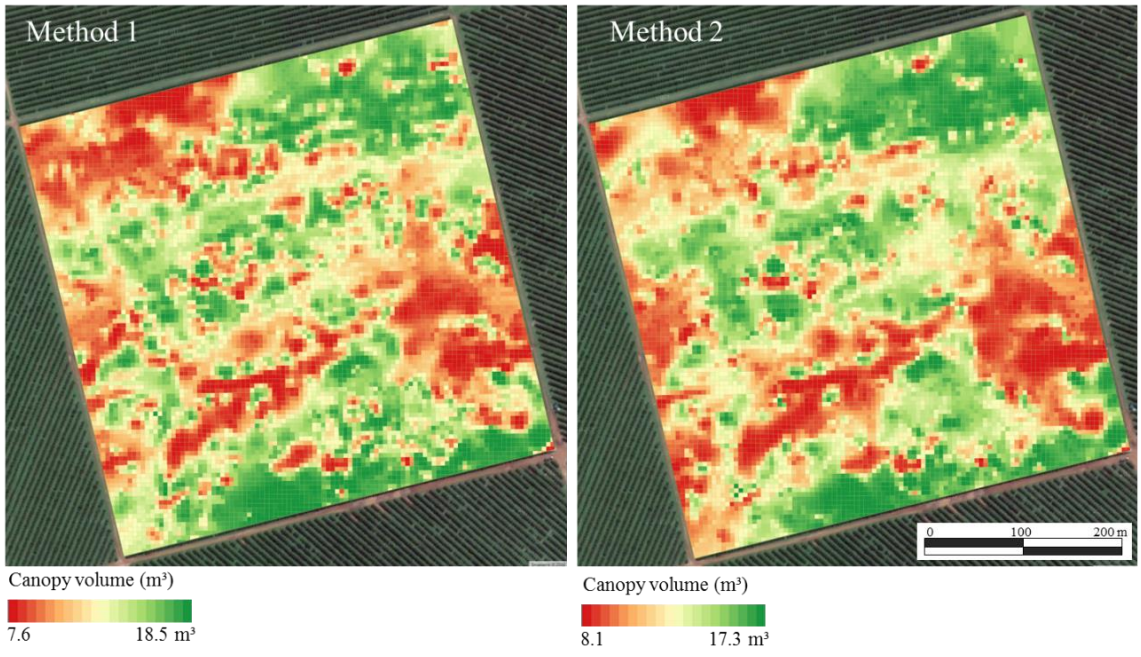

Figure 3.21: Canopy volume maps generated by two data processing methods: Alpha-shape modeled over individual trees (Method 1); Convex-hull modeled over sections of the row (Method 2)

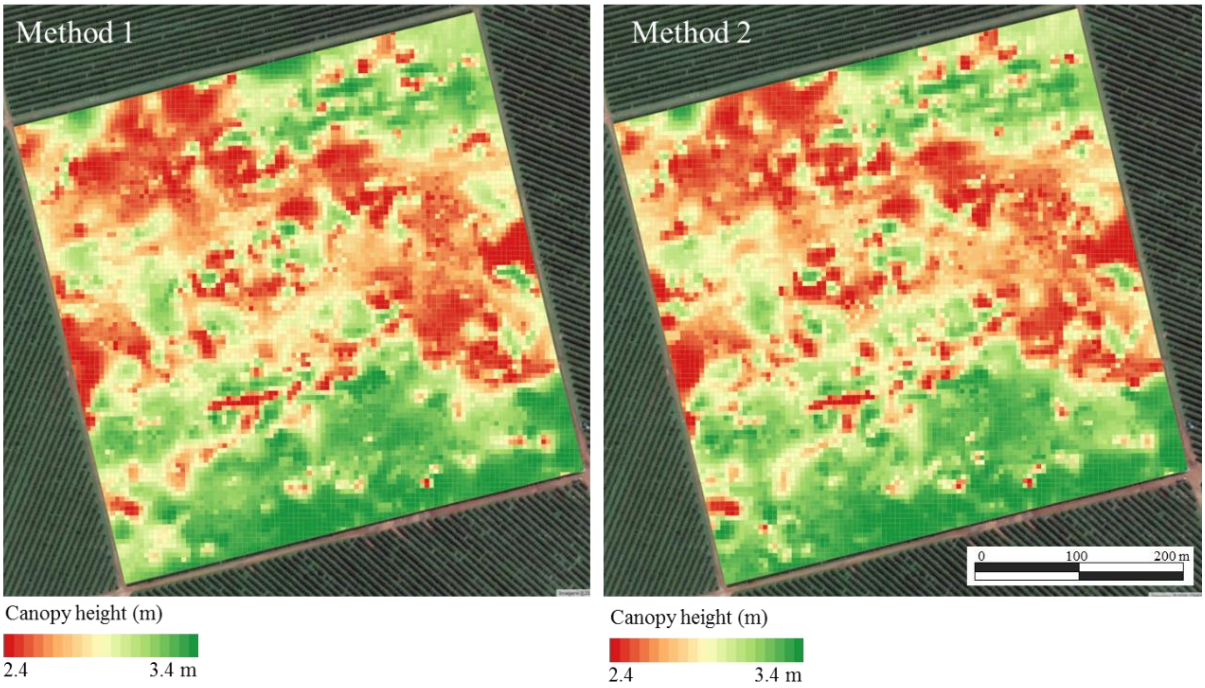

Figure 3.22: Canopy height maps generated by two data processing methods: Alpha-shape modeled over individual trees (Method 1); Convex-hull modeled over sections of the row (Method 2)

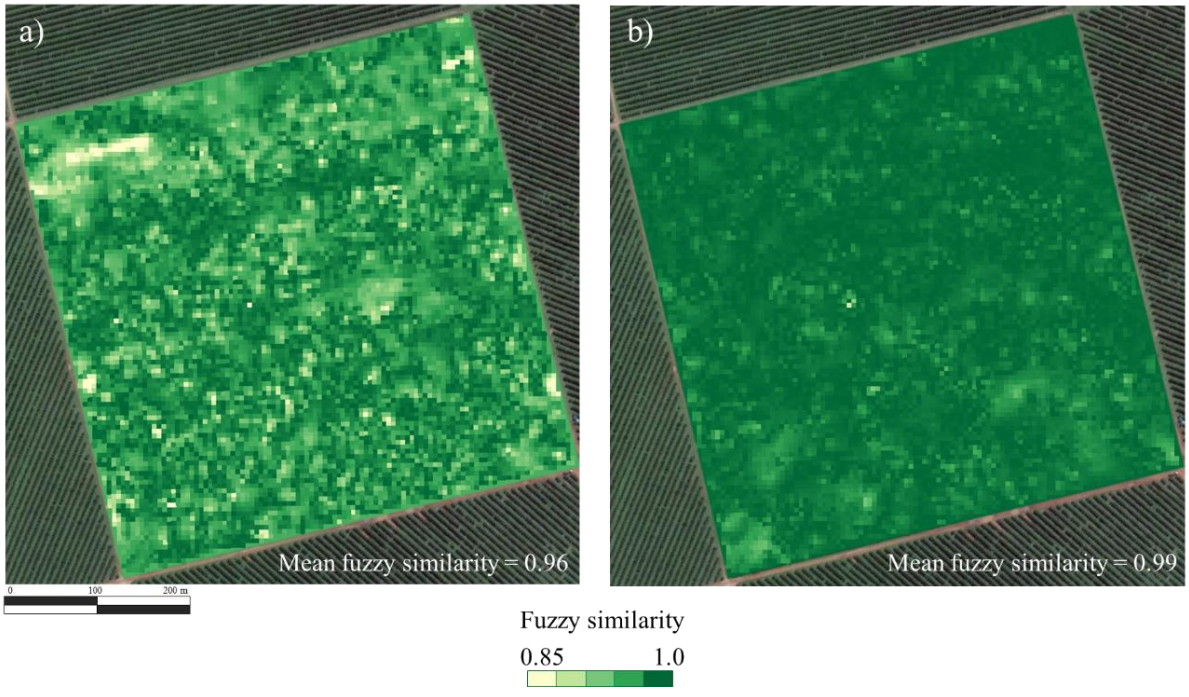

Figure 3.23: Fuzzy similarity maps resulted from the comparison between maps of canopy volume (a) and canopy height (b) generated by two different methods (cluster segmentation using alpha-shape reconstruction and transversal section segmentation using *convex-hull* reconstruction)

3.5. Conclusions

A methodology for 3D modeling and canopy geometry computation for orange groves was developed using a terrestrial georeferenced laser scanning system based on a LiDAR sensor. Variations over the data processing and 3D modeling algorithms were demonstrated and compared.

The method of data acquisition based on MTLS and 3D point cloud generation proved to produce reliable georeferenced point clouds of a commercial orange grove. The data acquisition set up was robust for large field scanning and could be implemented on current agricultural operations in the groves.

The *convex-hull* and *alpha-shape* ($\alpha = 0.75$) 3D modeling algorithms worked best when implemented over transversal sections of the row and over individualized plants, respectively. Nevertheless, the canopy volume and height maps produced by these two methods showed similar spatial variability in the evaluated grove. However, varying the type of segmentation of the cloud and the 3D modeling algorithms resulted in different values of canopy volume indicating the need for a reference method to be adopted. Nevertheless, the mapping of canopy volume and height by either cluster or section of the row resulted in similar maps.

The proposed data acquisition and processing systems were able to produce useful information for precision agriculture management. The LiDAR scanning and the proposed data processing and mapping reproduced the spatial variability in the grove in the format of thematic maps that can be used for variable rate applications and to guide management zones delineations within the grove. All the software used is open-source and freely available to any user.

References

AUAT CHEEIN, F. A. et al. Real-time approaches for characterization of fully and partially scanned canopies in groves. **Computers and Electronics in Agriculture**, Amsterdam, v. 118, p. 361–371, out. 2015.

AUAT CHEEIN, F. A.; GUIVANT, J. SLAM-based incremental convex hull processing approach for treetop volume estimation. **Computers and Electronics in Agriculture**, Amsterdam, v. 102, p. 19–30, mar. 2014.

COLAÇO, A. F.; MOLIN, J. P. Variable rate fertilization in citrus: a long term study. **Precision Agriculture**, Dordrecht, 13 maio 2016.

DEL-MORAL-MARTÍNEZ, I. et al. Georeferenced Scanning System to Estimate the LeafWall Area in Tree Crops. **Sensors**, New York, v. 15, n. 4, p. 8382–8405, 2015.

DEL-MORAL-MARTÍNEZ, I. et al. Mapping Vineyard Leaf Area Using Mobile Terrestrial Laser Scanners: Should Rows be Scanned On-the-Go or Discontinuously Sampled? **Sensors**, New York, v. 16, n. 1, p. 119, 2016.

ESCOLÀ, A. MARTINEZ-CASASNOVAS, J. A.; RUFAT, J. ARBONÉS, A.; SANZ, R.; SEBÉ, F.; ARNÓ, J.; MASIP, J.; PASCUAL, M.; GREGORIO, E.; RIBES-DASI, M.; VILLAR, J. M.; ROSELL-POLO, J. R. A monile terrestrial laser scanner for tree crops: point cloud generation, information, extraction and validation in an intensive olive orchard. In: EUROPEAN CONFERENCE ON PRECISION AGRICULTURE, 10., 2015, Tel Aviv. **Proceedings**... Wageningen: Wageningen Academic Publishers, 2015. p. 337 - 344.

FRIDGEN, J. J. et al. Management zone analyst (MZA): Software for subfield management zone delineation. **Agronomy Journal**, Madison, v. 96, p. 100–108, 2004.

HAGEN, A. Multi-method assessment of map similarity. In: AGILE CONFERENCE ON GEOGRAPHIC INFORMATION SCIENCE, 5., 2002, Palma. **Proceedings**… 2002.

LEE, K. H.; EHSANI, R. A laser scanner based measurement system for quantification of citrus tree geometric. **Applied Engineering in Agriculture**, St. Joseph, v. 25, n. 5, p. 777–788, 2009.

MENDEL, K. Rootstock-scion relationships in Shamouti trees on light soil. **Ktavim**, Rehovot, v.6, p.35-60, 1956.

ROSELL, J. R. et al. Obtaining the three-dimensional structure of tree orchards from remote 2D terrestrial LIDAR scanning. **Agricultural and Forest Meteorology**, Amsterdam, v. 149, n. 9, p. 1505–1515, set. 2009.

ROSELL, J. R.; SANZ, R. A review of methods and applications of the geometric characterization of tree crops in agricultural activities. **Computers and Electronics in Agriculture**, Amsterdam, v. 81, p. 124–141, fev. 2012.

SICK AG. Quick Manual for LMS communication setup - Hardware setup and measurement mode configuration. Version 1.1. 2002

SICK AG. Telegrams for Operating/Configuring the LMS2XX Laser Measurement Systems. Firmware version V.2.10/X1.14. 2003.

TUMBO, S. D. et al. Investigation of laser and ultrasonic ranging sensors for measurements of citrus canopy volume. **Applied Engineering in Agriculture**, St. Joseph, v. 18, n. 3, p. 367–372, 2002.

WEI, J.; SALYANI, M. Development of a laser scanner for measuring tree canopy characteristics: phase 1. Prototype development. **Transactions Of The Asabe**, St. Joseph, v. 47, n. 6, p. 2101–2108, 2004.

4. CANOPY VOLUME AND HEIGHT SPATIAL VARIABILITY AND SITE-SPECIFIC APPLICATIONS IN COMMERCIAL ORANGE GROVES

ABSTRACT

One key aspect when designing new site-specific management practices is the comprehensive understanding over the spatial variability of the fields. LiDAR technology trough mobile terrestrial laser scanners (MTLS) is able to provide with useful information about spatial variability of tree crop geometry. However, a general characterization of canopy volume and height variability in orange crops was not yet broadly explored by research. Once canopy variability is acknowledged, the sensor-based or map-based variable rate application of inputs is a suited solution to deal with canopy size variability. The relationship between canopy geometry and other relevant variables to the variability of crop performance should also be investigated in order to enhance site-specific practices. Therefore, the objective of this study was to characterize the variability of canopy volume and height in commercial orange groves in Brazil. In addition, it aimed to investigate the relationship between geometrical parameters of the trees with soil attributes and historical fruit yield. Five commercial orange orchards in São Paulo, Brazil, ranging from 10 to 25 ha, were selected to be scanned with a develop MTLS system based on LiDAR sensor. The canopy volume and height were computed for every 0.25 m section of the rows. The values of canopy volume and height of every ten adjacent sections were merged together and then interpolated into a 5 m pixel grid. A descriptive statistics and geostatiscal analyses were carried out to investigate the variability in canopy geometry. The input savings from sensor-based variable rate applications were estimated. Three out of the five initial groves were selected and their historical yield and soil map database were investigated. A pixel-based correlation analysis was carried out between the canopy geometry, yield and soil maps. One final analysis was performed in order to verify whether canopy geometry maps are effective on guiding the delineation of management zones within the groves. The selected groves were divided into three zones of different tree sizes. The mean values of historical yield and soil attribute were assessed for each zone and compared. The canopy volume and height of 0.25 m sections showed a coefficient of variation ranging from 31 to 41% and from 15 to 24%, respectively. The potential input savings provided by sensor-based variable rate applications were around 40% when compared to constant rate application base on the grove's maximum canopy volume. The canopy volume and height maps showed that these variables might significantly vary within short distances, but also large consistent regions of different tree sizes were recognized. The historical yield and soil database from the three selected groves showed that grove 1 was generally less variable with less temporal consistency then groves 2 and 3. Canopy geometry was more strongly related with yield and soil variables in groves 2 and 3 (R^2 up to 0.72). Nevertheless, the use of canopy volume and height information was successful on distinguishing zones of different yield performances and soil characteristics in all three groves. Given the variability found on canopy volume and height, this study proved the benefits of MTLS used for site-specific practices in commercial orange groves.

Keywords: canopy geometry; laser scanner; site-specific management; management zones; variable rate application

4.1. Introduction

Characterizing the spatial variability of different agronomical parameters and understanding the causes for such variabilities enables the development of new site-specific management strategies. The variables which are mostly investigated in precision agriculture research (plant or soil attributes) are usually assessed using georeferenced sampling or sensing techniques. Sensors have become important tools in the assessment of spatial variability due to their ability to collect a large amount of data with less effort than traditional sampling schemes.

Among the available technologies, the LiDAR scanning has showed potential for the site-specific management of tree crops. As exposed in Chapter 3, these systems are able to derive accurate 3D modeling of the canopies. The georeferenced data from mobile terrestrial laser scanners (MTLS) (based on LiDAR sensors) allows the assessment of the spatial variability of the tree geometrical attributes throughout large commercial groves. Once such variability is acknowledged, ranging sensors based on LiDAR or ultrasonic principles can be mounted on spreader or sprayer machines to guide variable rate application of inputs based on the variability of canopy size (SCHUMANN 2006b; GIL et al. 2007 and 2013; ESCOLÀ et al. 2013). This type of application on a single-tree basis can be performed in real time, by using prescription maps or even with the fusion of both techniques.

Some studies investigated the spatial variability in tree crops using ranging sensors and assessed the potential benefit of sensor-based variable rate applications. Zaman et al. (2005) and Schumman et al. (2006a) conducted ultrasonic sensor readings in a commercial orange grove in Florida. Through the analyses of histograms of canopy volume data, they found significant canopy size variation and a high occurrence of small trees due primarily to tree replacements. Zaman et al. (2005) performed variable rate applications of nitrogen using prescription maps and got up to 40% savings of fertilizer. In the spraying of vineyards, instrumented sprayers with ultrasonic sensors were designed in Spain for variable rate applications in real time. Gil et al. (2007) accounted average savings of 58% of pesticides. Later on, with a similar prototype, input savings reach up to 21% (Gil et al. 2013).

These studies have proven that sensor-based fertilizer spreading and spraying operations are viable alternatives to deal with canopy size variability in tree crops. Although real applications were performed through the design of machine prototypes, a general characterization of the spatial variability of large commercial groves was not yet broadly explored, especially with the use of MTLS. The variability in Brazilian groves is unknown and might be different from Florida due to different soil condition, disease occurrence and management practices. Therefore, the potential of sensor-based variable rate application for Brazilian orange groves is also unknown.

Besides the spatial characterization of geometrical parameters of trees, the relation of such parameters with other relevant field variables should be explored. Colaço and Molin (2016) showed the importance of soil electrical conductivity, soil texture, elevation and historical yield mapping in the understanding of spatial variability of crop performance and in guiding site-specific management strategies for orange groves in Brazil. The relationship between tree attributes and soil variables was also comprehensively assessed in two studies in Florida (ZAMAN and SCHUMANN, 2006 and MANN, SCHUMANN and OBREZA, 2010). The first study used the normalized difference vegetation index (NDVI) as the tree parameter. The latter actually used ultrasonically measured tree canopy volume together with NDVI as a growth indicator of the grove. Assessing the relationship between plant and soil attributes helped the authors delineating management zones in those groves and guiding different fertilization strategies in each zone.

The relationship between canopy geometry and other relevant variables was not yet assessed in Brazilian orange groves. Understanding such relationship is crucial for determining the use of geometrical attributes in the site-specific management of orange groves and in developing new site-specific management strategies based on canopy geometry.

4.2. Objective

The objective of this study is to characterize the variability of canopy volume and height in commercial orange groves in Brazil and assess the potential benefit of sensor-based variable rate applications of fertilizer and plant protection products. Secondly, it aims to investigate the relationship of the spatial variability of geometrical parameters of the trees with soil attributes and historical fruit yield. Lastly, this study evaluates the usage of the canopy geometry information on the site-specific management of orange groves.

4.3. Materials and Methods

4.3.1. Field characteristics

Five commercial orange groves located in the state of São Paulo, Brazil, were selected for this study. The general characteristics of these groves are listed in Table 4.1. These groves were grown in a rain-fed system. Grove 1 is the youngest and the tree rows were planted as straight lines that crossed over the terraces on the terrain contours (this is the same grove presented in Chapter 3). The groves 2 and 3 are older. These groves were also used in other research projects and they were chosen due to the availability of spatial database of different relevant variables (COLAÇO and MOLIN, 2016). The trees were fully developed and they are mechanically pruned every two years. The tree rows in these fields were implanted following the terrain contours (Figures 4.1.2 and 4.1.3). Groves 4 and 5 are smaller. They were chosen due to the higher occurrence of a disease infection that might affect the development and the geometrical attributes of the trees. The disease was the citrus trunk gummosis (*Phytophthora parasitica*), a fungal infection which can lead to a severe debilitation of the tree. Gaps and variation in canopy size can be seen in the overview photo of these groves (Figures 4.1.4 and 4.1.5).

Table 4.1: General characteristics of the orange groves used in this study

Grove	Location Latitude / Longitude (WGS84)	Variety Canopy/Rootstock	Area (ha)	Spacing Tree / Row (m)	Age (years)
1	-22°49'51.90" / -49°07'34.15"	Valencia / Swingle	25.4	2.6 / 6.8	6
2	-22°56'52.20" / -48°39'40.41"	Rubi / Swingle	25.7	4.0 / 6.8	12
3	-22°56'41.82" / -48°38'51.94"	Rubi / Swingle	25.7	3.5 / 7.5	11
4	-22°48'40.90" / -49°02'53.05"	Pera Rio / Sunki	10.8	2.3 / 6.5	8
5	-22°50'57.06" / -49°05'16.31"	Pera Rio / Caipira	12.1	2.6 / 6.8	9

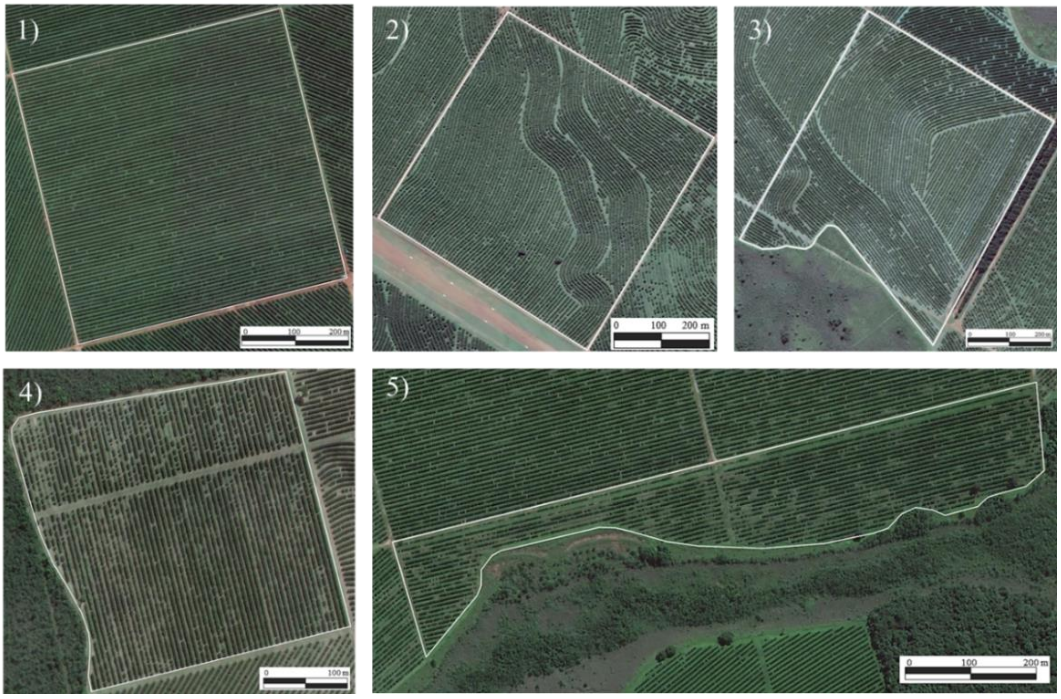

Figure 4.1: Overview of the orange groves 1 to 5 used in the study

4.3.2. LiDAR data acquisition and processing

The selected groves were scanned with a MTLS based on a LiDAR sensor in order to estimate and map the geometrical characteristics of the trees. The MTLS and data processing were based on the method described in Chapter 3. During the data acquisition, the vehicle moved along the alleys of the groves at a constant speed of 3 m s^{-1}. The scanning was performed at 75 Hz frequency with an angular resolution of 1º and the distance resolution set to mm. The canopy volume and height were computed along transversal sections of the rows. The length of each section was 0.25 m. The applied modeling algorithm was the *convex-hull*. Because the groves 2 and 3 were implanted as curved lines, the processing algorithm for segmenting the tree rows was adapted to suit this scenario as the segmentation method of the point cloud described in Chapter 3 was designed for tree rows implanted as straight lines. The segmentation algorithm requires a central line of the row in order to classify the point cloud into transversal sections. The central lines of the curve rows were obtained from the GNSS determined track of the vehicle along the two sides of each row. The row axis was computed by extracting the mid line between the two tracks.

4.3.3. Variability of canopy geometry and potential benefit of sensor-based variable rate applications

Prior to analyzing the LiDAR-derived geometrical data, a filtering step was carried out using the QGIS 2.10 software. The estimated values of canopy volume and height were imported into the software and a centroid point was created inside each section of the rows. The two geometrical attributes computed for each section were assigned to the centroid points. The points close to the beginning and ending of each row were excluded. In grove 1,

the points close to the terraces of the grove were also removed. A visual assessment of the point cloud, using the CloudCompare 2.6.1 software, was carried out in order to recognize undesired scanned targets (e. g., power poles, individual native trees inside the grove, etc) and spots where the point cloud was not generated correctly - due to malfunctioning of the sensor or rough and abrupt irregularities of the terrain. The centroid points within these spots were also excluded. The filtering process was performed manually.

After the filtering process, a descriptive statistic analysis was carried out with the remaining points (centroid points of each section) of each grove. A histogram was used to assess the data distribution for each variable (canopy volume and height) and grove.

In order to estimate the potential benefit of variable rate applications based on LiDAR sensors, different scenarios of input application (fertilizer or spraying) were designed based on the canopy volume data. The input consumption was considered directly related to the canopy volume. The amount of input was predicted in each field considering a constant rate for conventional application and considering the canopy volume for the sensor-based variable rate applications. In this study, it was considered that the farmers could calculate the application rate based on three different scenarios: the maximum, the average and the mode value of canopy volume from a set of sampled canopies in the grove. Adopting the maximum canopy volume as a base for constant rate applications is usually recommended as a safety strategy since the dose to be applied should cope with the worst situations and avoid disease and pest reinfection. However, it is noticed in the Brazilian groves that the average canopy volume is usually adopted and often very few trees are sampled. Besides, the conventional prescription is based on manual estimations of canopy volume, which might differ significantly from the MTLS derived volumes, as shown in Chapter 3.

In order to exclude the random error of the sampling, the actual estimation of the constant rate was based on the entire data, not on sampling. The average and mode canopy volume values were computed from the data, and the maximum canopy volume was given as two standard deviations above the average (considering that even with good sampling the grower would not find the absolute maximum canopy volume in the grove). Simulated variable rates followed the actual canopy volume of each transversal section of the row. The input consumption and the accuracy of each application method were compared among different scenarios in each grove.

4.3.4. Spatial variability of canopy geometry

To analyze the spatial variability of the groves the data were manipulated and prepared for geostatistical analysis and interpolation. After the filtering step over the centroid points of each section, adjacent points along the row were merged together into a central point, so they could represent larger segments of the row equivalent to individual trees (Figure 3.10). The number of merged points along the row for each field was based on the tree spacing of the grove; *e. g.* given that the centroid spacing was 0.25 m, if the tree spacing was 4 m, as in grove 2, the number of merged points was 16 (equivalent to one tree); if the tree spacing was not multiple of the point spacing, the number of merged point was rounded up. The values of volume and height assigned to the central point was the sum of the volume and the highest height of the merged sections, respectively. The objective of this step was to mask the within plant variability of volume and height, even though the merged points did not necessarily match the center of each tree individually. This step enabled better interpretation over the geostatistical analysis and the field's spatial variability.

With the new set of points a geostatistical analysis and an ordinary kriging interpolation was carried out using a pixel grid of 5 m. The canopy volume and height maps were generated for each grove using the Vesper 1.6 software and final editing of the maps was done using the QGIS 2.10 software.

4.3.5. Relationship between tree geometry, soil attributes and historical yield

To explore the possible causes of canopy variation and its relation with other agronomical parameters, a historical spatial database from groves 1, 2 and 3 was analyzed. The collected data were elevation, soil apparent electrical conductivity (ECa), soil texture and soil organic matter. These parameters were chosen due to their temporal stability, which considering a perennial crop, should affect the development of the crop throughout its lifetime. A series of yield maps was also analyzed.

The final maps were produced by interpolation of the original data, using ordinary kriging. To enable comparison with the canopy volume and height maps, the same 5 m pixel grid was used in all maps. The Vesper 1.6 and QGIS 2.10 software were used for interpolation and final editing of the maps.

Mapping of elevation and soil attributes

Elevation data was derived from the GNSS receiver track data during the LiDAR scanning (Figure 4.2). For soil texture and organic matter, georeferenced soil samples were collected throughout the fields. These data were available from other experiments carried out in those groves. 25 soil samples were collected in grove 1 (approximately one sample per hectare) and 50 in groves 2 and 3 (approximately two samples per hectare).

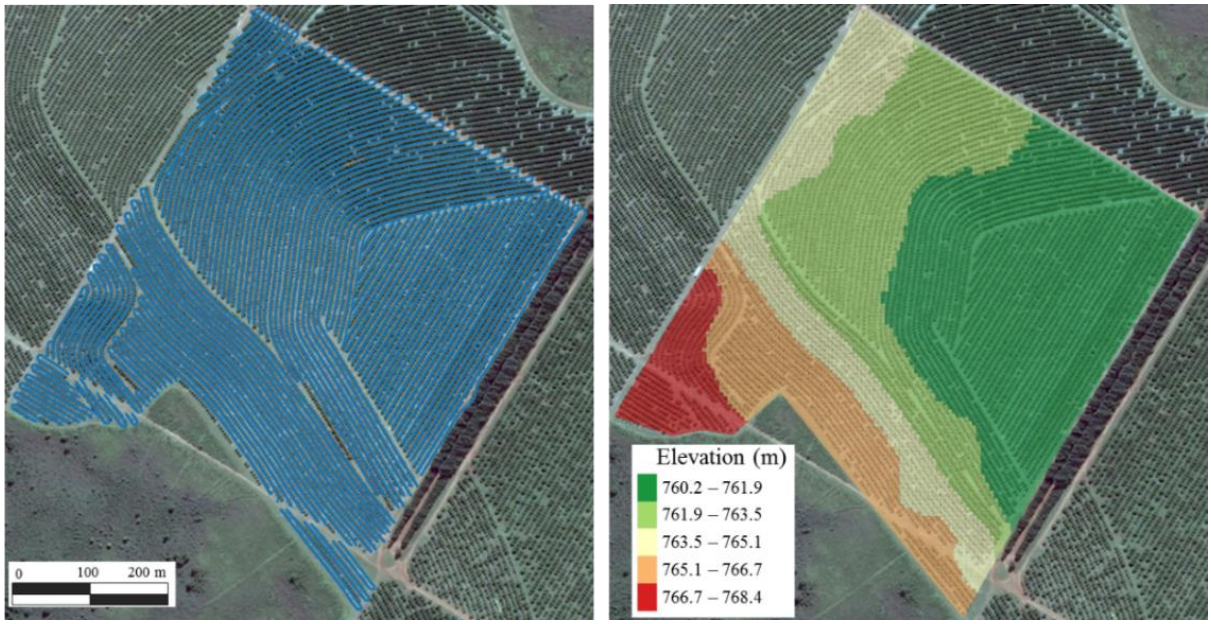

Figure 4.2: Elevation map derived from MTLS tracks in the grove

The soil ECa was obtained by using a Veris 3100 sensor (Veris Technology, Salina, USA). This instrument presents six electrodes which are inserted in the soil (Figure 4.3) and collects ECa data from two depth layers of approximately 0 – 0.3 m and 0 – 0.90 m. Given the similarity found between the two layers, only the shallow data

was used for analysis. The sensor was pulled by a tractor along the alleys of the groves at 2.8 m s^{-1}. The soil ECa data along with the GNSS coordinates were collected at a frequency of 1 Hz. Before generating the final map, discrepant values (exceeding two standard deviations from the average) were excluded. A local search for outliers was also carried out by applying the method proposed by Spekken, Anselmi and Molin (2013).

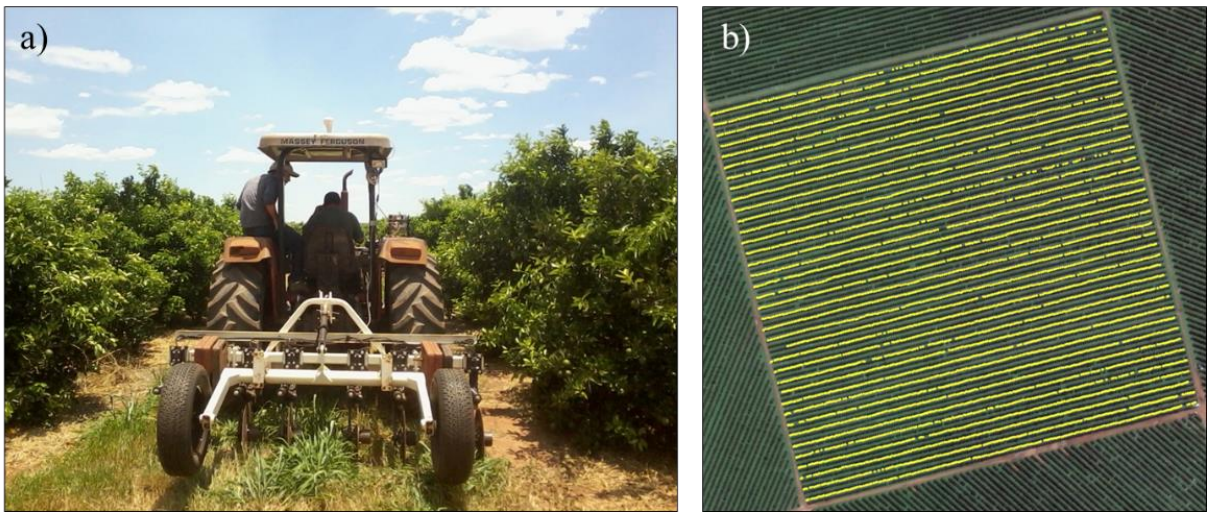

Figure 4.3: Veris sensor used to collect soil ECa data (a); georeferenced reading from the sensor in grove 1(b)

Yield mapping

Yield data were collected from 2012 until 2015 in grove 1 and from 2008 until 2013 in groves 2 and 3. Those data were also derived from other experimental activities carried out in those fields. The harvest of the fruits was manual so the method for yield mapping should suit the manual harvest procedure. During the harvest, the pickers used 'big bags' to store the fruits in the field while they carried out their harvesting work. To collect yield data, the location of these bags was georeferenced using a common navigation GNSS receiver (coarse acquisition code - C/A, accuracy of approximately 3 m). Yield values were calculated locally for each point based on the mass of the bag and the area which it represented in the field. The mass of each bag was visually estimated by the harvest crew leader (groves 2 and 3) or kept constant as 540 kg (grove 1). This visual estimation showed errors below 4% in Molin and Mascarin (2007) and Molin et al. (2012). The corresponding area of each point was computed using the 'Voronoi polygon' tool available in the QGIS software. This algorithm divides the field into smaller polygons, each corresponding to the coverage area of one point (Figure 4.4). The boundaries of those polygons are given by halving the distances between the point and its neighbors. The final yield value was calculated simply by diving the mass of the bag by the area of the 'Voronoi polygon' and converted into Mg ha^{-1}. This value was assigned to a centroid point inside each polygon. Given the logical of the Voronoi tool, the 'big bags' end up not in the centroid position of the polygon. Finally, the data were interpolated to produce the final yield map.

The logic behind this yield mapping technique is that yield should be higher with higher concentration of points throughout the grove. Similar methods were shown by Molin and Mascarin (2007), Molin et al. (2012) and Colaço and Molin (2016). Colaço et al. (2015) tested the Voronoi-based method against a modeled reference yield map. Results showed that this method is able to replicate the true spatial variability of yield with great level of detail. The comparison of the final interpolated yield map against the reference yield map showed an average error of 15 %.

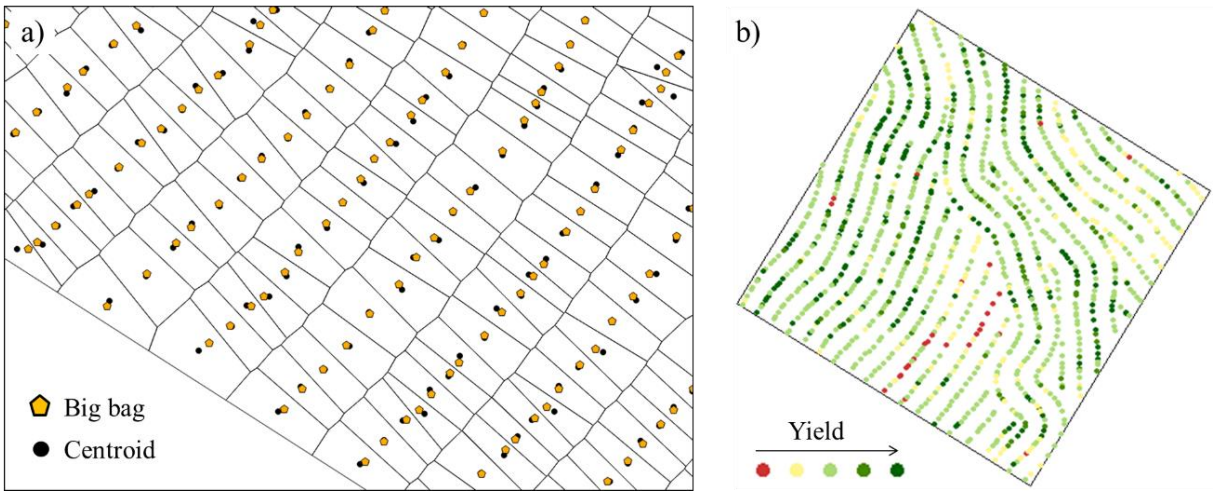

Figure 4.4: Georeferenced big bags and computed 'Voronoi' polygon (a); calculation of local yield in each point

Data analysis

A descriptive statistics analysis was carried out over the data from the yield maps, soil attributes, elevation and canopy geometry. A visual assessment of these maps was conducted in order to identify patterns in the spatial variability. Finally, a pixel-based correlation analysis was performed for each pair of maps.

Given the correlation found between canopy geometry and the soil and yield database, one additional analysis was performed in order to evaluate whether the canopy geometry is a suitable variable to guide management zones delineation in an orange grove. For that matter, based on the canopy volume map, the groves were classified into three classes of canopy volume: large, medium and small. The pixels from the canopy volume map were classified using the software MZA (management zone analyst) (FRIDGEN, 2004) by the fuzzy k-means clustering algorithm. Afterwards, using the R software, the average values of the different variables were computed for each zone and the Tukey test was performed ($p > 0.001$) to assess the differences between the three zones in the groves. This analysis was inspired by a similar study by Mann, Schumann and Obreza (2010).

4.4. Results and Discussion

4.4.1. Variability of canopy geometry and potential benefit of sensor-based variable rate applications

The filtering step over the data of transversal sections resulted in a different amount of data between the groves, even when the area of the fields were similar (Table 4.2). Descriptive statistics showed that, as expected, the average volume and height of the canopy sections were greater in the older groves (groves 2 and 3) (Table 4.2). The volume of sections in the evaluated groves presented a coefficient of variation between 31 and 36%, with exception of grove 5, which reached a coefficient of variation of 41%. The smallest variation was found in grove 1, which is the youngest grove. Greater variation was expected in groves 4 and 5 due to higher disease infection. The height coefficient of variation was lower than the variability of volume in all groves. It is noticed through the histograms that the height values were closer to the average than the canopy volume values (Figure 4.5). This is evidenced by the

lower kurtosis in the canopy volume histograms. The canopy volume is a more complex geometrical variable than height, and it was more variable in the fields than the canopy height.

Table 4.2: Descriptive statistics of canopy volume and height computed for 0.25 m sections along the crop rows

Grove	Canopy Variable	Mean	Med.	Mode	Min.	Max.	St. Dev.	C.V.	Kurt.	Skew.	Count
		---------- m³ (volume) or m (height) ----------									
1	Volume	1.22	1.23	1.30	0.00	3.33	0.38	0.31	0.80	0.06	96647
	Height	2.53	2.56	2.70	0.45	3.80	0.38	0.15	2.32	0.79	96647
2	Volume	2.54	2.64	3.20	0.01	5.36	0.87	0.34	0.50	0.31	124594
	Height	3.86	3.94	4.11	0.45	5.48	0.61	0.16	2.74	1.25	124594
3	Volume	2.60	2.69	3.20	0.00	5.42	0.93	0.36	0.34	-0.32	97880
	Height	3.89	3.98	4.17	0.46	5.48	0.72	0.19	2.94	-1.30	97880
4	Volume	1.47	1.54	1.65	0.02	3.43	0.50	0.34	0.72	-0.80	57589
	Height	2.75	2.87	2.96	0.46	4.01	0.59	0.21	3.56	-1.78	57589
5	Volume	1.42	1.50	1.70	0.00	3.62	0.59	0.41	-0.37	-0.42	59202
	Height	2.98	3.16	3.33	0.46	4.57	0.71	0.24	1.59	-1.40	59202

* Header abbreviations: Median (Med.); Minimum (Min.); Maximum (Max.); Standard Deviation (St. Dev.); Coefficient of Variation (C.V.); Kurtosis (Kurt.); Skewness (Skew.)

The histograms of canopy volume and height were asymmetric, especially for canopy height, with negative skewness (Figure 4.5). The distribution of canopy volume and height were closer to a normal distribution in grove 1. The negative skewness is caused by a large number of relatively smaller plants in the field. Through the histograms of canopy height, it is noticeable a thin tale in the left side of the distribution indicating the presence of very small trees in the grove. This is also noticed in the canopy volume histograms of groves 4 and 5. This is probably due to tree replacements. Those small trees are presented in a relatively higher frequency in groves 4 and 5, as expected due to higher disease occurrence. In the canopy volume and height histograms in grove 4 it is noticeable a second smaller pick in the left side. This might suggest that these small trees were replaced at the same occasion, whereas in the other groves, trees were replaced continuously in a steady pace.

Although the canopy volume histograms are also negatively skewed, this thin left tale is not present as in the canopy height histograms, at least for groves 1, 2 and 3. It is seen that canopies of small volume were more frequent than canopies with small height. In the correlation graphs between canopy volume and height in Figure 4.6, it is noticed that canopies with small volumes presented either shorter or taller heights (see in the regression graphs that for a fixed small value of canopy volume a broader range of canopy heights is noticed). This fact increases the frequency of small canopy volumes in relation to small heights. The negative skewness of the histograms of canopy volume in groves 2 and 3, and the relatively high frequency of volumes smaller but close to the average, indicates the presence of regions in the field with smaller canopy volumes. A generalization of these results indicates that very small trees from replacements are easily recognized from the histograms of canopy height, whereas the variation of canopy size due to different conditions in the field (*e. g.* regions with different soil fertility) are more evident in the canopy volume histograms.

The variability of ultrasonically measured canopy volume in a commercial orange grove in Florida was presented in the studies by Zaman, Schumann and Miller (2005), Zaman and Schumann (2005), Schumann et al. (2006a) and Zaman, Schumann and Hostler (2006). Schumann et al. (2006a) pointed out a significant variability on

tree canopy volume, ranging from less than 5 up to 245 m³ per tree. The histogram of tree canopy volume reveled three peaks representing the trees from the original planting plus two main resets. The 17 ha grove was over 40 years old at the time of the studies. The comparison between the studies from Florida and the results found in the present work, pointed out an important difference between the citrus management in the two countries. In Brazilian groves, the trees in one grove are entirely replaced every 20 years, approximately. Whereas in Florida, the original trees are kept for an indeterminate time and the trees are individually replaced as they turn ill or unproductive. These management strategies are reflected in the variability of canopy size, which is expected to be higher in Florida.

The relationship between height and volume of the 0.25 m sections was strong in all fields (Figure 4.6). The coefficient of determination ranged from 0.73 until 0.86, with a powered regression fit. This result suggests that canopy volume might be estimated (with a certain level of error) based on the canopy height. The mean square error of the regressions were 0.21, 1.96, 0.50, 0.23 and 0.27 m³ in groves 1 to 5, respectively. Based on the shape of the point cloud in the scatterplots it is noticed that the increase in height was not followed by an equal increase in volume, *i. e.* the plants first grow in height and later in volume.

These results have a significant impact in the current method of canopy volume estimation and spraying practices in Brazilian citrus groves. The per tree canopy volume is currently considered as a cube containing the tree. As exposed in Chapter 3, this method is extremely simplistic and inaccurate. Besides, it is time consuming resulting in few plants being measured. The high correlation found between canopy volume and height indicates that a simple measurement of height can be used to predict the canopy volume more accurately even if the purpose of this measurement aims to a constant rate application.

Since a significant variation in canopy volume and height was found in the evaluated groves it is reasonable to expect that sensor-based variable rate applications might provide a more rational use of inputs. In studies performed in Florida, this was already assessed proving the benefit of this technology. A variable rate application scenario was defined as if the application of plant protection products or fertilizers would employ proportional rates directly related with the canopy volume (*i e.* larger plants receive higher amount of inputs and *vice versa*). Operational application errors were not considered. The input savings obtained by this approach varied according to the way the constant rate was calculated. When the constant rate was stablished based on the average canopy volume, the total amount of input consumption would be equal to the amount applied with variable rate technologies. However, when the constant rate was determined based on the maximum canopy volume sampled in the grove (in this study, defined as two standard deviations above the average canopy volume), significant input reduction would result from variable rate applications. The over application caused when using a constant rate were generally close to 40% in the evaluated groves, reaching up to 45% in grove 5 (Figure 4.7), which is close to the results found by Zaman, Schumann and Miller (2005) of 40% saving on nitrogen fertilizer in an orange grove. Most studies pointed out in the literature review section showed savings around 30 to 40% on plant protection products in several different crops. If the approach adopted by the conventional treatment (constant rate), was based on the canopy volume of higher frequency (the mode value) the input consumption would be lower, as well as the input savings by the variable rate application. These over applications ranged from 6 up to 20% (Figure 4.7). It is to be noticed that constant rates were estimated based on MTLS derived volumes. In conventional practices those rates are based on manual estimations of canopy volume, which, as discussed, might differ significantly from estimations based on MTLS.

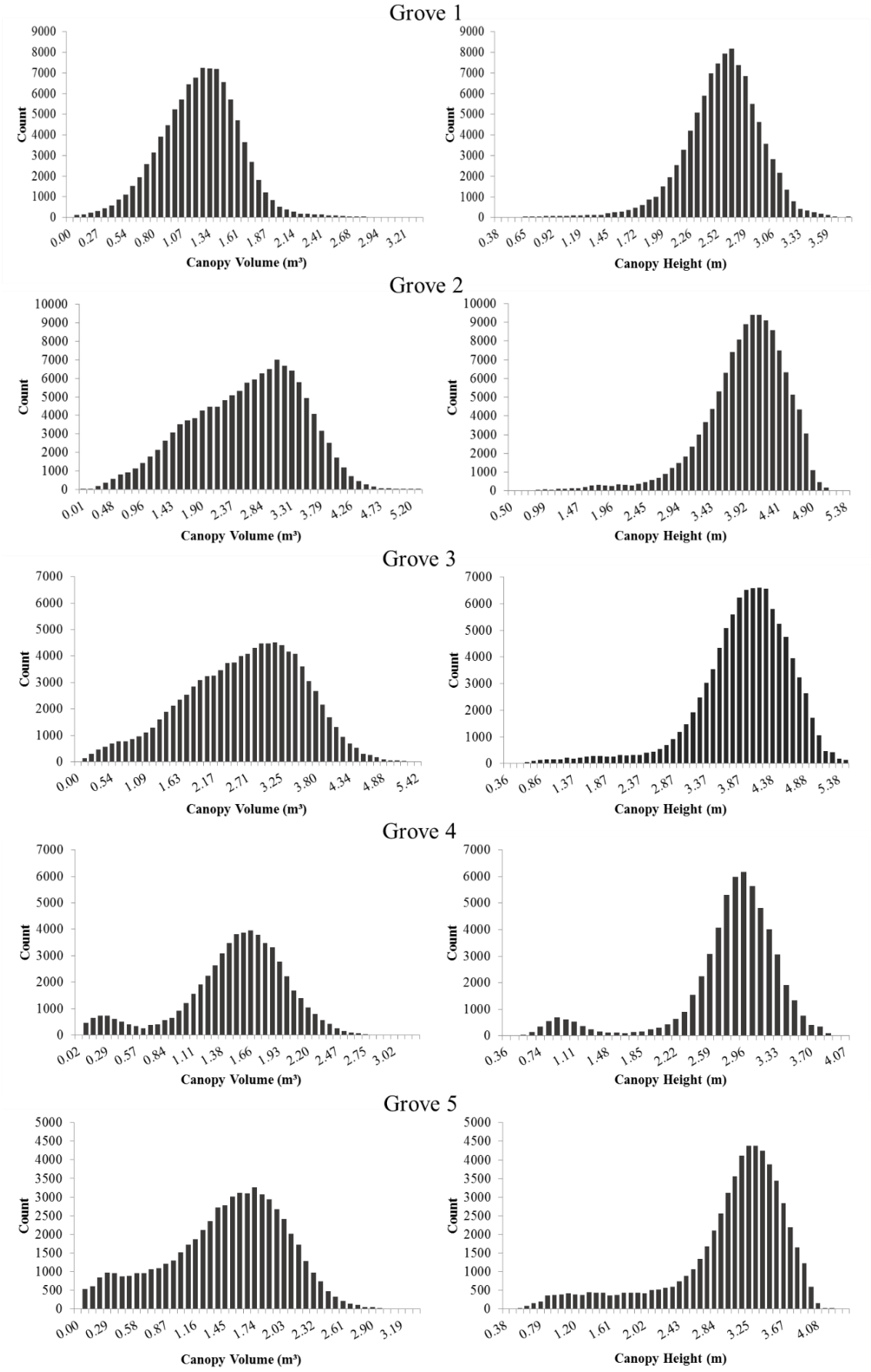

Figure 4.5: Canopy volume (left) and height (right) histograms for 0.25 m sections along the crop rows

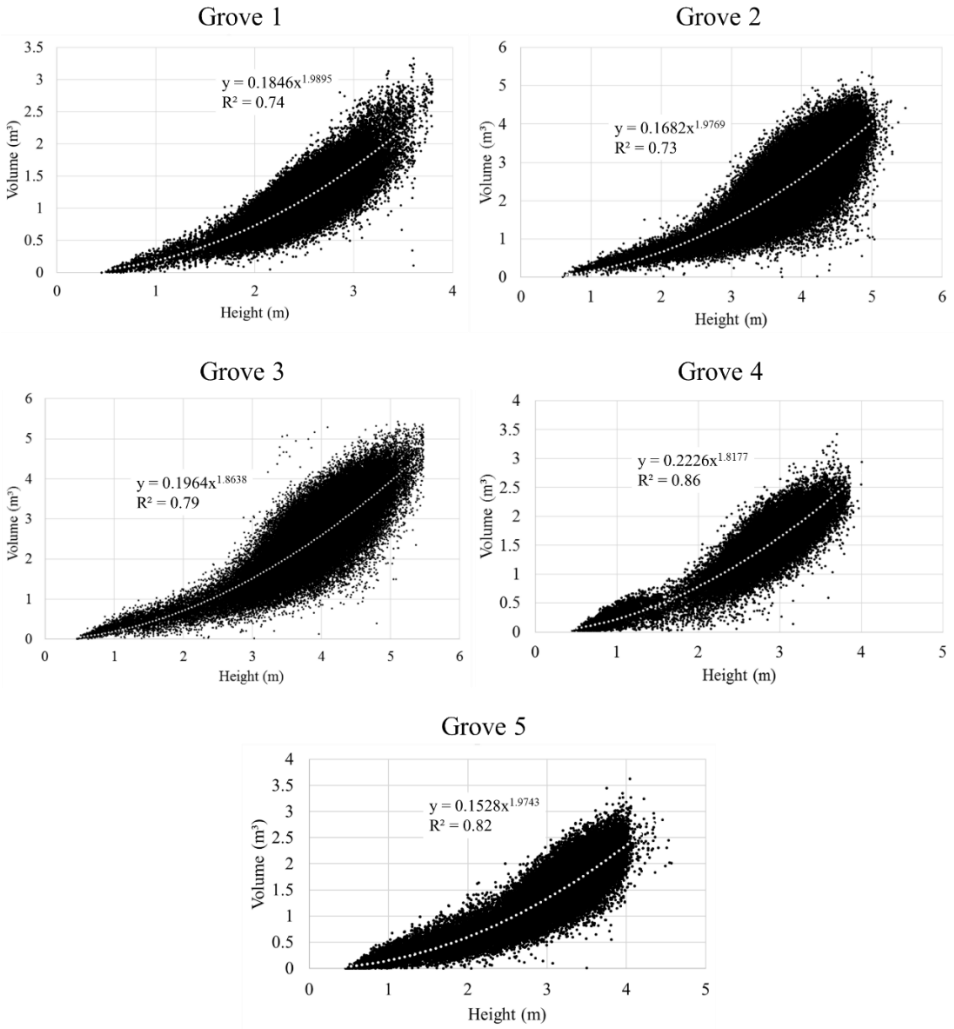

Figure 4.6: Regression analysis between canopy volume and height

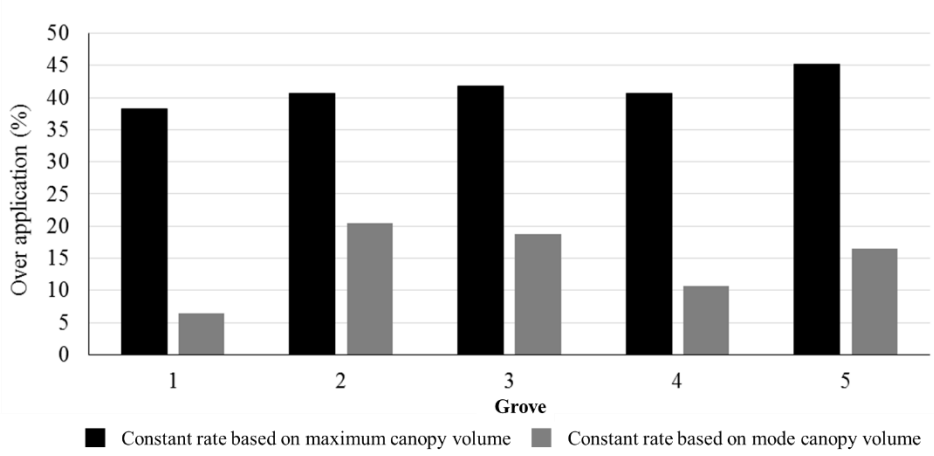

Figure 4.7: Over application of inputs based on a constant rate prescription

Besides the evaluation of the total amount of input used in each scenario and the potential input savings when using sensor-based variable rate applications, it is worth analyzing the accuracy of the conventional application by estimating the amount of canopies with over dosage or under dosage and the magnitude of such dose deviations. The graphs in Figure 4.8 shows the percentage of canopy sections in the grove (*y* axis) which would receive at least a

certain level of under or over dose in each application method (*x* axis). Steep inclination of the curves means that the amount of sections with dose deviation quickly decreases as the magnitude of the error increases. It is to be noticed that when the constant rate is defined based on the maximum canopy volume, nearly 100% of the trees would receive more product than necessary. If the application rate is based on the mode canopy volume, the over dosage is significantly reduced, however, under dosage errors starts to occur in the groves. For both approaches, the over dosage would affect more trees than the under dosage, which is not true for the constant rate based on the average canopy volume. In the graphs that the orange lines representing this approach start from the *y* axis with larger percentage of canopies with under dosage. This is a reflection of the distribution frequency of the canopy volume of these groves (Figure 4.5). Due to a large number of small plants in the grove, the average value of canopy volume is pulled down, getting further from the median value (which divides the distribution into two equal size number of sections). For that reason under dosage is more frequent than over dosage when the constant rate is based on the average canopy volume. The mode and (obviously) the adopted maximum values were greater than the median value of canopy volume. For that reason, over dosage was more frequent than under dosage. As the analysis is carried out in more intensive dose deviations (increasing the value on the *x* axis) the over dosage prevailed over the under dosage in all scenarios of constant rate. This is because in the extremities of the canopy volume distribution, smaller plants were more frequent in all groves.

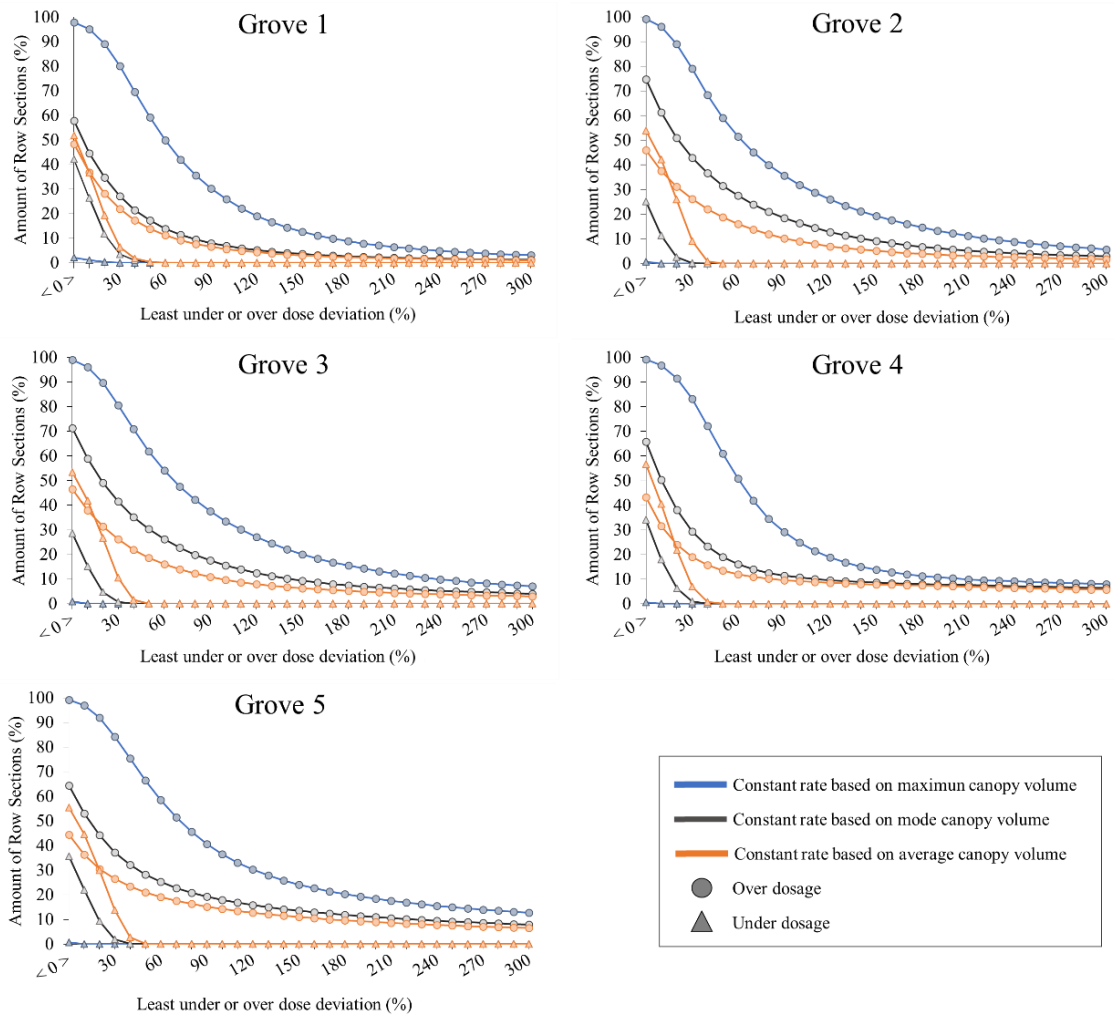

Figure 4.8: Amount of 0.25 m tree sections with increasing dose deviation (over or under supply of inputs)

4.4.2. Spatial variability of canopy geometry

Geostatistical analysis showed that canopy volume and height usually presented weak spatial dependence, since the nugget variance (C0) occupied a significant portion of the sill variance (C0+C1) (Figure 4.9), especially in the grove 1. Mann, Schumann and Obreza (2010) found a moderate spatial dependence on the canopy volume variogram in an orange grove in Florida (about 50% nugget/sill ratio). The weak spatial dependence means that these geometrical attributes varied significantly within short distances in the groves. The spatial dependence of canopy height was weaker than of canopy volume. The range was also shorter in the canopy height variograms. The range of these variables varying from 50 to 120 m, approximately, indicates that there were large regions in the groves with distinct canopy sizes (Table 4.3).

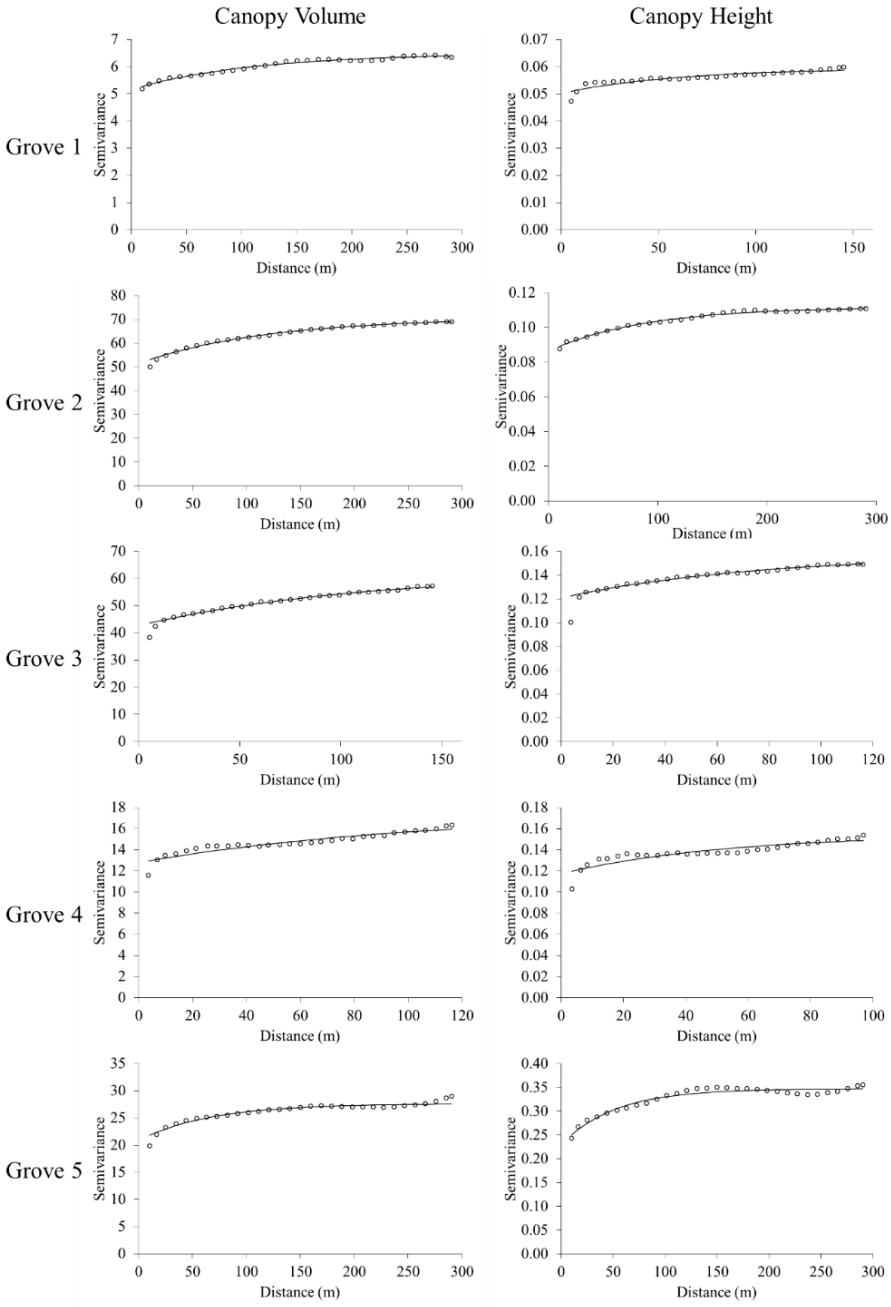

Figure 4.9: Variogram of canopy volume and canopy height in different groves

Table 4.3: Variogram parameters for canopy volume and canopy height from geostatistical analysis

Grove	Variable	C0	C1	A (m)	C0/C0+C1
1	Volume	5.16	1.33	111.20	0.80
	Height	0.05	0.01	59.35	0.85
2	Volume	51.49	19.12	117.80	0.73
	Height	0.09	0.03	88.25	0.77
3	Volume	42.65	19.38	109.00	0.69
	Height	0.12	0.04	75.15	0.77
4	Volume	12.78	4.69	103.90	0.73
	Height	0.12	0.04	51.86	0.76
5	Volume	20.85	6.76	66.47	0.76
	Height	0.23	0.12	51.22	0.66

* Header abbreviations: Nugget variance (C0); spatial dependent variance (C1.); range (A)

The maps of canopy volume and height (Figure 4.10 and 4.11) showed to be similar through visual assessment and were normally strongly correlated (Table 4.4). As pointed before, the canopy height might be a good estimator of canopy volume. The canopy height maps showed very similar variability patterns in the groves to the canopy volume maps. It indicates that the canopy height map can be used for spatial variability investigation when the measurement of canopy volume is not possible.

Some disagreements between these maps were more evident in grove 1. The coefficient of correlation of the canopy volume and height maps in grove 1 were significantly lower than in the rest of the groves. When the regression analyses were carried over the original data of row sections (and not with the merged sections approach) this lower correlation in grove 1 did not occurred (Figure 4.6). It means that in this specific grove, the correlation between canopy volume and height was higher when analyzing row sections instead of larger segments (representing the tree scale variability) of the row. As explained before, when adjacent sections are merged together the final data does not necessarily match the position of the individual trees. As exposed in Chapter 3, the relationship between maps of volume and height was slightly higher when the comparison was carried from individualized plants (using cluster analysis) ($r = 0.71$). In the present analysis, this effect is noticed only in grove 1 since this is the youngest grove and the trees did not completely filled up the gaps between each other. In the remaining groves, since these are older and trees are larger, a more continuous vegetative wall was already formed along the rows, so de effect of mismatching of the merged sections is not an issue. The choice of the merged sections approach to analyze the spatial variability in grove 1 was made in order to keep the same method for all groves. If the clustering segmentation approach was applied in all fields a greater error of classification would occur in groves 2, 3, 4 and 5. Besides, as exposed in Chapter 3, if the segmentation approach is different (clustering or sections) the optimal 3D modeling algorithm (*alpha-shape* or *convex-hull*) also varies.

Table 4.4: Correlation between maps of canopy volume and height

Grove	Coefficient of correlation
1	0.61
2	0.81
3	0.90
4	0.88
5	0.90

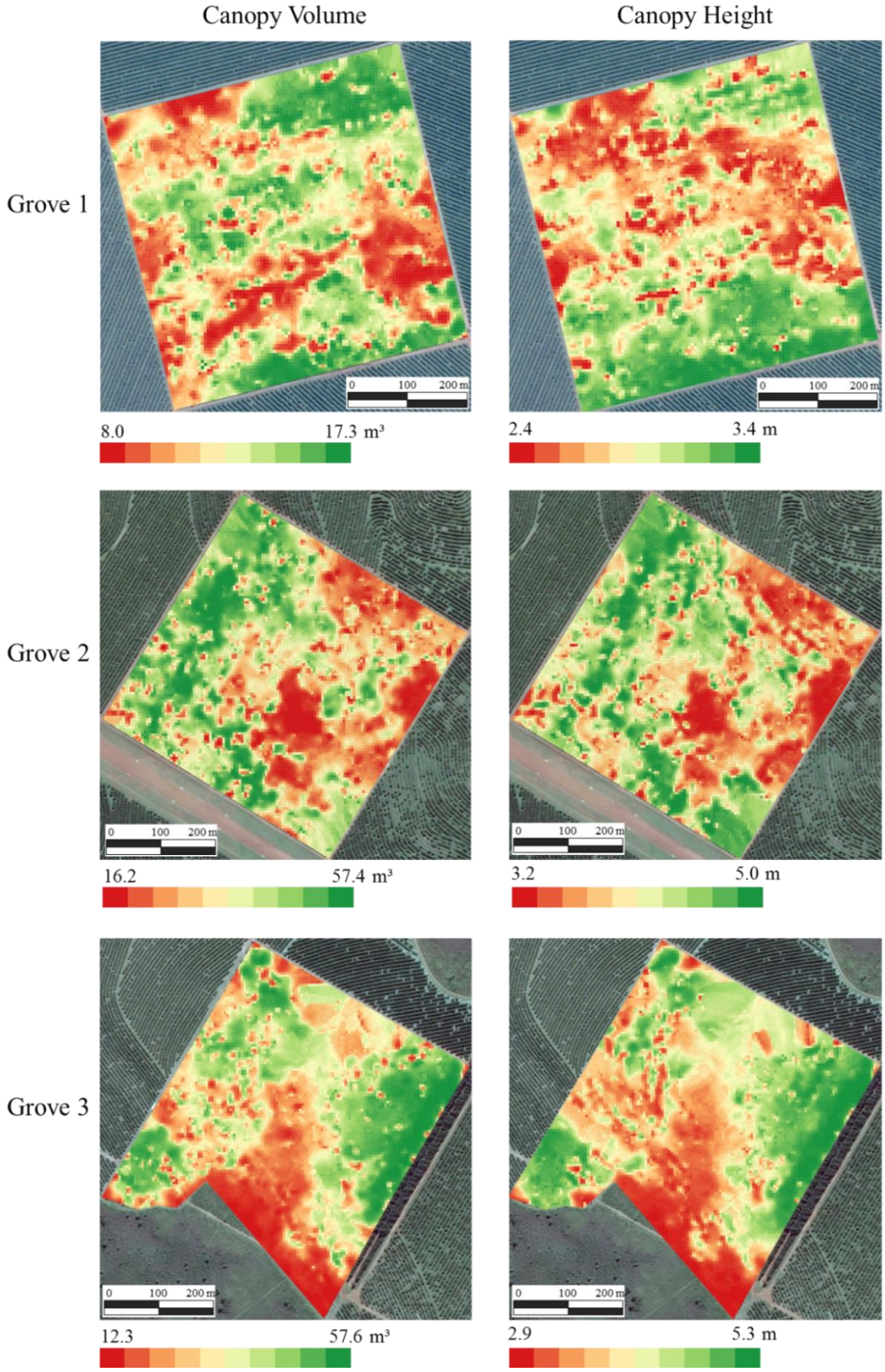

Figure 4.10: Canopy volume and height maps of in groves 1, 2 and 3

Regarding the shape and size of the variability zones in the maps of canopy volume and height (Figure 4.10 and 4.11), as a reflection of the geostatistical results, it is noticed either variation in short distances as well as large regions with similar canopy size. The appearance of these regions indicates that these groves can be divided

into different zones for site-specific management. Zaman and Schumann (2006) and Mann, Schumann and Obreza (2010) have approached this strategy, indicating that tree growth indicator such as canopy volume or NDVI are good options to segment the grove into distinct management zones. It is noticed that each grove could be divided into at least two management zones, one with larger trees and another with smaller trees. This delineation would enable different fertilization strategies for each zone. However, the establishment of different fertilizer prescriptions and how the differences in canopy size should be interpreted depends in a more profound understanding of the soil spatial variability in each grove.

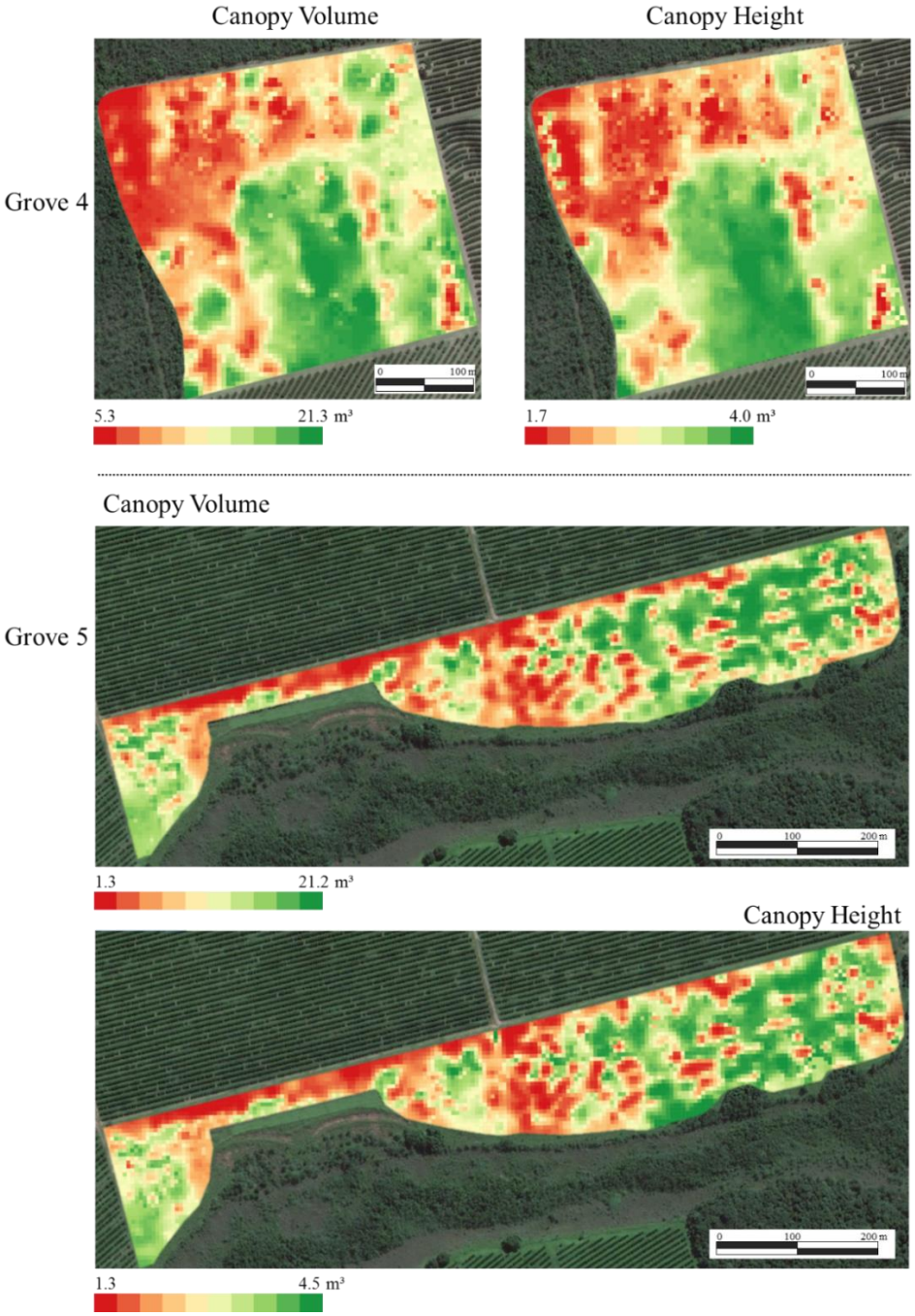

Figure 4.11: Canopy volume and height maps in groves 4 and 5

4.4.3. Relationship between tree geometry and soil attributes and historical yield

A database of soil and historical yield maps from groves 1, 2 and 3 were analyzed in order to understand the relationship between canopy geometry and other variables. Grove 1 has a more recent collection of yield maps, including the yield map from the same year as the laser scanning (2015). The other groves have a larger amount of yield maps; however, they are not as recent. The first noticeable fact when visually analyzing the maps from grove 1 is the lack of consistency in the variability patterns especially for the yield maps (Figure 4.12). This is evidenced by a general low coefficient of correlation between them (Table 4.6). The coefficient of variation of yield was also generally low, ranging from 7 to 13% (Table 4.5).The range of soil organic matter, clay content and soil ECa were also very low (Table 4.5), even though there is a 12 m variation in elevation. The resemblances between these soil maps is not very clear, but they might be perceived with a careful visual assessment. The correlation between these maps ranged from 0.48 to 0.61 (Table 4.6).

It is clear that such variability in soil did not reflect over the variability of yield. Higher yield usually occurred in the lower parts of the grove (see negative correlations in Table 4.6). However, the spatial patterns were not consistent throughout the years. There are numerous factor, besides soil variables, that might have affected the variability of yield in this grove.

The canopy volume usually got higher correlation with other variables than the canopy height. However, the variability found in the maps of canopy volume and height (Figure 4.10) also did not match clearly with any of the other variables. In fact, the coefficient of correlation was usually low, reaching between 0.2 and 0.3 in the best cases. As mentioned for the yield maps, the variability of the crop development did not follow the soil variability.

Table 4.5: Descriptive statistics from map data in grove 1

Variable	Unit	Mean	Minimum	Maximum	C.V.*
Canopy volume	m^3	12.14	8.05	17.31	0.09
Canopy height	m^3	2.87	2.45	3.43	0.04
Yield (2012)	Mg ha^{-1}	13.91	10.03	19.31	0.13
Yield (2013)	Mg ha^{-1}	34.44	26.80	41.63	0.07
Yield (2014)	Mg ha^{-1}	37.65	31.82	46.26	0.08
Yield (2015)	Mg ha^{-1}	41.13	35.04	50.67	0.07
EC_a (0 - 0.3m)	mS m^{-1}	2.45	1.63	3.25	0.12
Clay content	%	16.84	15.15	19.56	0.06
Organic Mater	%	1.37	1.12	1.50	0.63
Elevation	m	637.68	630.45	642.89	0.00

*Coefficient of variation (dimensionless)

Differently from the previous results, some resemblance in the spatial variability among different maps are visible in groves 2 and 3. These two fields were used in other studies and the relationship between soil attributes and yield were comprehensively investigated and reported by Colaço and Molin (2016). The clay content in grove 2 varied from 18 up to 50% (Table 4.7). The distributions of clay content and organic matter in this field are similar to the variation of elevation (higher clay content and organic matter in the lower part of the grove) (Figure 4.13). The soil ECa was also highly variable (values from 1.65 up to 14.1 mS m^{-1}). In one part of the grove, it is noticed some distinct variability patterns in the soil ECa map, which does not seem to be caused by natural soil variability. In the upper right corner of the grove, there is a straight line towards southwest dividing two zones with distinct soil ECa (Figure 4.13). This line matches a previous field boundary before the orange grove was planted (information discovered by analyzing old satellite images).

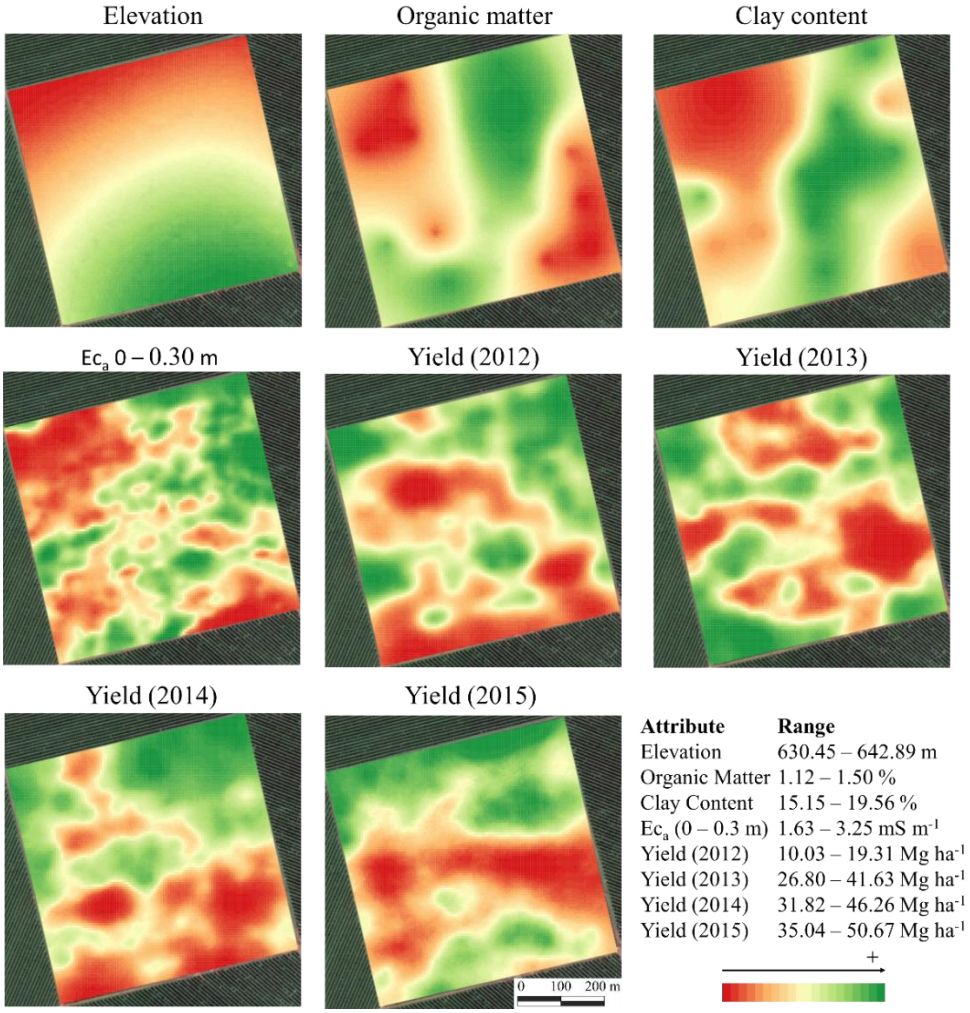

Figure 4.12: Maps of soil attributes and historical yield in grove 1

Table 4.6: Correlation matrix between different maps in grove 1

	Canopy Volume	Canopy Height	Yield (2012)	Yield (2013)	Yield (2014)	Yield (2015)	EC_a	Clay	O.M	Elev.
Canopy Volume	1.00	0.61	0.04	0.30	0.28	0.24	0.25	0.30	0.17	0.00
Canopy Height	0.61	1.00	-0.20	0.27	-0.19	0.08	0.03	0.11	0.18	0.47
Yield (2012)	0.04	-0.20	1.00	0.07	0.58	0.30	0.23	0.19	0.02	-0.48
Yield (2013)	0.30	0.27	0.07	1.00	0.11	0.33	-0.01	0.06	-0.20	-0.13
Yield (2014)	0.28	-0.19	0.58	0.11	1.00	0.46	0.23	0.36	0.00	-0.70
Yield (2015)	0.24	0.08	0.30	0.33	0.46	1.00	0.08	0.22	-0.20	-0.46
EC_a	0.25	0.03	0.23	-0.01	0.23	0.08	1.00	0.48	0.61	0.08
Clay	0.30	0.11	0.19	0.06	0.36	0.22	0.48	1.00	0.60	0.03
O.M.	0.17	0.18	0.02	-0.20	0.00	-0.20	0.61	0.60	1.00	0.54
Elev.	0.00	0.47	-0.48	-0.13	-0.70	-0.46	0.08	0.03	0.54	1.00

* Header abbreviations: EC_a, soil electrical conductivity in 0.3 m depth; O.M., organic matter; Elev., elevation

Table 4.7: Descriptive statistics from map data in grove 2

Variable	Unit	Mean	Minimum	Maximum	C.V*
Canopy volume	m^3	40.64	16.22	57.44	0.11
Canopy height	m^3	4.44	3.28	5.01	0.04
Yield (2008)	Mg ha^{-1}	18.36	10.62	32.95	0.17
Yield (2009)	Mg ha^{-1}	33.06	20.67	46.02	0.16
Yield (2010)	Mg ha^{-1}	20.07	8.59	38.68	0.18
Yield (2011)	Mg ha^{-1}	45.43	33.43	61.63	0.07
Yield (2012)	Mg ha^{-1}	66.09	30.37	102.96	0.13
Yield (2013)	Mg ha^{-1}	47.09	30.42	73.79	0.12
ECa (0 - 0.3m)	mS m^{-1}	4.52	1.65	14.10	0.31
Clay content	%	32.60	18.35	50.38	0.26
Organic Mater	%	2.39	2.10	2.93	0.09
Elevation	m	748.47	744.66	755.86	0.00

*Coefficient of variation (dimensionless)

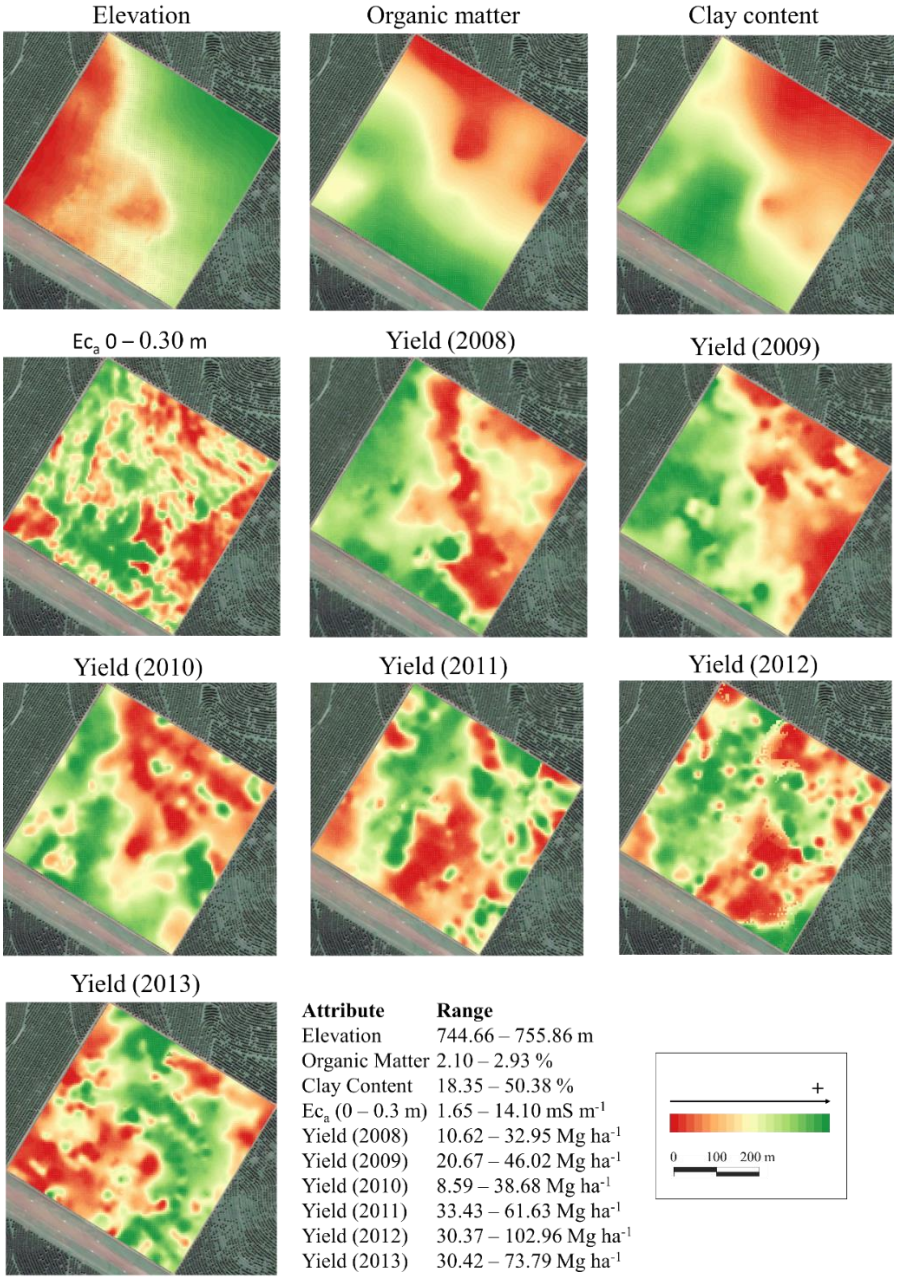

Figure 4.13: Maps of soil attributes and historical yield in grove 2

Generally, soil ECa also followed the variation pattern of elevation (higher values in the lowest part of the field). The correlation between soil variables and elevation ranged from -0.31 up to -0.75 (Table 4.8). The variability in the yield maps from 2008 until 2010 was similar to soil variability. This behavior was not as clear in the subsequent yield maps. The maps from 2011 and 2012 presented some similarity (r = 0.4).

Table 4.8: Correlation matrix between different maps in grove 2

	Canopy Volume	Canopy Height	Yield (2008)	Yield (2009)	Yield (2010)	Yield (2011)	Yield (2012)	Yield (2013)	EC_a	Clay	O.M.	Elev.
Canopy Volume	1.00	0.82	0.36	0.40	0.18	0.17	0.41	0.10	0.30	0.29	0.20	-0.37
Canopy Height	0.82	1.00	0.29	0.35	0.17	0.17	0.37	0.21	0.30	0.29	0.26	-0.37
Yield (2008)	0.36	0.29	1.00	0.70	0.42	-0.10	0.10	-0.30	0.34	0.56	0.52	-0.53
Yield (2009)	0.40	0.35	0.70	1.00	0.49	-0.14	0.15	-0.38	0.33	0.79	0.64	-0.76
Yield (2010)	0.18	0.17	0.42	0.49	1.00	-0.01	0.04	-0.26	0.08	0.52	0.51	-0.41
Yield (2011)	0.17	0.17	-0.10	-0.14	-0.01	1.00	0.40	0.14	-0.15	-0.24	-0.23	0.21
Yield (2012)	0.41	0.37	0.10	0.15	0.04	0.40	1.00	0.17	0.06	0.15	0.07	-0.18
Yield (2013)	0.10	0.21	-0.30	-0.38	-0.26	0.14	0.17	1.00	-0.09	-0.37	-0.20	0.18
EC_a	0.30	0.30	0.34	0.33	0.08	-0.15	0.06	-0.09	1.00	0.43	0.31	-0.31
Clay	0.29	0.29	0.56	0.79	0.52	-0.24	0.15	-0.37	0.43	1.00	0.83	-0.75
O.M.	0.20	0.26	0.52	0.64	0.51	-0.23	0.07	-0.20	0.31	0.83	1.00	-0.58
Elev.	-0.37	-0.37	-0.53	-0.76	-0.41	0.21	-0.18	0.18	-0.31	-0.75	-0.58	1.00

* Header abbreviations: EC_a, soil electrical conductivity in 0.3 m depth; O.M., organic matter; Elev., elevation

Regarding grove 3, a consistent variability pattern was found in most maps from soil and yield (Figure 4.14), even though the range on soil attributes were not very expressive (clay content varying 11.5 to 16.1 % and organic matter varying from 1.4 to 2 %) (Table 4.9). This is a relatively flat field, however, it is noticed that in the lowest part of the grove there is a low concentration of organic matter and clay (the correlations between elevation and organic matter was 0.64). Else, this is the region were lower yield occurred in practically all the evaluated years, especially in the yield maps of 2011, 2012 and 2013 (the correlation between yield in these years, clay content and elevation were between 0.50 and 0.60). The map of soil ECa showed that in this same region the highest values of ECa prevailed. This small portion of the field is known for having drainage problems, which explains higher levels of ECa and lower yields.

This grove presented the highest correlations between canopy geometry and soil parameters and yield, especially the canopy volume (as for the other groves the canopy height yielded lower correlations than canopy volume). The maps of canopy volume and height (Figure 4.10) showed that in the region with soil drainage problems the tree development was armed. A negative correlation between canopy volume and soil ECa (r = -0.51) was found. The map of canopy volume was also similar to most of the yield maps (excluding the yield maps from 2009 and 2010). Given that the LiDAR scanning was carried out a few years after the yield maps were gathered, and still the same variabilities patterns appeared, it indicates the consistency and the importance of the soil characteristics to the intrinsic variability in this grove.

Table 4.9: Descriptive statistics from map data in grove 3

Variable	Unit	Mean	Minimum	Maximum	C.V.*
Canopy volume	m^3	35.87	12.50	57.63	0.15
Canopy height	m^3	4.50	2.96	5.34	0.06
Yield (2008)	Mg ha^{-1}	12.28	7.87	19.80	0.13
Yield (2009)	Mg ha^{-1}	21.30	13.42	31.09	0.11
Yield (2010)	Mg ha^{-1}	22.96	14.43	38.77	0.14
Yield (2011)	Mg ha^{-1}	47.24	13.58	62.24	0.18
Yield (2012)	Mg ha^{-1}	57.50	22.32	83.54	0.18
Yield (2013)	Mg ha^{-1}	38.89	15.27	58.96	0.16
ECa (0 - 0.3m)	mS m^{-1}	1.03	0.25	6.15	0.53
Clay content	%	14.53	11.51	16.12	0.06
Organic Mater	%	1.71	1.49	2.02	0.06
Elevation	m	765.67	760.34	768.37	0.00

*Coefficient of variation (dimensionless)

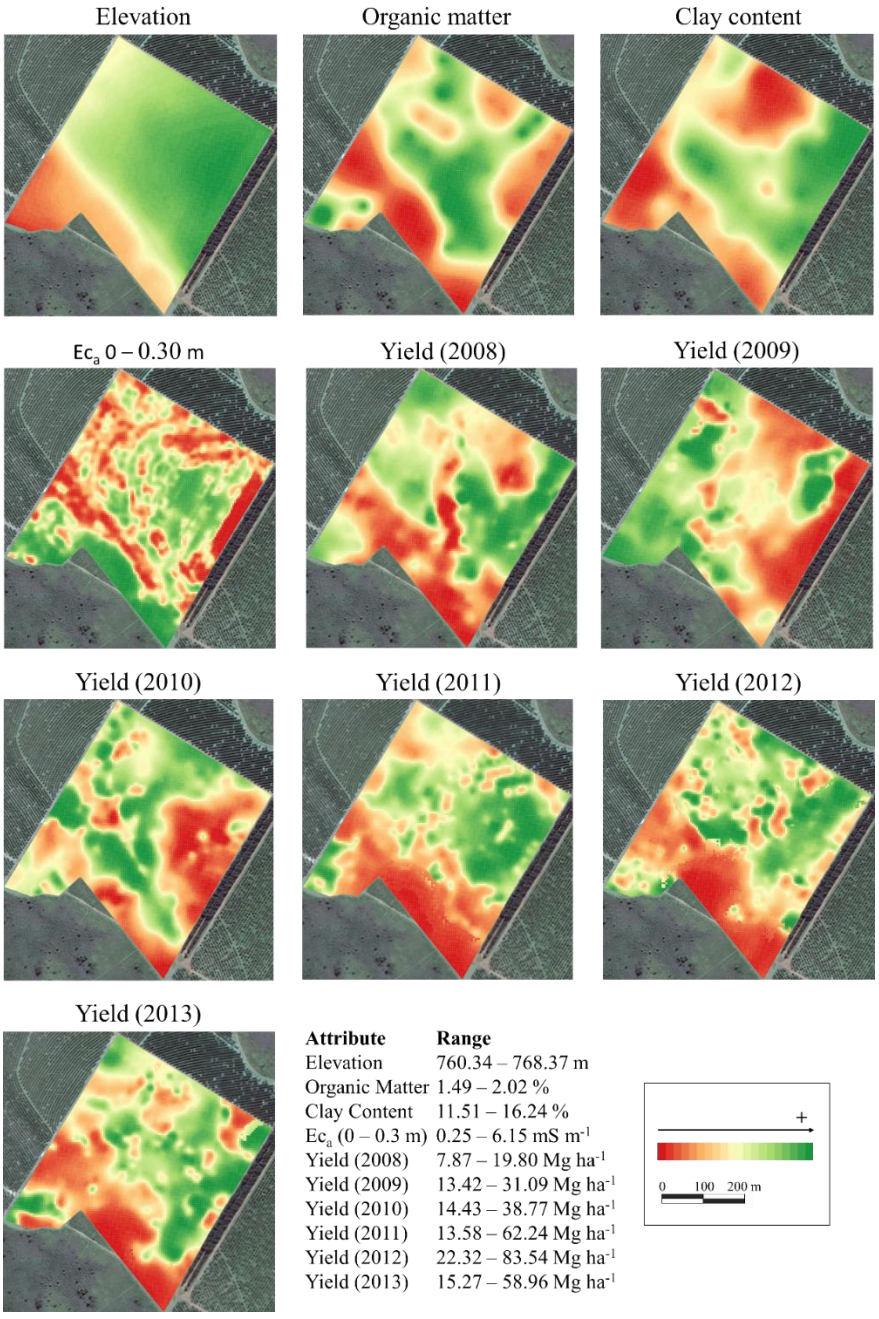

Figure 4.14: Maps of soil attributes and historical yield in grove 3

Table 4.10: Correlation matrix between different maps in grove 3

	Canopy Volume	Canopy Height	Yield (2008)	Yield (2009)	Yield (2010)	Yield (2011)	Yield (2012)	Yield (2013)	EC_a	Clay	O.M.	Elev.
Canopy Volume	1.00	0.91	0.53	-0.16	-0.09	0.72	0.54	0.62	-0.51	0.27	0.41	0.44
Canopy Height	0.91	1.00	0.49	-0.14	-0.09	0.67	0.52	0.59	-0.51	0.25	0.35	0.36
Yield (2008)	0.53	0.49	1.00	-0.19	-0.19	0.56	0.42	0.54	-0.23	0.30	0.44	0.41
Yield (2009)	-0.16	-0.14	-0.19	1.00	0.11	-0.04	-0.08	-0.25	0.15	-0.02	-0.32	-0.46
Yield (2010)	-0.09	-0.09	-0.19	0.11	1.00	0.09	-0.02	-0.02	-0.33	0.10	-0.23	-0.12
Yield (2011)	0.72	0.67	0.56	-0.04	0.09	1.00	0.72	0.71	-0.58	0.56	0.34	0.58
Yield (2012)	0.54	0.52	0.42	-0.08	-0.02	0.72	1.00	0.60	-0.35	0.62	0.31	0.53
Yield (2013)	0.62	0.59	0.54	-0.25	-0.02	0.71	0.60	1.00	-0.42	0.53	0.34	0.53
EC_a	-0.51	-0.51	-0.23	0.15	-0.33	-0.58	-0.35	-0.42	1.00	-0.29	-0.22	-0.34
Clay	0.27	0.25	0.30	-0.02	0.10	0.56	0.62	0.53	-0.29	1.00	0.20	0.43
O.M.	0.41	0.35	0.44	-0.32	-0.23	0.34	0.31	0.34	-0.22	0.20	1.00	0.64
Elev.	0.44	0.36	0.41	-0.46	-0.12	0.58	0.53	0.53	-0.34	0.43	0.64	1.00

* Header abbreviations: EC_a, soil electrical conductivity in 0.3 m depth; O.M., organic matter; Elev., elevation

A general evaluation of the spatial variability in these groves indicates that the youngest grove, grove 1, presented less variability in yield, soil attributes and canopy volume. The variability found in the maps was not very consistent and there was little resemblance between them. As discussed in the first section of the results, the canopy volume showed a frequency distribution close to normality and a weak spatial dependence indicating a certain level of randomness of the spatial variability of canopy volume. Grove 3 presented higher variability in soil conditions, significant yield variability and consistency along the years. The canopy geometry variation usually matched the variability found in soil and yield. Grove 2 showed intermediate results. Significant variation was found in altitude and soil attributes, which was reflected in yield variability in some years. The canopy volume and height maps were not strongly correlated with yield. The canopy volume histograms in groves 2 and 3 were more asymmetrical than in grove 1, presenting a slightly stronger spatial dependence than grove 1, indicating more consistent regions with distinct canopy sizes in those groves.

Some studies in Florida have shown strong correlations between orange fruit yield and ultrasonically measured canopy volume. However, different methods were applied in order to correlate these two variables. The highest correlation was reported by Mann, Schumann and Obreza (2010). They reached an R^2 of 0.85 when correlating the canopy volume and yield from 30 selected locations from a 10 ha orange grove. Zaman, Schumann and Hostler (2006) divided an orange grove into forty 0.4 ha plots and got an R^2 of 0.80 by applying a linear correlation over data from twenty out of the forty plots (the other half was used as a validation data-set). In the same grove, Schumann et al. (2006a) correlated yield and canopy volume using the data from all plots and got an R^2 of 0.64. The canopy height was slightly less correlated ($R^2 = 0.54$) with yield than canopy volume. In the present work, the canopy height was also less correlated with yield and soil attributes than canopy volume. Those groves in Florida presented significantly higher variability in canopy volume than the Brazilian groves evaluated in this study. The coefficient of variation of canopy volume in the study of Mann, Schumann and Obreza (2010) was 54%. Besides, the approach employed by the present study was a pixel-based correlation between maps, which might have contributed

to lower correlations. Schumann et al. (2006a) reported that the variability found in canopy volume was much higher than yield variability because the method of yield mapping do not allow the yield estimation on a single-tree basis as the ultrasonic sensor does for canopy volume. Nevertheless, visual resemblance between canopy volume and yield maps was pointed out by Zaman, Schumann and Hostler (2006) and Mann, Schumann and Obreza (2010).

The correlation between canopy geometry and yield or soil attributes might indicate whether canopy geometry is a suitable parameter to guide management zones delineation in a given grove. Figure 4.15 shows the cluster classification of the groves into three zones based on the canopy volume (canopy volume was chosen over canopy height due to its higher correlations with other variables). The classification in grove 3 produced continuous zones matching with spatial patterns viewed in soil and yield maps. The resulting zones were more diffuse in groves 1 and 2. The classification of canopy volume in grove 2 resembled the elevation, soil attributes and some yield maps. Regarding grove 1, the classification of the canopy volume, as the canopy volume maps itself, did not clearly match any of the yield or soil maps in a visual assessment.

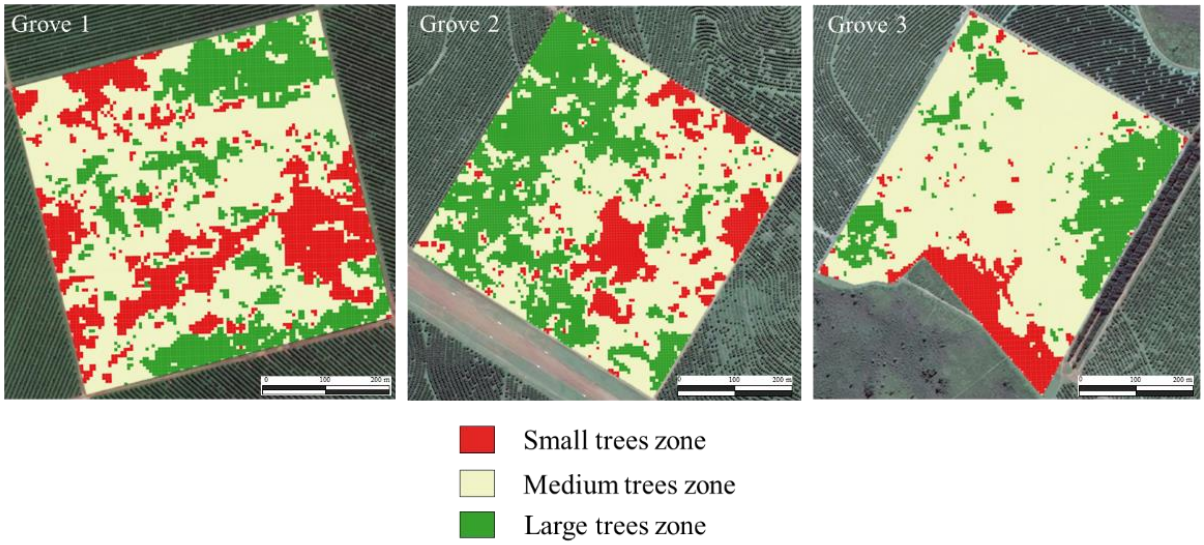

Figure 4.15: Classification of orange groves into different tree size zones

The mean values of each variable in the database (historical yield and soil attributes) were computed for each canopy volume zone (Table 4.11). As expected, zones with large trees were found in sites with higher clay and organic matter content. The soil ECa was also higher in those regions, with the exception of grove 3, where the higher ECa was found in the zone with smaller trees (in that grove high ECa is related to bad soil drainage). Regarding the yield in each zone, in a few cases some illogical results were found where the highest yield occurred in the zones with medium (grove 2 in 2013 and grove 3 in 2010) or small trees (grove 3 in 2009). This shows that the classification was not effective in those cases, probably due to the fact that the canopy volume was measured in 2015 and did not reflect the yield variability in the past or because the spatial variability in these years was unusual.

Table 4.11: Mean values of canopy volume, yield and soil attributes in three zones delineated based on canopy volume

Grove	Canopy volume zones	Canopy volume (m^3)	Yield (1)*	Yield (2)*	Yield (3)*	Yield (4)*	Yield (5)*	Yield (6)*	Eca	Clay content	O. M.	Elev.
			(Mg ha^{-1})						(mS m^{-1})	(%)	(%)	(m)
1	Large	13.58 a	14.00 a	35.11 a	39.10 a	42.09 a	-	-	2.53 a	17.26 a	13.93 a	638.02 a
	Medium	12.14 b	13.94 a	34.73 b	37.55 b	41.24 b	-	-	2.44 b	16.86 b	13.68 b	637.60 b
	Small	10.79 c	13.78 b	33.21 c	36.52 c	39.99 c	-	-	2.36 c	16.41 c	13.62 b	637.50 b
2	Large	44.93 a	19.65 a	35.44 a	20.52 a	45.85 a	68.91 a	47.05 b	4.93 a	35.02 a	2.43 a	747.10 c
	Medium	39.51 b	17.80 b	32.04 b	20.07 b	45.46 b	65.94 b	47.68 a	4.35 b	31.81 b	2.37 b	749.20 b
	Small	32.94 c	16. 86 c	30.22 c	18.83 c	44.18 c	58.86 c	44.98 c	3.95 c	28.85 c	2.33 c	749.70 a
3	Large	42.91 a	13.36 a	21.09 b	20.98 b	52.82 a	62.09 a	42.39 a	0.90 b	14.43 b	1.78 a	766.50 a
	Medium	35.52 b	12.23 b	21.28 b	23.80 a	48.45 b	58.73 b	39.48 b	0.92 b	14.74 a	1.69 b	765.80 b
	Small	25.54 c	10.64 c	21.80 a	21.24 b	29.76 c	41.63 c	28.97 c	1.91 a	13.42 c	1.65 c	763.50 c

* In grove 1, yield (1) to (4) represent yields from 2012 until 2015 sequentially. In grove 2 and 3, yield (1) to (6) represent yields from 2008 until 2013 sequentially

** Means with the same letter within columns in each grove are not significantly different according to the Tukey test ($p > 0.001$)

*** Header abbreviations: EC_a, soil electrical conductivity in 0.3 m depth; O.M., organic matter; Elev., elevation

Nevertheless, practically all variables differed significantly ($p > 0.001$) between zones in the three groves. Mann, Schumann and Obreza (2010) obtained similar results by classifying an orange grove into five zones based on canopy volume. These results indicate that the canopy volume map can provide zones where soil and historical yield are different. Therefore, the canopy volume map can be used in order to guide zones delineation for different management. Management zones are usually delineated based on the combination of several layers of information. In this case, all available variables should be considered as management zones indicators. However, in the absence of a large database, the canopy volume alone can help revealing zones of different soil and yield performance.

The establishment of management zones based on canopy volume does not mean that application rates must be kept constant inside each zone. As shown in the first section of this study, the MTLS system is able to provide information of variability even within each plant (along sections of the row). The optimum use of such technology should be a system which combines the real-time variable rate application based on MTLS with a base-map layer of the established management zones. In this system, the sensor readings should adjust the application rate proportionally to the canopy volume variation along the transversal sections of the row. Simultaneously, the management zone base map should guide the fertilization strategy (*e.g.*, choosing the optimal fertilization algorithm) which will achieve the yield goal for that specific zone.

4.5. Conclusions

The variability of canopy volume and height was assessed in commercial orange groves with the use of a mobile terrestrial laser scanner (MTLS) in order to evaluate i) the potential benefit of sensor-based variable rate application, ii) how does canopy geometry correlates with yield and soil attributes and finally iii) how canopy geometry information might be useful in precision agriculture management.

A significant variability in canopy volume and height was found in the five evaluated groves, especially in one with high occurrence of disease (grove 5). The frequency distribution of canopy geometry was usually negatively skewed. Canopy height histograms were useful for recognizing young tree resets in the groves. The canopy volume

and height computed for each transversal section of the tree rows were strongly correlated, indicating that canopy volume might be predicted by canopy height.

The simulation of sensor-based variable rate application of plant protection products or fertilizer showed that this technology could provide about 40% savings on input and an improvement in the accuracy of such applications.

The canopy geometry presented weak spatial dependence. The canopy volume maps showed variations within short distances as well as in large regions in the groves with distinct canopy sizes. The correlations between maps of canopy geometry and yield or soil attributes were usually low, especially in the youngest grove (grove 1) (R^2 up to 0.41). In the older groves (groves 2 and 3), which presented higher variability in soil attributes, the correlations between canopy volume and yield or soil parameters were higher, especially in grove 3 (R^2 up to 0.72). The patterns of the spatial variability of canopy geometry matched with the variability in yield and soil maps in those groves.

The classification of the groves into zones based on the canopy volume was successful in distinguishing regions in the groves with different soil features and yield performance, suggesting that canopy volume maps could be useful for the delineation of management zones in orange groves.

This study showed a high potential of sensor-based variable rate application of inputs in Brazilian orange groves due to the possibility of significant input savings by this technology. The canopy volume information showed to be a useful information to the understanding of spatial variability in an orange grove as well as an important variable for the site-specific management.

References

COLAÇO, A. F.; MOLIN, J. P. Variable rate fertilization in citrus: a long term study. **Precision Agriculture**, Dordrecht, online, 2016.

COLAÇO, A. F.; TREVISAN, R. G.; KARP, F. H. S.; MOLIN, J. P. Yield mapping methods for hand harvested crops. In: EUROPEAN CONFERENCE ON PRECISION AGRICULTURE, 10., 2015, Tel Aviv. **Proceedings**... Wageningen: Wageningen Academic Publishers, 2015. p. 225 - 232

ESCOLÀ, A.; ROSELL, J. R.; PLANAS, S.; GIL, E.; POMAR, J.; CAMP, F.; LLORENS, J.; SOLANELLES, F. Variable rate sprayer. Part 1 – Orchard prototype: Design, implementation and validation. **Computers and Electronics in Agriculture**, Amsterdam, v. 95, p. 122–135, 2013.

FRIDGEN, J. J. et al. Management zone analyst (MZA): Software for subfield management zone delineation. **Agronomy Journal**, Madison, v. 96, p. 100–108, 2004.

GIL, E.; ESCOLÀ, A.; ROSELL, J. R.; PLANAS, S.; VAL, L. Variable rate application of plant protection products in vineyard using ultrasonic sensors. **Crop Protection**, Guildford, v. 26, n. 8, p. 1287–1297, 2007.

GIL, E.; LLORENS, J.; LLOP, J.; FÀBREGAS, X.; ESCOLÀ, A.; ROSELL, J. R. Variable rate sprayer. Part 2 – Vineyard prototype: Design, implementation, and validation. **Computers and Electronics in Agriculture**, Amsterdam, v. 95, p. 136–150, 2013.

MANN, K. K.; SCHUMANN, A. W.; OBREZA, T. a. Delineating productivity zones in a citrus grove using citrus production, tree growth and temporally stable soil data. **Precision Agriculture**, Dordrecht, v. 12, n. 4, p. 457–472, 2010.

MOLIN, J. P.; COLAÇO, A. F.; CARLOS, E. F.; MATTOS Jr., D. Yield mapping soil fertility and tree gaps in an orange orchard. **Revista Brasileira de Fruticultura**, Jaboticabal, v. 34, n. 4, p. 1256-1265, 2012.

MOLIN, J. P.; MASCARIN, L. S.; Colheita de citros e obtenção de dados para mapeamento da produtividade (Characterization of harvesting systems and development of yield mapping for citrus). **Engenharia Agrícola**, Jaboticabal, v. 27, n. 1, p. 259-266, 2007.

SCHUMANN, A. W.; HOSTLER, K. H.; BUCHANON, S.; ZAMAN, Q. U. Relating citrus canopy size and yield to precision fertilization. **Proceedings of Florida State Horticultural Society**, Tallahassee, v. 119, p. 148–154, 2006a.

SCHUMANN, A. W.; MILLER, W. M.; ZAMAN, Q. U.; HOSTLER, K. H.; BUCHANON, S.; CUGATI, S. A. Variable rate granular fertilization of citrus groves: Spreader performance with single-tree prescription zones. **Applied Engineering in Agriculture**, St. Joseph, v. 22, n. 1, p. 19–24, 2006b.

SPEKKEN, M.; ANSELMI, A. A.; MOLIN, J. P. A simple method for filtering spatial data. In: EUROPEAN CONFERENCE ON PRECISION AGRICULTURE, 9., 2015, Lleida. **Proceedings**... Wageningen: Wageningen Academic Publishers, 2013. p. 259-266.

ZAMAN, Q. U.; SCHUMANN, A. W. Performance of an ultrasonic tree volume measurement system in commercial citrus groves. **Precision Agriculture**, Dordrecht, v. 6, p. 467–480, 2005.

ZAMAN, Q. U.; SCHUMANN, A. W.; HOSTLER, K. H. Estimation of citrus fruit yield using ultrasonically-sensed tree size. **Applied Engineering in Agriculture**, St. Joseph, v. 22, n. 1, p. 39–44, 2006.

ZAMAN, Q. U.; SCHUMANN, A. W.; MILLER, W. M. Variable rate nitrogen application in Florida citrus based on ultrasonically-sensed tree size. **Applied Engineering in Agriculture**, St. Joseph, v. 21, n. 3, p. 331–336, 2005.

ZAMAN, Q. U; SCHUMANN, A. W.; Nutrient management zones for citrus based on variation in soil properties and tree performance. **Precision Agriculture**, Dordrecht, v. 7, p. 45–63, 2006.

5. SUMMARY AND FINAL REMARKS

Modern agriculture has acknowledged the importance of taking the spatial variability of agronomical parameters into account in the management of crops. Sensors are the most promising solution to acquire data from crops aiming for the site-specific diagnostics, prescriptions and interventions. Sensing systems based on LiDAR technology have being developed in the past two decades for precision horticulture. These systems are able to provide with information about tree geometrical attributes such as canopy volume and height. The present research developed a mobile terrestrial laser scanner and new data processing methods in order to obtain 3D models of large commercial orange groves in Brazil. The system was able to provide accurate information about the canopy geometry and represent its spatial variability in the format of thematic maps supporting the decision making for site-specific applications.

The spatial variability of canopy geometry in commercial orange groves was characterized, providing enough information to elaborate scenarios and assumptions about the potential input savings of sensor-based variable rate applications. A broad understanding was provided about how canopy size relates with other agronomical variables traditionally used in precision agriculture studies. Suggestions were made on how to incorporate sensor-based canopy geometry information into future site-specific management practices.

This research project showed unprecedented results over the application of mobile terrestrial laser scanners in commercial orange groves. The first large scale scanning with such a system was reported. Viable solutions to improve the current management of orange groves in Brazil were proposed.

This is the first research project of its nature in Brazil. Future studies in such production environment should continuously enhance and optimize the data acquisition and processing systems towards its full applicability for growers. Besides, this project should encourage similar investigation in other relevant tree crops in Brazil.